Development of Novel Direct Arylation Methodology for the Synthesis of Conjugated Polymers

Jason A. Lee

A dissertation

submitted in partial fulfillment of the

requirements for the degree of

Doctor of Philosophy

University of Washington

2018

Reading Committee:

Christine K. Luscombe, Chair

Samson Jenekhe

Alshakim Nelson

Program Authorized to Offer Degree:

Chemistry

University of Washington

Abstract

Development of Novel Direct Arylation Methodology for the Synthesis of Conjugated Polymers

Jason Albert Lee

Chair of the Supervisory Committee:
Professor Christine K. Luscombe
Material Science and Engineering

Conjugated polymers (CP) represent an important class of materials in the field of organic electronics. From the seminal Nobel prize-winning studies on the semiconducting properties of polyacetylene in the 1970s, the development of CP for various novel applications has increased tremendously over the past two decades. However, although much focus has been on optimizing material performance in devices such as organic-based transistors and photovoltaics, there has been less study on the optimization of atom-economical polymerization methodology. C-H functionalization can provide a pathway towards reducing the amount of synthetic steps and waste produced via traditional aryl coupling reactions (Stille, Suzuki, Kumada, etc.). Specifically, direct arylation polymerization (DArP) can allow for more cost-effective and environmentally responsible syntheses that would be more amenable to industrial scale-up of these technologies. The following dissertation presents original research to develop new conditions for DArP.

TABLE OF CONTENTS

LIST OF SCHEMES

LIST OF FIGURES

LIST OF TABLES

ACKNOWLEDGEMENTS

First, I would like to thank my advisor, Professor Christine K. Luscombe, for her support, patience, and guidance throughout my graduate career. Her temperance and understanding greatly helped me during times of difficulty and frustration.

Next, I'd like to recognize some specific members in the Luscombe group for their contribution to my graduate experience:

Professor Ken Okamoto was my mentor when I first joined the group. He was vital in refreshing my synthetic and laboratory skills. He was patient with me and was always available to answer my questions. His help allowed me to better adjust to the lab during my first year.

Dr. Sabin-Lucian Suraru helped contribute to the C-H functionalization project that I would eventually take over. We understood the frustrations of C-H functionalization research and he was always a friendly resource for discussing chemistry.

Lauren Kang has always been a wonderful colleague and peer to discuss both chemistry and graduate student life in general. I appreciate her cheerful and welcoming attitude, which I believe helped to establish a similar atmosphere within our research group. It was invaluable to discuss our projects with one another in order to gain a better sense of our goals and to encourage each other whenever we hit a roadblock.

Erik Ho and Alin Miksi Kalayjian were two of my undergraduate students who I mentored in the lab. Their synthetic efforts helped contribute to some of the projects within this work.

Viktoria Pakhnyuk has been instrumental to my personal growth during my last year at UW. As much as I've grown academically, she helped to remind me that one's principles and

character are even more important. Through the roller coaster of trying to finish my graduate studies, her moral support has helped me find my ground in the face of uncertainty.

I cannot forget to give mention of my previous undergraduate mentors. I thank them for their patience and motivation for me to pursue graduate studies. From UCLA, I would like to acknowledge my advisor, Professor Paula Diaconescu, as well as my mentors Brian Williams and Dr. Selma Duhovic. From Caltech (summer undergraduate research), I would like to acknowledge Professor Robert H. Grubbs and my mentor, Dr. Rosemary Kiser, who helped instill my interest for research.

I would also like to acknowledge the efforts of my committee members, Professor Samson Jenekhe, Professor Alshakim Nelson, and Professor Buddy Ratner (GSR).

Last, but not least, I would like to thank my family friends who have supported me in multiple ways and who have believed in me. I hope I have and will continue to make you proud: Mom, Dad, Jessica, Chris, Kelvin, Jason H., Paula D. Julie H., Kevin V. Khai N., Kevin H., Takayuki K., Melrose M., and Chris G.

DEDICATION

To God for His grace and mercy.

To my family and friends for their support and encouragement.

Chapter 1. SEMICONDUCTING POLYMERS

1.1 INTRODUCTION TO POLYMERS

A polymer is comprised of macromolecules, of high molecular mass, which are made up of many repeated discrete covalently linked small molecules. Many common products we use are made from polymeric materials, and a common term for such materials is plastics (PE, PVC, PET, PS, PU, etc.). Plastic materials have revolutionized various consumer industries

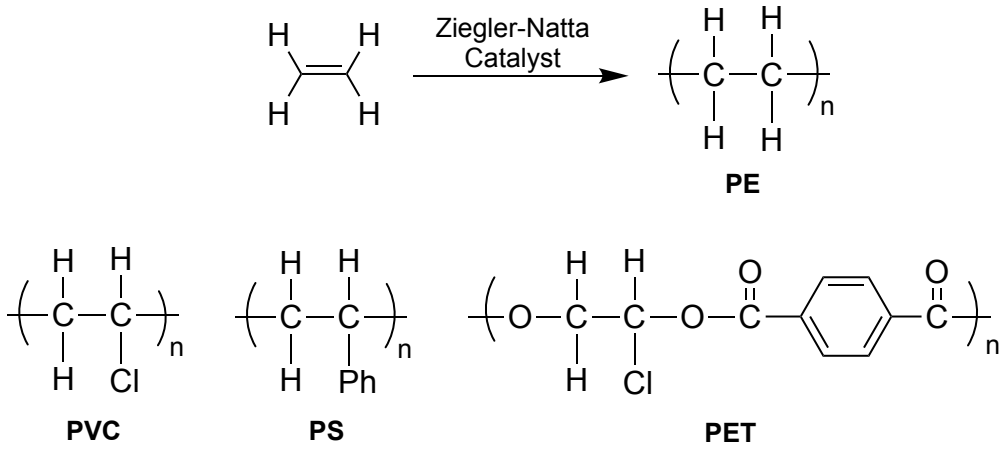

Scheme 1-1. ***Synthesis of polyethylene (PE) and common consumer plastics.*** *Polyvinylchloride (PVC), polystyrene (PS), polyethylene terephthalate (PET).*

(packaging, clothing, transportation, etc.) in terms of providing easily synthesized and cheap materials with structurally-tunable higher order properties including: tensile strength, hardness, and opacity. Some polymers are sized on the order of millions of grams per mole. Molecular weight plays a role in a polymer's applications and it is the most basic metric to characterize them. There are two definitions for estimating the molecular weight of a polymer sample known as the number-average molecular weight (M_n) and the weight-average molecular weight (M_w),

(**Equation 1-1 and 1-2**). In practice, not every macromolecule in the sample will have the same molecular weight and therefore understanding the distribution of molecular weights in a given sample is important. This metric is called the dispersity (Đ) and is defined as the M_w divided by the M_n. To showcase a large degree of control over a polymerization, a dispersity value approaching 1.0 is ideal, and it should be noted that dispersity can also be a factor in determining bulk properties. Commonly, vinyl or carbonyl-containing precursors are used to form non-conjugated linkages between repeat units (**Scheme 1-1**). In general, typical consumer plastics are electrically insulating due to the chemical structures of the monomers.

$$M_n = \frac{\sum X_i M_i}{\sum X_i}$$

Equation 1-1. ***Number-average molecular weight.*** *X_i is the number of moles of mass M_i.*

$$M_w = \frac{\sum X_i M_i^2}{\sum X_i M_i}$$

Equation 1-2. ***Weight-average molecular weight.*** *X_i is the number of moles of mass M_i.*

1.2 Semiconducting Polymers

Towards the end of the 20th century, Heeger, MacDiarmid, and Shirakawa's studies[1] showcased novel phenomena and applications for polymers, namely semiconducting polymers, or conjugated polymers (CP) (**Scheme 1-2**). Their shared Nobel prize in 2000 exemplified the significance of their work, and subsequent interest and research in the field has since burgeoned.

Semiconducting polymers continue to be a mainstay in the field of organic-based electronic functional materials research, where the drive towards high performance materials for potential

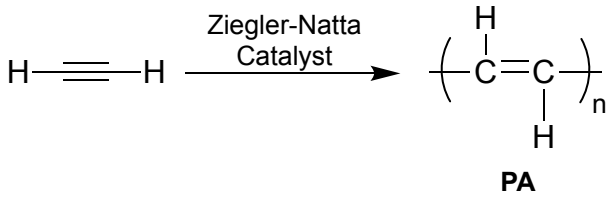

PA

Scheme 1-2. ***Synthesis of polyacetylene (PA).*** *Semiconducting properties characterized by Heeger, MacDiarmid, and Shirakawa.*

applications in organic photovoltaics (OPV), organic light-emitting diodes (OLED), organic field-effect transistors (OFET), and sensors has only increased.[2–4] Interest in these macromolecules not only stems from their intrinsically useful electronic properties but also from their structural modularity and potential mechanical robustness in novel conformations.[5] CP can have their elastic modulus tuned based on structure to allow for use in non-planar or higher tension surfaces, although incorporation in blends can greatly affect this property.[6] This is in contrast to inorganic semiconductor alternatives that are naturally brittle in nature. Due to their handling in organic solvents, CP can also be processed via solution-based roll-to-roll methods, while the production of inorganic materials require expensive specialized equipment, energy-intensive processes, and stringent working conditions.

Characteristic of a CP (visualized by Lewis structures) is a series of alternating single and double bonds that run along the polymer backbone. Looking at the atomic orbitals, the presence of overlapping p-orbitals along the atoms of the polymer chain allow for delocalization of π-electrons. In a small conjugated molecule, such as napthalene, this effect is not as pronounced, whereas a polymer has an increased conjugation length, which is directly proportional to

increasing the number molecular orbitals and decreasing the energy between the highest occupied molecular orbital (HOMO) and the lowest-unoccupied molecular orbital (LUMO). This energy difference becomes analogous to the differential magnitude between the valence and conduction bands in traditional inorganic semiconductors, which is known as the band gap (**Figure 1-1**). Therefore, with increased conjugation length to high approximation, a narrowing of the conjugated polymer's band gap is observed, allowing for lower barrier of a molecule's outer electrons to be extracted, thus yielding semiconducting properties. Materials with band gap values generally less than 1 eV are considered conductors while band gap values higher than 4 eV are considered insulators with semiconductors, and subsequently CP, falling in the middle range.

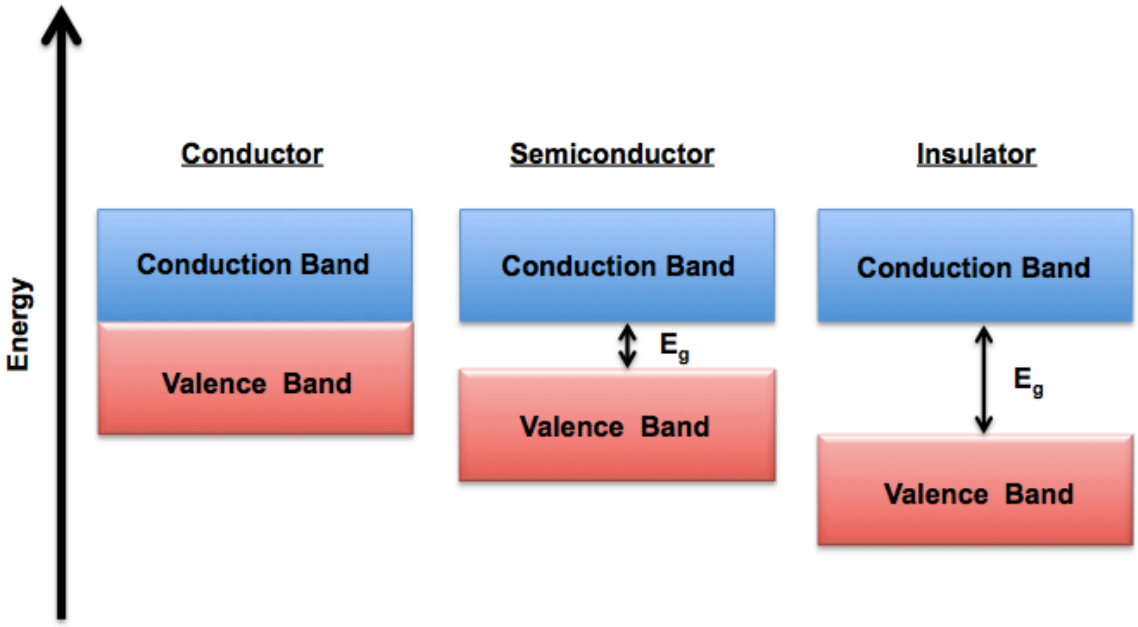

Figure 1-1. ***Example of band structures for various materials.*** *E_g denotes the band gap, or energy difference, between the conduction and valence bands of the material. A narrow E_g is characteristic of a semiconducting polymer.*

1.3 Motivating Applications for Conjugated Polymers

In order to inspire motivation for pursuing research on CPs, it might be of interest to discuss one of the possible applications. OPVs represent one of the more intriguing and challenging uses for CPs, especially in addressing the issues of environmentally conscious and sustainable energy. Although solar energy is not a new technology, the traditional inorganic materials used have placed bottlenecks on its widespread adoption. Current single-junction silicon solar technologies are able to reach efficiencies of over 25%.[7] However, the cost to manufacture these panels is expensive and the fabrication facilities are prohibitively costly from expanding the availability of these technologies geographically. Although optimum OPV efficiencies have yet to reach that of traditional technologies, hovering slightly above 10%,[7] they show promise in their potentially lower processing costs and physical properties. Because of their intrinsically high optical absorption, CPs can be implemented in thin films, which decrease the amount of material and bulk required for a given device.[8]

CP mainly fall into two categories, p-type and n-type, with the former being the more common due to performance and stability.[9,10] P-type CP (donor) possess higher electron density, so positively charged holes can be transported throughout .the material. Conversely, an n-type CP (acceptor) is more electron-deficient and thus is amenable for electron mobility. For an OPV to function, it is necessary to have both donor and acceptor materials, though the acceptor may or may not be polymeric.

The charge carriers in the conjugated polymers of these OPVs stem from a bound electron-hole pair, called an exciton. Excitons can be generated by the molecular absorption of photons of energy sufficient to match the bandgap of the given polymer, which is tuned by the chemical structure of the monomers as well as the conjugation length. Due to the fact that most

of the solar spectrum that the earth receives lies in the range of 450-700 nm,[11] lower band gap materials that require higher wavelength photons (less energetic) are ideal. As an electron is excited from its ground state via the energy from the absorbed photon, the coloumbically-bound pair may then be separated, aided by the help of an electron acceptor material (commonly fullerenes). The successful generation, splitting, and flow of charge allows for electrical current that can be used in different device architectures. However, the lifetime of the exciton is less than 1 ns with diffusion lengths less than 20 nm with the possibility of the charged particles recombining or undergoing other quenching mechanisms.[2,12] The ability to efficiently harvest electrons involves many material, morphological, architectural, and procedural factors that must be optimized, which heavily rely on structure-property relationships of the semiconducting materials.

Because of the low lifetime, diffusion length, and risks of quenching or recombination, the typically studied architecture for an OPV is that of a bulk heterojunction (BHJ) whereby a mixture of donor and an acceptor material are mixed together between two electrodes (cathode and anode). This effectively increases the interfacial surface area between the two material types. It is the interpenetrating domains of the donor and acceptor materials that allow for the photo-generated excitons to be split and for charge to be subsequently harvested. There may also be other additive layers to help create ohmic contacts of low electrical resistance with the electrodes and facilitate higher charge carrier mobility or to stabilize the morphology. Although a given CP can have high mobility properties on its own, the integration of the material with the other components of the device is non-trivial as there can be related physical and electronic boundaries brought about by their complex interactions.[13,14]

The modularity of changing monomer structure to investigate desired electronic and physical properties allows for more systematic optimization of polymer materials. However, the preparation of these monomers can be synthetically complex and environmentally burdensome. Simple CP such as polyacetylene have been replaced by intricate heterocyclic arenes, which have become the standard in the field. In order to utilize such materials for sustainable energy applications, the development of novel methodologies to mitigate these potential problems has so far been largely understudied and non-trivial.

1.4 POLY(3-HEXYLTHIOPHENE)

Much of the work described in the following chapters utilizes poly-(3-hexylthiophene) (P3HT) and thiophene precursors as model compounds for study. P3HT is one of the more ubiquitous polymers that have been examined in the field of organic electronics (**Figure 1-2**). Its physical characterization is quite well understood and its synthesis has also been greatly optimized.[15–18] At sufficiently high M_n (~10 kg/mol), P3HT appears as a purple solid with a

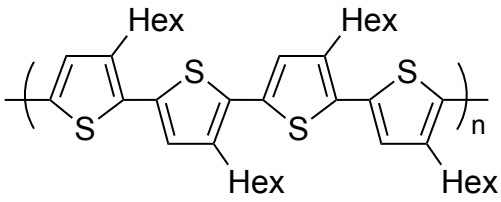

Figure 1-2. ***Poly(3-hexylthiophene) structure.***

metallic sheen. As a p-type CP with simplistic molecular structure, thiophenes are more synthetically accessible than complex monomer structures for use in studying fundamental structure-property relationships. Generally, thiophenes are functionalized in the 3-position with alkyl groups that help promote solubility. It was found via alkyl chain screening that the ideal

chain length is six (hexyl) for optimal properties in various optoelectronic applications.[19–21] The alkyl chain has contributions to the crystallinity, phase incorporation, and subsequently morphology. These aspects contribute to the hole mobility based on the ability of charge to hop from chain to chain. Anisotropic charge transfer has been reported based on the orientation and stacking of P3HT chains,[22] which highlights the importance of molecular packing that is affected by both substituents (including alkyl chains) as well as defects in the connectivity along the polymer backbone (regioregularity). Regioregular P3HT consists of 3-hexylthiophene units covalently connected from the 2-postion of one monomer to the 5-position of the next monomer. This is referred to as head-to-tail coupling, while other "defect" couplings exist such as head-to-head and tail-to-tail (**Figure 1-3**). High regioregularity is generally desired due to the higher degree of crystallinity that can be achieved, which promotes charge transport within the polymer domains.[13] However, defects alone do not necessarily yield lower performing devices.[23]

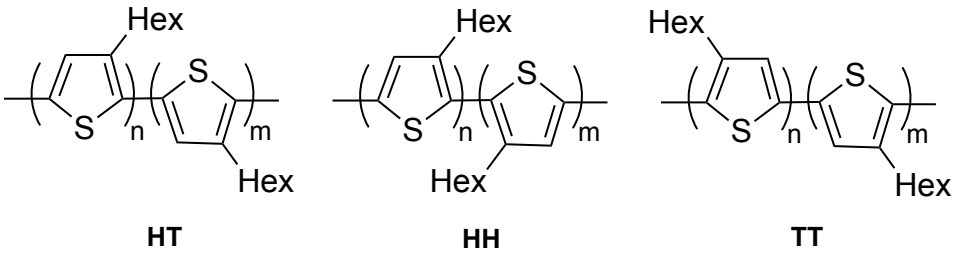

Figure 1-3. ***Examples of regioselective connectivity in P3HT.*** *Head-to-tail (HT), head-to-head (HH), and tail-to-tail (TT) are shown.*

Although P3HT is not considered the state-of-the-art when it comes to modern solar cell applications, showing optimal power conversion efficiencies of 6-7%,[24,25] it continues to be a reliable substrate to continue pushing the development of OPV technology. P3HT has been synthesized via micro-flow reactors with controlled regioselectivity, molecular weight, and

dispersity.[26–28] The development of these alternatives to traditional lab syntheses show promise for P3HT and other CPs to be utilized in scale-up processes for potential roll-to-roll printing, which will be necessary for future kilogram scale production of materials for industry. Even if P3HT itself is not utilized, thiophene units are still incorporated as components of large conjugated monomer systems for their donating character and reliable reactivity to act as π-bridges.[29,30]

1.5 Synthesis of P3HT: Living Polymerization Method

Kumada catalyst transfer polycondensation (KCTP) is the common methodology for synthesizing P3HT.[31,32] KCTP is a living polymerization scheme that incorporates Grignard metathesis (GRIM) in the presence of a nickel catalyst. **Scheme 1-3** below shows the typical polymerization conditions. All of the materials are commercially available and are not prohibitively expensive, making P3HT an ideal choice for model studies and often as a benchmark material for comparison.

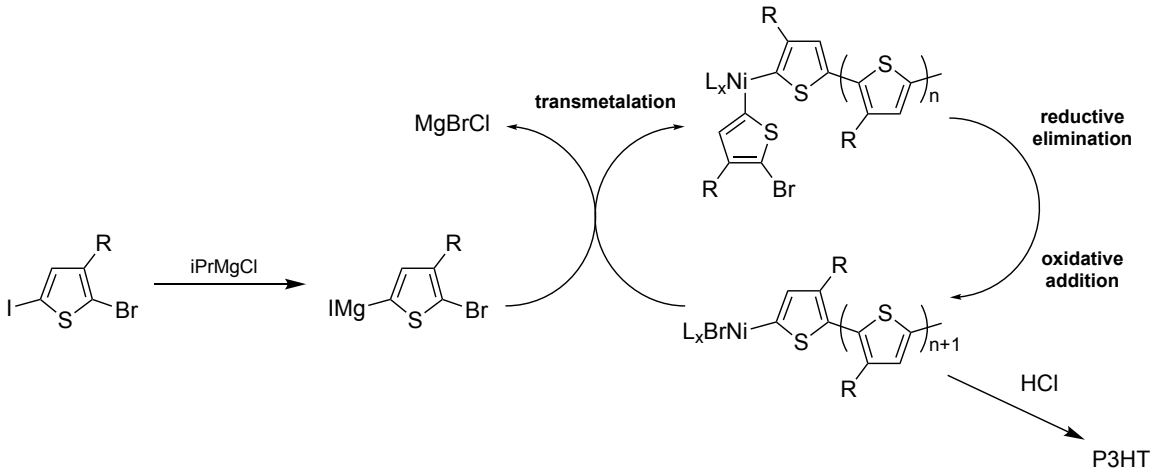

Scheme 1-3. ***General KCTP Mechanism for the synthesis of P3HT.***

The first step of KCTP involves the Grignardization of a di-halogenated thiophene monomer. In **Scheme 1-3,** the 2-bromo-5-iodo-3-hexylthiophene contains regioselectivity at the iodinated 5 position. Stoichiometric addition of Grignard is added to ensure the highest conversion of un-activated to activated monomer. Subsequent addition of the Ni catalyst species begins the polymerization. The impressive aspect of KCTP is the fact that it is a living polymerization, which has not been readily applied to many types of CP systems. One of the main conditions that characterize the methodology as living is that there is no chain termination, meaning a single catalyst is able to stay associated with a single polymer chain throughout the synthesis.[33,34] After reductive elimination and subsequent coupling of thiophene monomers, the now zero-valent Ni catalyst forms an associative π-complex with the electron rich thiophene ring (**Figure 1-4**). This "stickiness" prevents the Ni from dissociating away from the growing polymer chain long enough that the Ni can then oxidatively add into the halogen functionality in the terminal monomer. Depending on the monomer species, this complex may be too stable and trap the Ni from effectively chain walking.[35] As the catalyst remains active, or "living," after each coupling turnover, once the initial loading of monomer is consumed, more monomer can be added to increase the chain length, if desired. Due to the catalyst's chain association, the target M_n can be achieved by adding the correct equivalence of monomer-to-catalyst. This ratio determines the

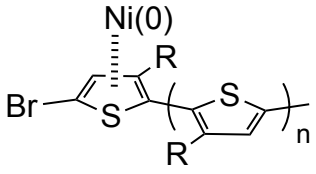

Figure 1-4. ***Ni chain association pi-complex with growing P3HT chain.***

degree of polymerization and subsequently the molecular weight. For example, a target M_n of 10 kg/mol would require about 60 molar equivalents of 3-hexylthiophene monomer to 1 equivalent of catalyst or more commonly measured as 1.67 mol% of catalyst with respect to monomer. The reaction is terminated via acid quenching, which cleaves the pendant catalyst and protonates the terminal end. From the above example, the majority of expected end-groups would be an H and Br. Additionally, the reaction can be quenched by specific groups, such as thiols or ethyne, to end-functionalize the P3HT chain.[36,37] High degree of control over the molecular weight is invaluable for studying systems identifying morphological and electronic consequences based on molecular weight. Another impressive aspect to this methodology is that the rate of initiation by the Ni species to a given monomer is much greater than the rate of propagation, meaning that all catalyst molecules should begin growth at similar time points. This allows for narrow dispersities, which is ideal for decreasing batch-to-batch variation and obtaining a high yield of the desired polymer size.

Although the KCTP method is quite robust, in practice it can be quite a sensitive reaction with some difficulties. The starting monomer, 2-bromo-5-iodo-3-hexylthiophene, is difficult to purify via column chromatography from its 2-bromo-3-hexylthiophene precursor. Although the monomer can be bought commercially, it is considerably more expensive than the constituent reagents. Additionally, the use of Grignard reagents means the entire process is highly water sensitive and that knowing the exact concentration of Grignard added is important for both maximizing the amount of monomer conversion to the activated monomer as well as minimizing the possibility for side reactions. Without proper loading of monomer, the precise control over the polymerization is lost. To ensure this, the entire reaction should be run under an inert gas atmosphere with every component and glassware as dry as possible. KCTP has been applied to

various other monomer types including alternating copolymers,[38,39] but has not been widely incorporated into more complex systems.

One of the inherent problems of the KCTP or GRIM polymerization involves the use of highly basic Grignard species. Current state-of-the-art polymers utilize both electron-rich and electron-poor molecules within a single polymer unit. These types of polymers are called donor-acceptor (DA) polymers and they have the ability to lower the energy band gap of the polymer and in the case of OPV, effectively increase the amount of low-frequency light that can be absorbed. The presence of electron-deficient monomers are often not compatible with highly basic moieties that could effectively attack electron-poor groups or possibly open up ring structures. Lack of electron density in acceptor monomers may also possess low affinity for the Ni catalyst, which prevents the associative ring-walking complex.

1.6 Traditional Conjugated Polymer Syntheses

The number of practical reactions for the polymerization of conjugated monomers is limited. Inspired by small-molecule cross-coupling reactions, the most common polymerization techniques are Stille and Suzuki coupling. Similar to GRIM, monomers must be pre-functionalized at two positions and require stoichiometric equivalents of organometallic reagents (**Figure 1-5**). Stille involves the use of organotin reagents, which are considered quite toxic to the environment and must be handled and disposed of in specialized waste streams.[40] Suzuki coupling employs boronic acids/esters, which are not as water sensitive as other techniques, but the compounds can be difficult to purify and incompatible with various monomers. P3HT has been made via both Stille and Suzuki coupling.[41,42] Both of these methods primarily utilize

palladium catalysts as opposed to nickel, which generally has lower affinity for forming π-complexes with monomers such as thiophene.[43]

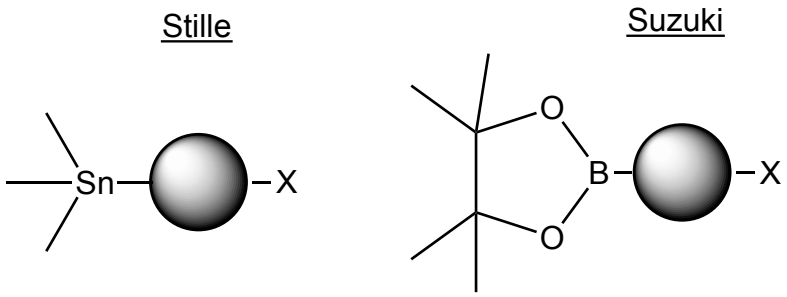

Figure 1-5. ***Example of Stille (organotin) and Suzuki-type (boronic ester) functionalities.***

Another important difference between these methods and KCTP is that they are not considered a living polymerization. That is, each subsequent coupling reaction regenerates free catalyst that must again undergo intermolecular oxidative addition transmetalate with another activated monomer species. This is opposed to the intramolecular oxidative addition in the GRIM method that affords one catalyst per chain, which remains active until quenched. Step polymerizations are slower and the rate of initiation versus propagation is not necessarily uniform throughout the course of the reaction. This behavior can be described by the slow growth of oligomers up to very high monomer conversion where the oligomers then stitch together and form polymers. This means that the predictability of the molecular weight as well as the dispersity is not as certain from batch-to-batch as you can have the presence of short chains or inter-chain coupling. Theoretically, the dispersity of step growth polymerizations approaches a value of 2 while controlled chain growth polymerizations tend towards 1.

Currently, in the interest of using semiconducting polymers as more environmentally-friendly and accessible technologies, the plethora of reagents required for complex monomers

poses questions about the actual environmental impact that mass-production of these materials may impart. The necessity to pre-functionalize two sites per monomer can often be non-trivial, especially when trying to activate electron-deficient monomers as they often require particularly harsh conditions, although recent iodination reactions involving perfluoroiodinated compounds appear promising.[44,45] Thus, it would seem that although optimization of optoelectronic properties of a given semiconducting polymer is obviously an important aspect of the field, it might also be relevant to be able to find alternatives to the current synthetic methodologies. Not only would this allow for easier, less time and resource intensive fabrication, but also it would help to quell some of the concerns about the fate and transport of potential environmental and biological hazards that are often associated with these syntheses. For that, we can look towards an increasingly growing field known as carbon-hydrogen functionalization, which aims to achieve such a goal.

Chapter 2. C-H FUNCTIONALIZATION

2.1 Introduction to Atom Economy

In the synthesis of conjugated polymers, carbon-carbon (C-C) bonds need to be formed to create the covalent backbone of the polymer. Generally, there are a few traditional C-C bond-forming reactions that are employed for small molecules that are also applied towards polymerizations (Suzuki, Stille, Kumada, etc.). However, these reactions require pre-functionalization of the substrates in order to sufficiently activate the desired carbon sites. This is commonly in the form of a carbon-hydrogen (C-H) bond transformation into a C-X, where X is often a halogen (**Figure 2-1**). Even after the carbon site is pre-functionalized, the use of stoichiometric amounts of organometallic reagents is required in order to facilitate the C-C bond formation, which may require additional purifications.

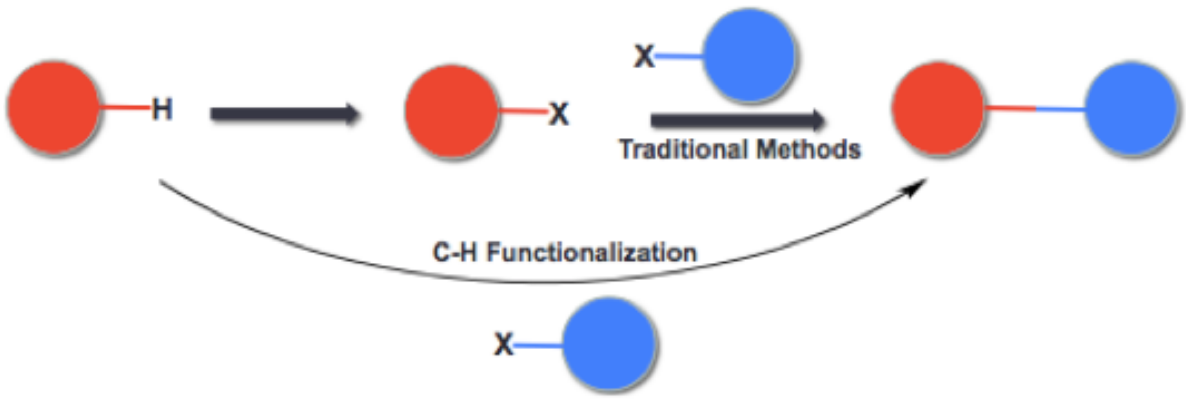

Figure 2-1. ***General C-H functionalization scheme versus traditional methods.*** *X is an activating group such as a halogen or organometallic group.*

The necessity of these extra steps can greatly contribute to increased synthetic complexity and cost. Even less obviously considered are the potential costs associated with the fate and transport of the subsequent byproducts and waste from these additional reactions. Ideally, we would be able to limit the number of pre-functionalization steps required in a given syntheses by finding conditions to increase the reactivity of C-H bonds. This is the principle of C-H functionalization (CHF), where we can utilize specific reagent and conditions in order to both activate the typically inert C-H bond, and directly functionalize it with a desired substrate. This methodology can effectively eliminate one, if not several, steps in a given syntheses. Another way to describe CHF is atom-economy, where the number of reactant atoms is conserved, as much as possible, in relation to the atoms present in the desired products. CHF becomes more essential in downstream synthetic pathways of complex molecules, which is a growing need for biologically and pharmaceutically relevant targets.[46] Although CHF with respect to materials synthesis has not traditionally been a focus in the field, the surge of conjugated materials research has opened up renewed motivations for evaluating CHF's possible role.

2.2 Direct Arylation

On any given molecule or monomer, there can exist many potential C-H bonds, which is what makes study of selective CHF the more challenging endeavor. Specifically, in the context of conjugated materials, consideration is shifted towards unsaturated sp^2-hybridized carbons in aromatic molecules. A more specific term for CHF applied to this class of substrates is called direct arylation (DA). **Figure 2-2** shows a comparison of substrates found in DA reactions. Some of the early reports on DA conditions came in the 1980's by Itahara, who studied the arylation of

aromatic heterocyclic compounds such as thiophenes, furans, and indoles.[47] In that report, $Pd(OAc)_2$ was used with mixed solvents containing acetic acid at reflux. Surprisingly, these conditions are not too different from some of the more modern systems for DA used nearly 40 years later.[48,49] Palladium-based catalytic conditions for DA have become quintessential.[50]

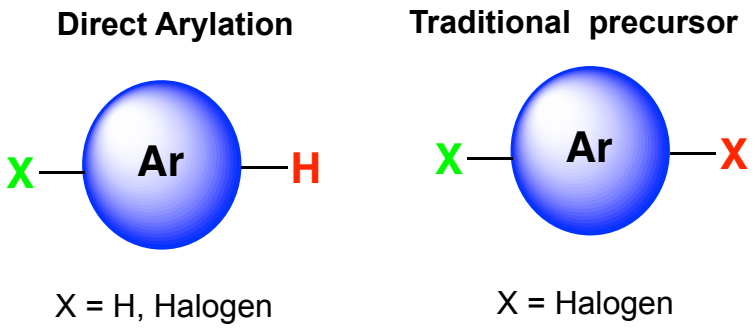

Figure 2-2. ***Examples of aryl substrates and their pre-functionalization for DA and non-DA conditions.***

In the last decade, exploration into understanding DA reactions has greatly developed with some more novel systems being investigated without Pd. For example, Larrosa has investigated the use of gold as the primary catalyst.[51–53] Fagnou was one of the modern contributors to DA understanding, having developed substrate scopes,[48,54] mechanistic insight,[55] as well as general reaction conditions[49] that have generally been referenced for inspiring other DA conditions. Still, there remain mysteries into the necessary of contributing roles of certain additives (for example, oxidants or types of bases) as well as the mechanism of more non-traditional DA conditions. Although ample occurrence of sp^2-hybridized C-H activation has been demonstrated, control and efficiency of such systems is the next step in pushing the methodology forward.

2.3 Concerted Metalation Deprotonation Mechanism

Fagnou's group published many works on substrate scope for DA of aromatic heterocyclic molecules including thiophenes. He also worked to elucidate the mechanism and energetics for DA as well as the effects incurred by various arene species.[56,57] Today, it is widely accepted that many DA that stem from these seminal works undergo what is known as concerted metallation-deprotonation (CMD). From experimental and computational collaboration, it was found that the deprotonation of the carbon site occurs nearly simultaneously with the metalation of the carbon. It was observed that carboxylate ligands or additives (commonly pivalic acid) were necessary to help facilitate this concerted mechanism.[49] Pivalic acid and other small molecule carboxylates have been characterized as proton shuttles and reactions without them have significantly less reactivity.

In general, the C-H activation process is the rate-limiting step of DA and two energy barriers have been recognized as playing a contributing factor based on the substrate (**Figure 2-3**). Firstly, there is a distortion energy associated with the bond strain of the target hydrogen as it enters the transition state conformation. Secondly, there is a beneficial interaction energy contribution where the metal center and ligand approaches the substrate. It was generally found that electron-rich arenes experience higher distortion energies, due to repulsion via their increased electron density, as opposed to electron-deficient arenes. However, it was also observed that electron-rich arenes benefit from a higher energetic gain due to the interaction with catalyst, which would be expected with the generally electron-poor metal center. Meanwhile, electron-deficient arenes do not get the energetic benefit of this interaction, or stabilization energy, likely due to the lessened electronic affinity between substrate and catalyst. In general, it

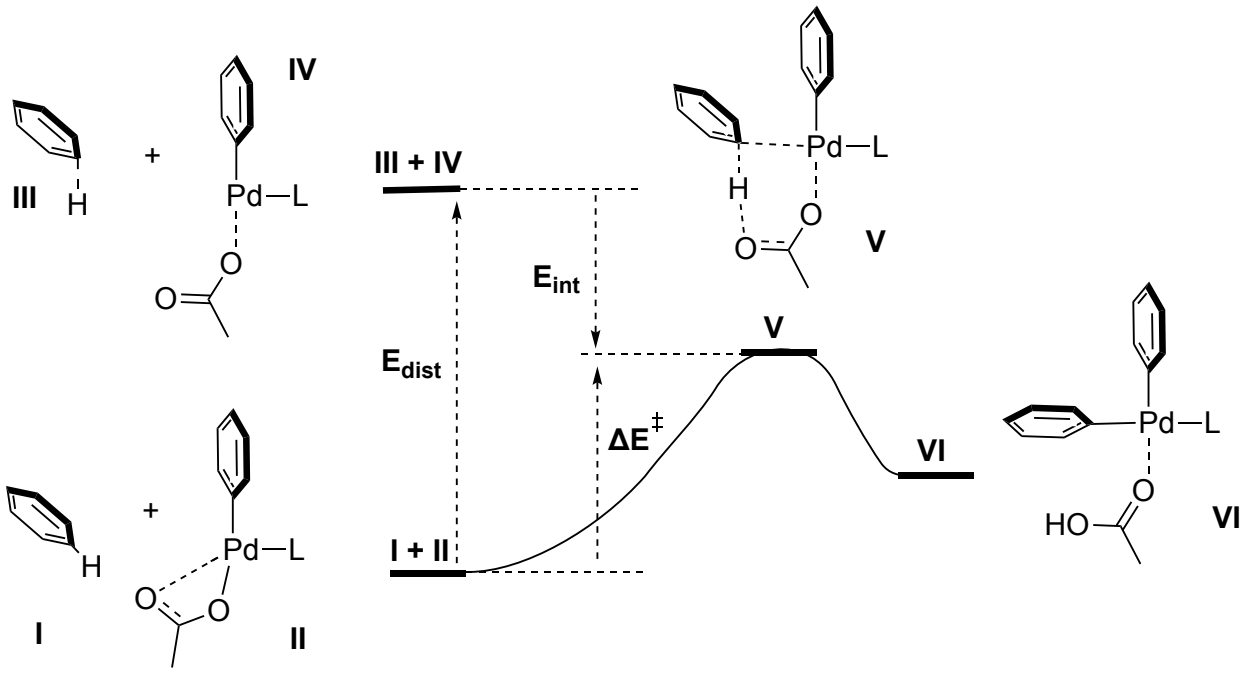

Figure 2-3. ***CMD distortion and interaction energy contributions for C-H activation***.[57]

has been observed that electron-deficient molecules are more prone to C-H activation. These experimental and computational results were significant in CMD's acceptance as the prevailing mechanism in CHF over other previously hypothesized mechanisms such as electrophilic aromatic substitution. Even Cl substitution has been shown to lower the proton distortion energy barrier compared to non-chlorinated compounds (~3-5 kcal/mol), promoting site selectivity.[58] Based on the reaction coordinate, the distortion energy plays a greater role in achieving the transition state over the interaction energy.

2.4 Direct Arylation Polymerization

Similarly as the traditional C-C coupling methods for small molecules have inspired polymerization conditions, DA conditions have also been applied to conjugated polymers.[59,60]

Specifically, the methodology is called direct arylation polymerization (DArP). DArP has seen an increase in its usage in conjugated polymer materials research. The current focus has been on donor-acceptor type polymers with co-monomers using A-A and B-B motif for their reactive site. There have also been several reports of P3HT being synthesized via DArP.[61–63] Thompson looked to explore the regioselectivity of 2-bromo-3-hexylthiophene in DArP conditions by screening for carboxylate additives.[64] His group found that a mixture of neodecanoic acid isomers prevented undesired β-branching, which would lead to lower performing non-linear P3HT architectures.[65] Also, Cheng and coworkers showed P3HT and poly(3-hexylselenophene) using pyridine-enhanced precatalyst preparation stabilization and initiation (PEPPSI) Pd catalysts.[66] However, due to the nature of the CMD mechanism, DArP-synthesized polymers undergo step-growth kinetics with inherent lack of control. Also, as stated previously, step-growth behavior leads to higher molecular weight distributions and potentially more batch-to-batch variation. These are undesirable characteristics because they have larger implications on device performance and fabrication. Thus far, attempts at trying to achieve chain growth DArP systems[62] has been lacking, and it will require more development and understanding of reaction conditions to eventually push it towards controlled polymerizations. Materials research has been driven by novel properties, while sustainable and atom-economical syntheses appear to be secondary. Therefore, if DArP is to ever fully compete with such methods as KCTP, it will be necessary to achieve similar robustness and utility.

2.5 Cost Incentives for DArP

As previously mentioned, the pursuit of conjugated polymers is attributed to the attractive ease in device processing via roll-to-roll and other solution-based methods as opposed to many inorganic counterparts. However, as the race towards optimization of the highest efficiencies and mobilities continues to develop, the importance of scalability of manufacturing these materials is a necessary consideration. The materials and synthetic costs involved in many of the organic monomers and subsequent polymers are non-negligible if one were to seriously consider implementing technologies such as OPV in a commercial venture where the target metric of cost per energy produced is less than $1/watt. Some reports have given studies to model the importance in the cost for synthesizing some of the most recognized semiconducting polymers in the field. Aside from cost implications, it is also important to consider, although difficult to predict, the impact of waste and toxicity treatment engendered by these lengthy syntheses. It would seem counter-intuitive to look towards alternative energy as a way to promote sustainability and protection of our natural environment but in the meanwhile requiring the generation of large-scale potentially hazardous chemical wastes that could have similar or worse consequences than conventional energy resources.

One of the metrics considered by Osedach et al, is the cost-per-gram-step (CPGS),[67] which calculates the cost of materials (including solvents) in each step of a polymerization as well as estimated purification costs associated with each step. Although the price of chemicals used are based on lab-scale chemical suppliers, thereby giving an overestimate in material cost, their estimate does not even factor in waste treatment, energy input, or maintenance and operational costs, which could potentially exceed the CPGS estimate of the materials synthesis alone. In an idealized and impractical model, not factoring in the cost of purification, they found

a correlation of over $6 per gram-step. When calculating estimates incorporating necessary purification and work-up, they found a nearly 5-fold increase up to $31 per gram-step (**Table 2-1**). It could be envisioned that for the higher efficiency donor-acceptor polymers consisting of complex and structurally unique co-monomers, these costs could climb quickly. CPGS may not

Polymer	**Number of Steps**	**Cost (no work-up) ($ per g)**	**Cost ($ per g)**
P3HT	3	3.56	16.18
DBP	3	7.88	89.60
PDPP3T	6	14.95	164.46
DTS	8	12.34	163.25
PBDTTPD	10	85.90	447.83

Table 2-1. ***Materials cost estimate for conjugated polymers in OPV.***[67]

DBP: dibenzo([f,f0]-4,40,7,70-tetraphenyl) diindeno[1,2,3-cd:10,20,30-Im]perylene,
PDPP3T: poly[(2,5-bis(2-hexyldecyl)-2,3,5,6-tetrahydro-3,6-dioxopyrrolo[3,4-c]pyrrole-1,4-diyl)-alt-([2,20:50,20- terthiophene]-5,50-diyl)],
DTS: 5,5-bis(4-(7-hexylthiophen-2-yl)thiophen-2-yl)- [1,2,5]thiadiazolo[3,4-c]pyridine-3,3-di-2-ethylhexylsilylene-2,20- bithiophene,
PBDTTPD: poly((4,8-diethylhexyloxyl)benzo([1,2-b:4,5-b0]dithiophene)-2,6-diyl)-alt- ((5-octylthieno[3,4-c]pyrrole-4,6-dione)-1,3-diyl).

be the most accurate in determining actual cost estimates, especially only factoring in active layer materials. However, it does highlight the importance of cost considerations for complex synthetic pathways. As expected, the more steps, the higher correlation of costs associated with the material.

Another group has attempted to develop their own metric known as the synthetic complexity index (SC), which places a non-monetary value on the feasibility of scale-up.[68] Ranging from 0 to 100, this index incorporates a weighted average of various components including the number of steps, the number of purification steps, the number of column chromatographies needed, and consideration for the number of hazardous chemicals used (**Equation 2-1**). This value is then normalized over the reported PCE to give a figure-of-merit (FOM) value to analyze more of a relative cost-utility analysis. After analysis on various donor and acceptor CPs, it was observed that many of the highest efficiency materials in the literature contain high SC values and subsequently, high FOM, showing their potential lack of scalability. It is noteworthy that P3HT was rated as one of the lowest FOM. Unlike the CPGS, the FOM

$$SC = 35\frac{NSS}{NSS_{max}} + 25\frac{\log(RY)}{\log(RY_{max})} + 15\frac{NUO}{NUO_{max}} + 15\frac{NCC}{NCC_{max}} + 10\frac{NHC}{NHC_{max}}$$

Equation 2-1. ***Synthetic complexity index (SC).*** *Number of synthetic steps (NSS), reciprocal yield of monomers (RY), number of unit operations for isolation/purification of monomers (NUO), number of column chromatographic purifications (NCC), and number of hazardous chemicals used for monomer preparation (NHC) are all considered.*[68]

metric takes into account the performance of the material, which indirectly takes into account other component factors of the device. The aim should be to find the best balance of low synthetic and processing cost versus device performance. Of course, one way is to push towards higher efficiencies. However, the other way would be to develop synthetic pathways that could decrease the SC. That is where the potential of CHF can be realized and implemented.

Chapter 3. REGIOSELECTIVITY IN HYPERBRANCED P3HT

3.1 Introduction to Hyperbranched Conjugated Polymers

There has been much focus on achieving linear regioregular polymer architectures in the interest of increased conjugation length, higher structural planarity, as well as the degree of crystallinity.[14] These characteristics are correlated with desirable characteristics such as narrower band gaps and higher charge mobilities. For that reason, branched conjugated polymer structures have not been as heavily explored for optoelectronic applications. However, that does not mean branched morphologies are without unique and interesting properties.[69] Branched thiophenes have shown lower HOMO and LUMO levels, which may be desirable for electronic band matching in devices.[70] Additionally, branched polymers tend to exhibit increased solubility over their linear counterparts, which can be explored for applications requiring modular and even aqueous-based solubility.[71] Finally, intense fluorescence emissions have been shown to be tunable with the degree of branching (DB) or functional groups.[72,73] DB, which is the unique metric developed to differentiate branched from linear polymers is exemplified in **Figure 3-1** and is defined by **Equation 3-1**.

Although traditional applications such as OFETs and OPVs may not immediately benefit from understanding of conjugated hyperbranched polymers, biomedical applications such as imaging technologies may be more appropriate.[74–76] Additionally, there have been chemical sensors such as detection of explosive precursors, including in aqueous environments, which have garnered some attention.[77–79] Incorporation of controlled branched architectures in other devices may prove to have uses that have yet to be realized. Another reason for the lack of branched conjugated polymer exploration could be due to the general difficulties found in their

syntheses. Such difficulties include designing and synthesizing branched monomers, low-yielding polymerizations, and uncontrollable branching.

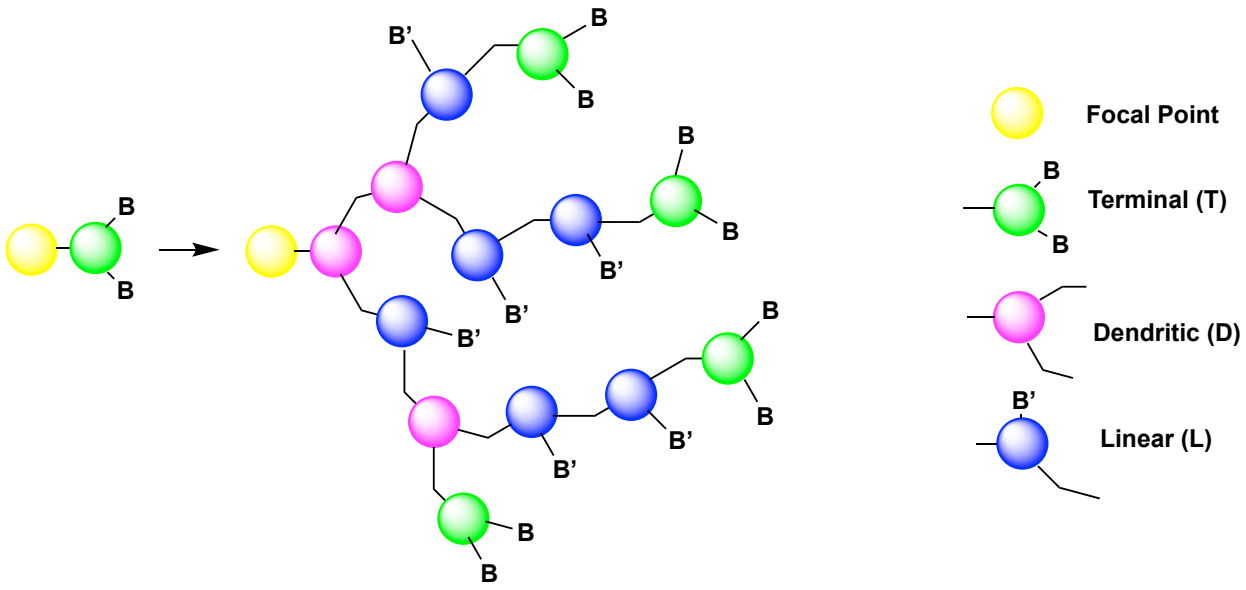

Figure 3-1. ***Example of linkages in hyperbranched polymers.***[80]

$$DB = \frac{D + T}{D + T + L}$$

Equation 3-1. Degree of branching equation. *Dendritic (D), terminal (T), and linear (L) monomer connections.*

3.2 Motivation From Tunable Hyperbranched DArP Work

In 2012, the Luscombe group published conditions for using C-H activation on 2-bromo-3-hexylthiophene, yielding tunable branching, involving C-H activation of the 4-position and/or 5-position of the thiophene monomer (**Scheme 3-1**).[81] One system identified as condition, A,

used $Pd(OAc_2)$ and KOAc to give a DB of 0.1. The second system referred to as, B, used $PdCl_2$ and KF to yield a DB of 0.4. Various other additives were then applied to these general conditions to vary the DB. Interestingly, it was found that the DB for condition B began to approach a value of 0.5, which would theoretically imply that the 4 and 5-position have nearly equal reactivity. This is a result that would not be expected in small molecule reactions, which often require more difficult methods to selectively activate the 4-position.[82] It was of interest to determine the cause and mechanism of this regioselectivity such that we could obtain more control over polymer branching. Such synthetic control could aid in rational design of novel materials that have not yet been explored in the realm of conjugated polymers.

Scheme 3-1. ***Previously published conditions for hyperbranched P3HT.*** *Condition A: KOAc (2 eq.), $Pd(OAc_2)$ (1 mol %), 24 hr, DB = 0.1, M_W = 31 kg/mol. Condition B: KF (4 eq.), $PdCl_2$ (3 mol %), 48 hr, DB = 0.4, M_W = 25 kg/mol.*[81]

3.3 Regioselectivity Model Reaction Studies

Due to the apparent difference in reactivity between small molecule coupling and the branched polymerization observed, it was thought that perhaps the increase in conjugation has an effect on the reactivity. We hypothesized that with increase in polymer length there would be higher reactivity at the 4-position. In order to track the reactivity and regioselectivity of 3-alkylthiophene, a small-molecule analogue model reaction was proposed for easier analysis

(**Scheme 3-2**). Bromine from the original monomer was replaced by chlorine in order to prevent polymerization due to ease of oxidative addition into the C-Br bond versus C-Cl bond. 2-Bromotoluene was chosen as a coupling partner in these reactions. Being a relatively electron-rich compound while bearing some steric resemblance to the original monomer, this coupling partner seemed like an acceptable substitute. Additionally, the methyl group provided an easy way to identify the presence of coupling products via NMR. An upfield methylene proton signal would be more easily identifiable as opposed to any aromatic protons in the crowded and complex aromatic region.

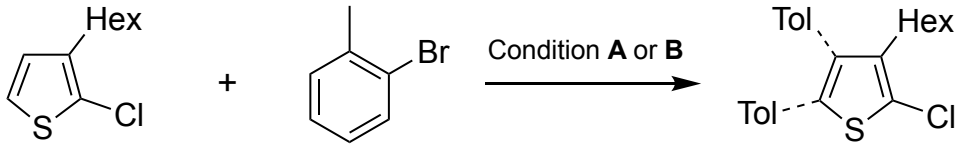

Scheme 3-2. ***Small molecule model reaction used to determine distribution of C-H functionalization.***

For analyzing each model reaction, the ^{1}H-NMR spectrum was examined for disappearance of aromatic thiophene protons of the starting monomer as well as an uncoupled proton signal for reacted monomer. The methyl peak of the 2-bromotoluene was also observed for chemical shifts due to differences in free and coupled moieties. Condition A and B of the original polymerization reaction were used following the exact same procedure as published. Three trials for each condition, with increasing monomer lengths (dimer and trimer) were performed (**Table 3-1**). In these trial reactions, a general trend of higher reactivity for condition

Substrate[a]	Condition	Major Products (% Yield)[b]	Trace Products [c]
Monomer	A	Mono-substituted (96)	-
	B	Mono-substituted (11)	Dimer
Dimer	A	Mono-substituted (90)	-
	B	-	Mono-substituted
Trimer	A	-	Mono-substituted
	B	-	Mono-substituted

Table 3-1. ***Hyperbranched P3HT model reactions.*** *[a] Substrate is 2-chloro-3-hexylthiophene and its oligomers. [b] Mono-substituted product was only observed with substitution at the 5-position of thiophene. Absolute yield was determined by NMR with napthalene as a reference. [c] Mono-substitution and dimer formation of substrate was observed in trace amounts via GC-MS.*

A and low to no reactivity for condition B was observed. Additionally, with increasing monomer length, a general lack of reactivity was seen. In all cases, there were no readily observable products with reactivity at the 4-position, which was unsupportive of the original hypothesis. Trace amounts of monomer dimerization were observed through gas chromatography-mass spectrometry (GC-MS). These results would imply that the thiophene reactivity is actually decreased with increasing chain length, although this would not explain the previously reported polymerization results where high molecular weight and branching were observed.

3.4 MECHANISTIC COMPUTATIONAL-EXPERIMENTAL COLLABORATION

The next step was to look towards computational methods to see if the mechanism could give clues on how to experimentally explain the reactivity results. We collaborated with the computational group of Musaev from Emory University. Calculations were first done on the proposed model reactions so that results could be experimentally corroborated. From the computations, a coupling pathway via a CMD mechanism was proposed (**Scheme 3-3**), illustrating a kinetically favored offshoot homocoupling pathway of thiophene to eventually yield a DMAc solvent-coordinated Pd(0) active catalyst. Additionally, as expected, preliminary energy comparisons confirmed that C-H activation at the 5-position is more thermodynamically favored than the 4-position for the monomer model. It is also reasonably seen that the presence of base is required for any C-H activation to occur, which re-directed the focus on the base's participation in these reactions. To help test some of the computational results, model reactions were run to evaluate the efficacy of Pd(0) as well as evaluate the base effects (**Table 3-2**).

The use of palladium (0) tetrakistriphenylphosphine yielded similar results to the original condition A model reaction with very high conversion of the monomer to the monosubstituited product at the 5-position, which was seen as an encouraging sign for corroborating the preliminary calculations. Base-catalyst pairings were then interchanged in order to evaluate trends with the base. It was seen that KF had an overall decreased reactivity with both palladium (II) and palladium (0) source catalysts. Overall, the effect of the base on the reaction seemed to play a more significant role than the starting catalyst species. To verify this further, a mixed reaction condition of $Pd(OAc)_2$ and KF was used in the polymerization reaction of 2-bromo-3-

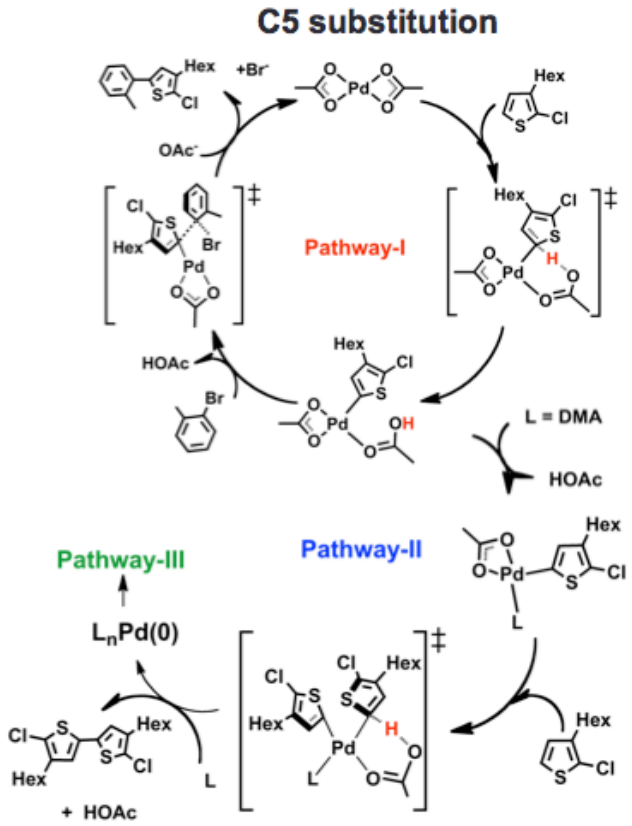

Scheme 3-3. ***Catalytic cycle proposed by Musaev group via DFT calculations for C5 substitution of the small molecule model reaction.*** *$L_nPd(0)$ is proposed to be $Pd(DMA)_2$.*

hexylthiophene, yielding a degree-of-branching of about 0.39, which is close to the degree of branching of condition B (DB = 0.4). Although this did not reconcile the lack of reactivity in the small molecule reactions, it highlighted the significance that the base has in influencing the course of the reaction.

Entry	Catalyst	Base	Conversion (%) [a]
1	$Pd(PPh_3)_4$	KOAc	> 90%
2	$Pd(OAc)_2$	KF	~ 40%
3	$Pd(PPh3)_4$	KF	~ 40%
4	$PdCl_2$	KOAc	> 90%

Table 3-2. ***Pd source and base screening.*** *[a] Conversion is the approximate ratio of mono-substituted (5-position) product to starting material via ^1H NMR integration.*

3.5 KF Clustering Computational Studies

More calculations were carried out by the Musaev group to determine how KF might be affecting reactivity. Upon developing a Pd(0) coupling pathway in the model reaction, it was observed that KF might have a potential to cluster during ligand exchange after oxidative addition of the catalyst to 2-bromotoluene in the "Ligand Exchange" regime of the reaction coordinate (**Figure 3-2**). Under a simplistic model of sequential addition of KF molecules, a continual decrease in Gibbs free energy seemed to favor a clustered arrangement (**Figure 3-3**). At six KF molecules, a barrier of over 100 kcal/mol compared to reductive elimination was

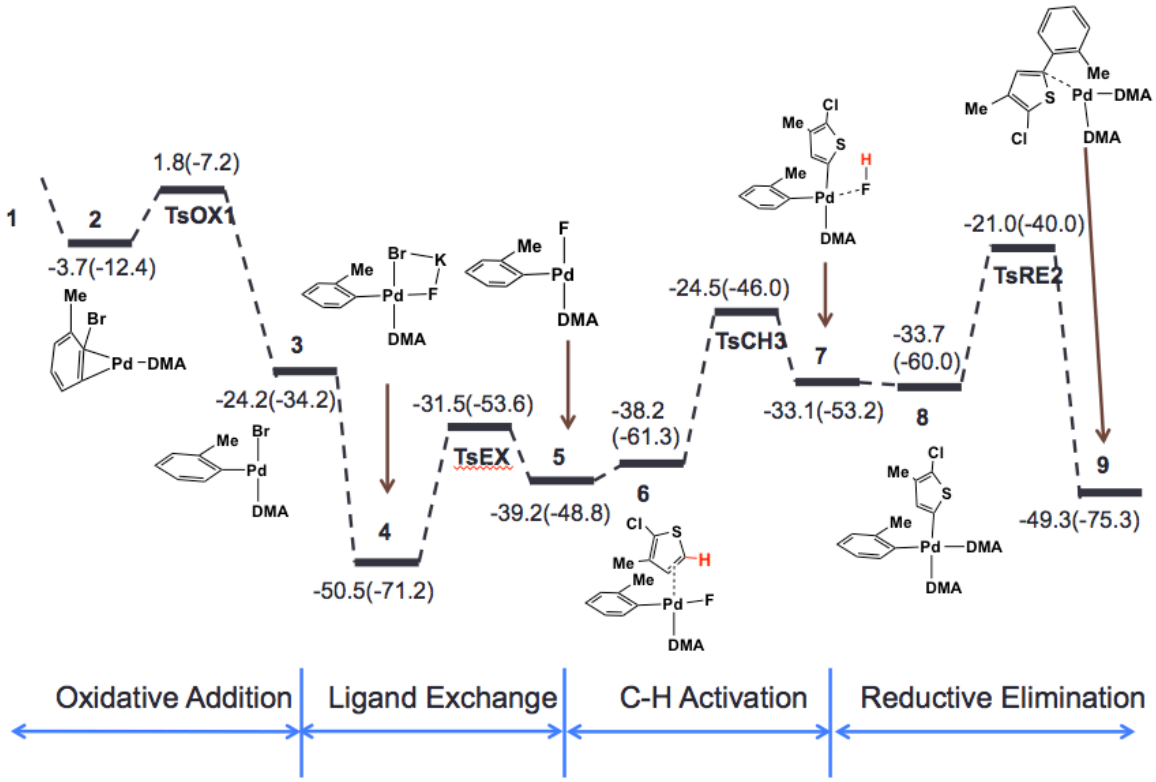

Figure 3-2. Proposed pathway III of small molecule model reaction. *ΔG(ΔH) kcal/mol. State **1** is Pd(DMA)$_2$ and 2-bromotoluene before oxidative addition. Graphic provided by Musaev group.*

calculated. This low energy state is proposed to disfavor reactivity in the model reactions with the 2-chloro-3-hexylthiophene, which might explain the overall lack of reactivity seen for condition B. Analogous clustering calculations were done for KOAc, though those results showed that multiple acetate coordination is thermodynamically neutral, which predicts less likelihood of clustering.

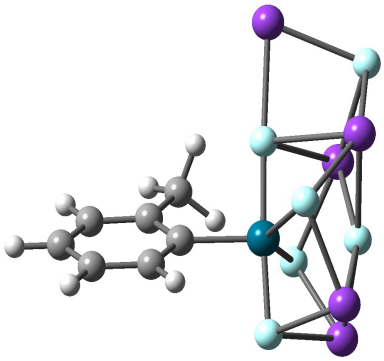

Figure 3-3. Calculated model of a six KF-clustered palladium-toluene complex during ligand exchange of pathway III. *One K is lost as KBr. There is about a 130 kcal/mol drop in free energy as compared to only one KF. Palladium is dark blue, fluoride is light blue, potassium is purple, carbon is gray, and hydrogen is white. Model provided by Musaev group.*

3.6 KF Clustering Test Reactions

To further examine the possibility of KF clustering, test reactions were performed to experimentally observe how to possibly disrupt clustering and the effect on reactivity (**Table 3-3**). Beginning with the monomer reaction, the base was changed to tetrabutylammonium fluoride (TBAF) as an alternative fluoride salt. With the relatively long alkyl chains, it was thought that TBAF would have less likelihood of clustering in the same way as KF due to the steric bulk of the cation. As a result, there was a marked increase in the amount of converted coupling product as compared to the original condition B. Another test involved the use of a chelating agent, 18-crown-6 ether, in an attempt to trap potassium ions that would disrupt the proposed clustered structure. First, a half equivalent of the crown ether was added with respect to the base, which gave more than a doubling in the conversion of coupled product to starting material as compared

to the reaction without it. This would seem to suggest that a lack of clustering may contribute to higher reactivities. Additionally, a trial was run in which a full equivalent of the crown ether with respect to the base was added and only a slight increase in coupled product conversion was observed. The current explanation for this may be due to the need for some clustering to form the active catalyst species and that chelation of the majority of KF may have an undesirable effect on reactivity. Despite the increased C-H activation, no reactivity at the 4-position was observed.

Entry	Catalyst	Base	Additive	Conversion (%)[a]
1	$PdCl_2$	TBAF	-	> 90
2	$PdCl_2$	KF	18-crown-6 (0.5 eq.)[b]	~ 40
3	$PdCl_2$	KF	18-crown-6 (1 eq.)[b]	~ 40

Table 3-3. ***Trials to prevent KF clustering.*** *Monomer model reaction was used in all cases. [a] Conversion is the approximate ratio of mono-substituted (5-position) product to starting material via ^1H NMR integration. [b] 18-crown-6-ether equivalence are with respect to the base, KF.*

These same tests with the TBAF and varying equivalents of crown ether were then performed in the polymerization reaction (see SI). There was a marked decrease in the degree of branching (DB = 0.15) of the TBAF reaction, which would be expected based on the current computational hypothesis. Decreases in DB in the crown ether reactions were not as pronounced, but there still was an overall decrease in DB with higher amounts of crown ether added (DB = 0.38 and 0.31, respectively). In general, although it appears that these additives and the

possibility of clustering have an effect on overall reactivity, the regioselectivity has still not yet been determined. It appears that an increase in 5-position reactivity occurs in these "less clustered" systems. Taking this direction and applying it towards calculations for the polymerization reaction would be the next step.

3.7 Conclusions and Future Considerations

Based on previous work in our group on C-H activated branched polythiophenes, model reactions and computational calculations were performed to try and elucidate the cause of unexpected regioselectivity in a 2-bromo-3-hexylthiophene monomer at the 5-position for condition B. Initial hypotheses correlating the reaction at the normally inactive 4-position of thiophene with increased monomer length were inconclusive when attempting to perform similar small molecule reactions with 2-chloro-3-hexylthiophene and 2-bromotoluene. Mechanistic insight with the help of computational collaborators shifted focus onto the role of the base in each reaction and it was postulated that KF might cluster around the palladium catalyst. Small molecule model reactions using either TBAF or 18-crown-6 ether in order to disrupt possible clustering showed marked increased conversion of coupling product, but still no 4-position reactivity. When applying the same reagents to polymerization conditions, a decrease in the degree of branching was observed. From these results, it appears that the model reaction substrate is not an accurate representation of the reactivity found in the monomer for the polymerization condition.

For future work, it would be interesting to take aliquots of each condition at various time points to determine both the molecular weight and the degree of branching. It would also be

interesting to synthesize linear regioregular P3HT of varying molecular weights and narrow dispersity, and then attempting to subject them to the C-H activation conditions and observe how the degree of branching is affected. If there is a correlation between the molecular weight and the degree of branching observed for a given condition, then it is possible that the reactivity is statistically related to the number of opportunities for the catalyst and additives to interact with the polymer backbone at exposed beta sites. Additionally, the trend between 18-crown-6 ether and KF loading could be further explored. In condition B, KF is used at 4 equivalents with respect to the monomer, while only up to equivalent of the chelating ether was used. Increasing the amount of the crown ether might better elucidate the importance for the K ions if indeed the DB continued to decrease.

Once this can be accomplished, it would be our aim that the synthetic toolbox for controlling polymer branching can be expanded so that it may become possible and more practical to achieve unique branched polymers for novel applications in various devices.

3.8 SUPPORTING INFORMATION

Experimental Methods

General polymerization procedure:

Polymerizations were performed in an inert nitrogen atmosphere with oven-dried glassware using standard Schlenk techniques. Exact procedures were taken from reference 80.

General small molecule reaction procedure:

All small molecule reactions were performed in an inert nitrogen atmosphere with oven-dried glassware using standard Schlenk techniques. To a Schlenk flask was added 2-chloro-3-hexylthiophene (1 mmol, 1 eq.), 2-bromotoluene (5 mmol, 5 eq.), and DMAc (4 mL). Base and catalyst were then added in the equivalence outlined in the polymerization procedure, specific to each condition. Flask was then heated to 130 °C under reflux and allowed to stir for 24-48 hr. Reaction was removed from heat and quenched with saturated aqueous NH_4Cl. Chloroform was used to extract material. Organic layer was then washed 8-10 times with DI water to remove DMAc. After rotary evaporation, crude compound was analyzed via ^1H NMR (300 MHz) to determine presence of coupling products.

Computational parameters:

Calculations were performed using Gaussian 09 and GaussView5 for visualization. M06L functional with GENECP basis set with effective core potential was used throughout all calculations.

Determination of degree of branching via NMR:

Degree of branching was determined via ^{1}H NMR as outlined in reference 80.

In short, DB was determined by NMR using integrations for the alpha methylene peaks on the hexyl chain of 2-bromo-3-hexylthiophene. The location of the shifts were obtained from previously synthesized and analyzed model polymers.

The following regions (ppm) were identified for specific types of thiophene linkages: Linear (2.65-2.90), Bent (2.65-2.38), Dendritic (2.18-2.38). Linear linkages are thiophenes reacted at the 5-position. Bent linkages are thiophenes reacted at the 4-position. Dendritic linkages are thiophenes reacted at the 4 and 5-positions. The region from 2.18-2.90ppm would estimate all repeat units of the polymers.

Degree of branching is defined as: DB = (D+T)/(D+T+L), where D are the dendritic units, T are the terminal units, and L are the linear units. (D+T+L) equals the number of all repeat units. From here, the equation was simplified to: DB = (D+T)/(All repeat units). In order to simplify the calculation such that terminal units did not need to be considered, an approximation for longer polymers, D ~ T was used. Thus, the final estimated DB = 2D/(All repeat units). These values were determined by integrating the appropriate regions in the NMR spectrum.

Entry	Catalyst	Base	Additive	DB
1	$Pd(OAc)_2$	KF	-	0.39
2	$PdCl_2$	TBAF	-	0.15
3	$PdCl_2$	KF	18-crown-6 (0.5 eq.)	0.38
4	$PdCl_2$	KF	18-crown-6 (1 eq.)	0.31

Table 3-4. ***Polymerization test reaction summary.*** *2-bromo-3-hexylthiophene was used as the substrate as in the original polymerization reaction. DB was calculated by NMR ratios as explained previously.*

Chapter 4. C-H/C-O DIRECT ARYLATION POLYMERIZATION

4.1 INTRODUCTION TO C-H/C-O COUPLING

Aside from traditional C-H/C-X type reactions, there has been exploration of C-H/C-O direct arylation with consideration for the abundance of phenol moieties that are commercially available and relatively inexpensive. The Itami group[83] has explored the coupling of benzoxazole with various aryl C-O electrophiles such as pivalate, triflate, carbamate, and mesylates (**Scheme 4-1).** They also reported the use of Ni-catalyzed direct arylation, which is advantageous over more commonly expensive metals such as Pd, Ru, and Ir. The subsequent acidic or highly polar byproducts of the reaction can be readily removed via purification. Several mechanistic studies[84,85] have shown similar intermediates as found in traditional direct arylation whereby the metal is coordinated to the carboxylate group, which is widely seen as a proton shuttle that helps activate the C-H bond via an agostic interaction. However, in this case there is no proton at the reactive phenol site and the carboxylate is directly attached to the arene. Inspired from this work, our goal was to apply this particular reaction scheme for DArP, which has yet to be shown

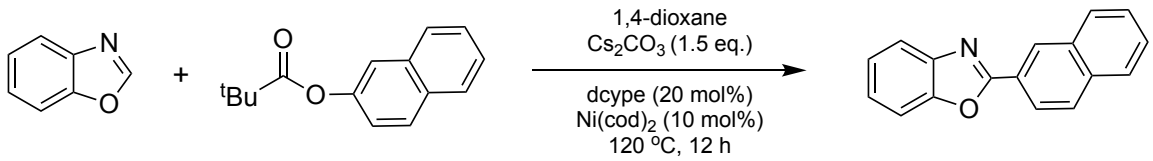

Scheme 4-1. ***Example of C-H/C-O coupling by Itami.***

4.2 Design of A-B Type Monomer for C-H/C-O DArP

Benzoxazole is an electron-deficient monomer and thus could be used as a model template for synthesizing an alternating donor-acceptor conjugated polymer. However, we first chose to focus on developing a homopolymer to simplify our scope. Rather than two monomers consisting of A-A and B-B orthogonal functionalities, we attempted to design an A-B monomer. First attempts focused on a fused ring system, drawing inspiration from Itami's previously reported small-molecule substrates (**Figure 4-1**). The aim was focused on mimicking the potential catalyst ring-walking observed via KCTP mechanism (**Figure 4-2**).[86] Ideally, after one coupling event, the subsequent Ni(0) species would not be liberated from the growing polymer and instead oxidatively add into the C-O bond of the electrophile functionality. Computational studies of Itami's original work have shown that this is a non-rate limiting intermediate stage in the reported small molecule couplings.[84] Observance of this chain-association behavior would allow for a controlled polymerization via DArP conditions, which still has not yet been reported.

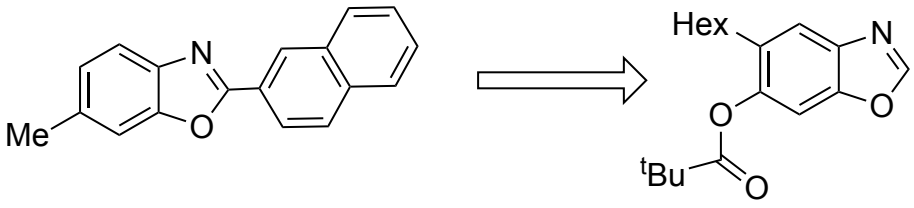

Figure 4-1. ***Coupling product reported by Itami (left) and proposed A-B monomer (right).***

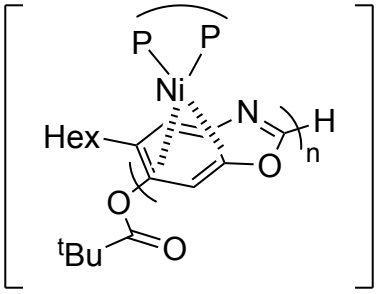

Figure 4-2. ***Possible pi-complex for catalyst ring-walking.***

4.3 Synthesis and Evaluation of Fused-Ring Benzoxzaole Monomer

The synthesis of the monomer precursor is shown in **SI, Scheme 4-5**. Choice of the triflate for the C-O electrophile resulted from its reported reactivity. Itami explored various different types of functionalities for the phenol and found that triflates were the most reactive. Generally, triflic reagents and their subsequent products are known to be quite electrophilic, which lends to their higher reactivity, but also nucelophilic sensitivity. It was important that the triflate moiety could be successfully isolated without risk of hydrolysis.

Triflation of the monomer was found successful in the presence of triflic anhydride and pyridine in dichloromethane (**Scheme 4-4**). However, subjecting the monomer to the same reaction conditions as reported in the small molecule couplings did not result in any reaction. Instead, it was observed via NMR that hydrolysis of the triflate was observed, even though the starting monomer was able to be isolated and confirmed beforehand. Thinking that perhaps the triflate group was too sensitive, the C-O electrophile was switched to pivalate. Yet again, not even oligomerization was observed under the reported conditions.

One possible reason for the lack of reactivity could be due to steric crowding. The hexyl chain is relatively close to the reactive carboxylate functionalities. When examining reported

mechanistic studies, not only are the dcype ligands quite large, but there was computational evidence of a three-Cs cluster (from the cesium carbonate base) helping to lower the barrier for C-H activation. It was observed that without the base, the CMD rate-limiting step was 34.7 kcal/mol versus 26.6 cal/mol while in the presence of the Cs-cluster.[84] Due to the length, and flexibility of the alkyl chain, this could be detrimental to either forming the oxidative addition product or in forming the subsequent Cs-cluster complex. Also apparent was that none of the other reported small molecule substrates had any large alkyl or other functional groups near the C-O electrophile site, which led to a redesign of the monomer for this polymerization system.

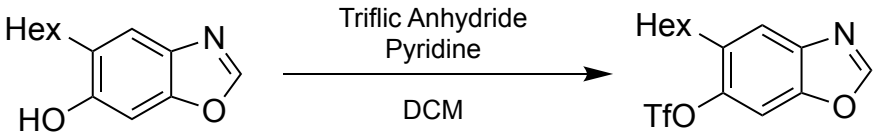

Scheme 4-2. ***Triflation of phenol group.***

4.4 Design of Non-benzoxazole Monomer

Therefore, taking into account the potential steric limitation, we again looked for inspiration from previously synthesized C-H/C-O coupling products in order to obtain proof-of-concept polymerization rather than immediately pursuing an ideal controlled synthesis. **Figure 4-3** shows the next designed monomer. The proposed monomer structure also resembles more of a donor-acceptor motif, which would be beneficial in minimizing potential homocoupling byproducts when using two co-monomers. Also of note, the intended solubilizing hexyl chain is now two positions away from where the C-O electrophile would be. Rather than immediately pursuing polymerization conditions, we looked at whether the hypothesized steric problems were

actually addressed. Our model reaction (**Scheme 4-3)** involved using just oxazole with the alkylated phenol-derivative as if the terminal end of a polymer was reacting with additional monomer. Indeed, we observed the desired coupling product as confirmed by GC-MS (**Figure 4-4**). Although this does not take into account electronic effects of the actual intended monomer, this was encouraging enough to pursue the synthesis.

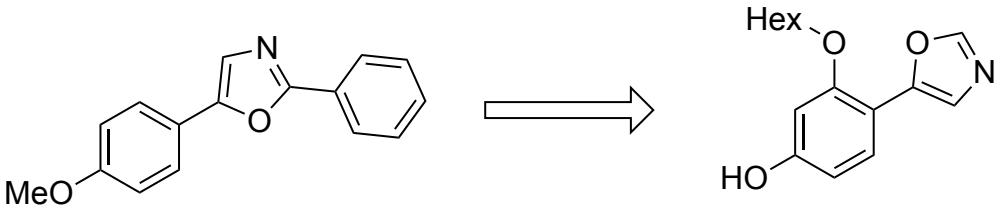

Figure 4-3. ***Reported oxazole coupling product via Itami[83] (left) and newly designed monomer (right).***

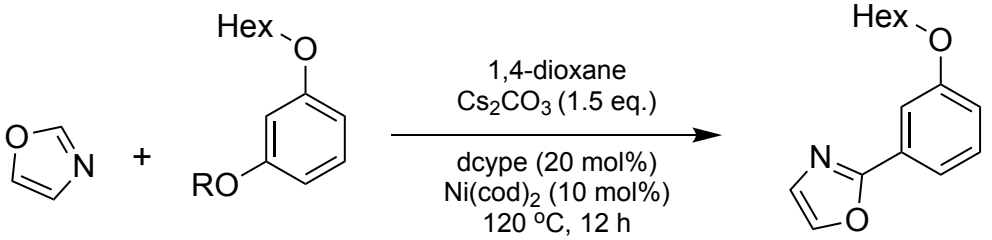

Scheme 4-3. ***Test reaction to simulate terminal ends of new monomer.***

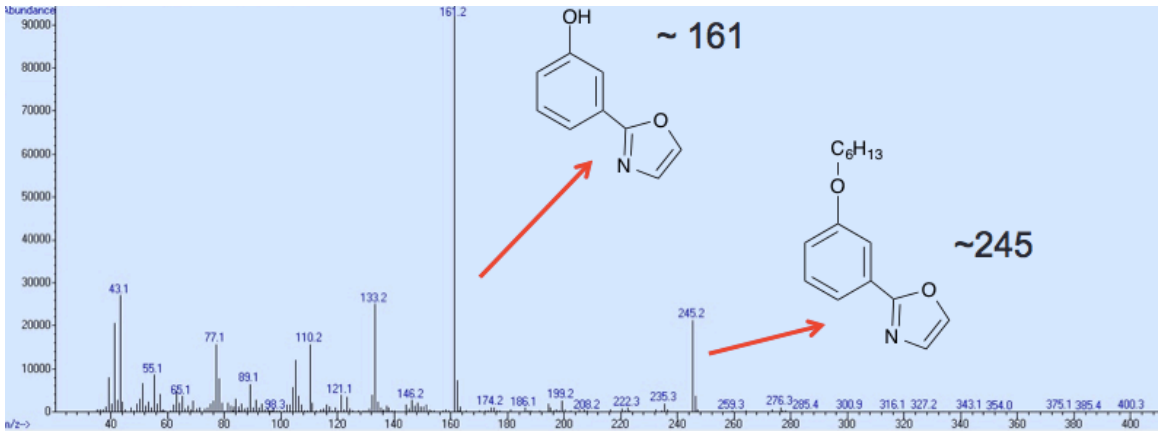

Figure 4-4. ***GC-MS analysis of successful coupling products.***

4.5 Synthesis of Oxazole-Phenol Monomer

Encouraged by the preliminary result, focus then shifted to the synthesis of the monomer. Our original synthetic route (**SI, Scheme 4-6**) planned to begin with the abundant starting material, resorcinol and included the Pd-catalyzed direct arylation of oxazole to the phenyl substrate. First, resorcinol would be selectively mono-brominated at the site of eventual oxazole attachment. Next, was the protection of the least sterically hindered alcohol via a tosylate, which would later be de-protected and transformed into another C-O electrophile at the end. This was done in planning for the eventual nucleophilic mono-alkylation in the penultimate step. Although the first two steps were successful, the attachment of the oxazole proved to be difficult. Despite the expected preferential reactivity found at the 2-position of oxazole, we did find reported conditions that could supposedly activate the 4-position of oxazole.[87] However, despite several attempts, the desired monomer was never formed.

Instead, an alternate pathway was used attempted by using classic van Leusen oxazole synthesis (**Scheme 4-4**).[88] We also decided to use the tosylate protecting group as the C-O

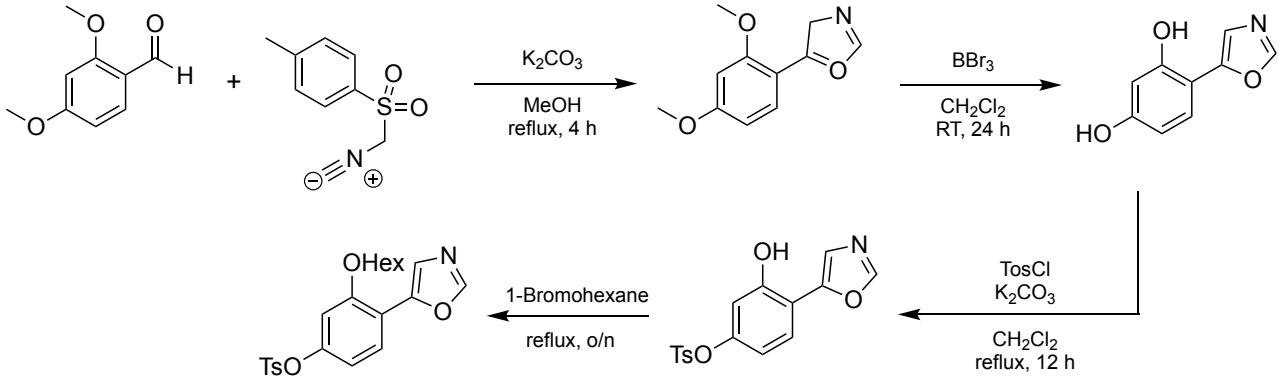

Scheme 4-4. ***Van Leusen oxazole synthesis approach.***

electrophile to eliminate additional steps as the total synthetic yield was relatively low due to the oxazole formation stage having only a 20% yield on its own. We were able to confirm product via NMR up to the dealkylation step. However, due to low yield, we were unsuccessful in achieving the final monomer structure.

4.6 Conclusion and Future Considerations

Based on the design of two monomer types, it was observed that the position of solubilizing alkyl chains may have to be considered so that they are sufficiently far from the C-O electrophile to reduce steric hindrance. For future directions, it would be of interest to explore replacement of the tosylate group with triflate to examine if polymerization occurs. Additionally, if solubility becomes an issue, it may be possible to begin the synthesis with 2,4,6-trimethoxybenzaldehyde, and attempt to append two hexyl chains, or the hexyl chain could be replaced by a branched alkane instead. Once the appropriate monomer and polymerization conditions are found, investigation of the growth kinetics would help us observe whether the Ni catalyst maintains chain association behavior. Although C-H/C-O DArP conditions would be novel and interesting, creating more complex conjugated monomer systems may be difficult due to the multi-step syntheses building from phenols. Generally, it is difficult to attach hydroxyl groups to heterocyclic arenes. Additionally, hydroxyl groups have some nucleophilic tendency, which could interfere with other pendant functional groups, ligands, or catalysts. Itami did report the use of thiazoles and benzothiazoles, which is encouraging for more commonly used conjugated monomer designs such as benzobisthiazole (BBT), however they were generally lower yielding than the oxazole varieties, which would be a hindrance in efficient polymerization.

4.7 SUPPORTING INFORMATION

Experimental Methods

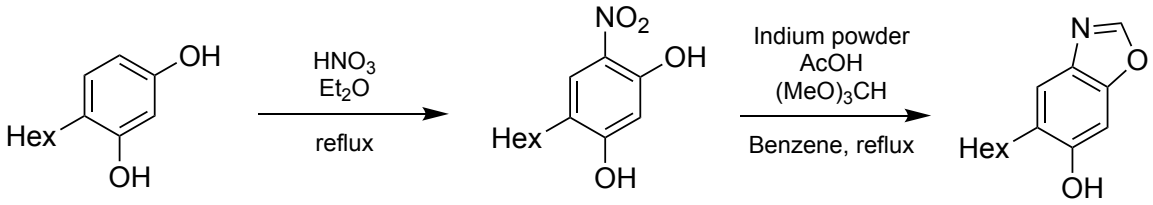

Scheme 4-5. ***Synthesis pathway for 5-Hexyl-6-hydroxybenzoxazole.***

5-Hexyl-6-hydroxybenzoxazole

Step 1:

To a Schlenk flask was added 4-hexylresorcinol (1 eq.) and anhydrous diethyl ether (0.2 M). Fuming nitric acid (1.01 eq.) was added drop wise. The solution was stirred overnight. The reaction mixture was extracted via saturated K_2CO_3 solution and chloroform. The organic layer was dried under reduced pressure and used directly in the next step.

Step 2:

The crude 2-nitro-4-hexylresorcinol (1 eq.) from step 1 was added to a Schlenk flask under nitrogen atmosphere. Anhydrous benzene (0.3 M) was added via syringe. The flask was purged under nitrogen over the course of 10 minutes. Indium powder (4 eq.), AcOH (10 eq.), and $(EtO)_3CH$ (4 eq.) were added under positive nitrogen pressure and the reaction was refluxed at 90 ^oC overnight. Reaction was extracted via aqueous work-up in dichloromethane. Product was purified via column chromatography and isolated as a pale yellow solid.

3-Hexoxyphenol

To a round bottom flask was added resorcinol (3 eq.) and bromohexane (1 eq.). Ethanol was then added to the round bottom flask (1M) as the mixture was then refluxed. Potassium hydroxide (1.1 eq.) was added in DI water (2M) and then added drop wise to the reaction. The reaction was refluxed for 3 hours. Diethyl ether was used to extract the desired compound via aqueous extraction. The organic layer was collected and dried under reduced pressure. Product was purified via column chromatography using dichloromethane and acetic acid (99:1).

1-Hexoxy-[3-(trifluromethyl)sulfonyl]benzene

To a Schlenk flask under nitrogen atmosphere as added 3-hexoxyphenol (1 eq.) with a small scoop of DMAP. Anhydrous dichloromethane (0.7M) was added followed by anhydrous triethylamine (1.2 eq.). The Schlenk flask was cooled in an ice bath for 10 minutes. Triflic anhydride (1.1 eq.) was then added drop wise to the reaction and allowed to stir overnight. The reaction mixture was extracted in three times in minimal saturated sodium bicarbonate solution and dichloromethane. The organic layer was dried via sodium sulfate and the product was eventually dried under reduced pressure. The desired product was purified via column chromatography.

2-[3-(hexoxy)phenyl]oxazole

See **Scheme 4-6**. Cesium carbonate (1.5 eq.) was added to a Schlenk tube and dried with a heat gun under vacuum. The tube was allowed to cool to room temperature before 1-hexoxy-[3-(trifluromethyl)sulfonyl]benzene (1.5 eq.) was added under positive nitrogen pressure. The Schlenk tube was brought into a nitrogen-filled glovebox where $Ni(COD)_2$ (0.1 eq.) and dcype

ligand (0.2 eq) wad added. The sealed tube was then removed from the glovebox and oxazole (1 eq.) was added followed by anhydrous dioxane (0.2M) under positive nitrogen pressure. The reaction was heated to 120 ^{o}C for 12 hours. Reaction was extracted via chloroform in saturated ammonium chloride followed by a brine wash.

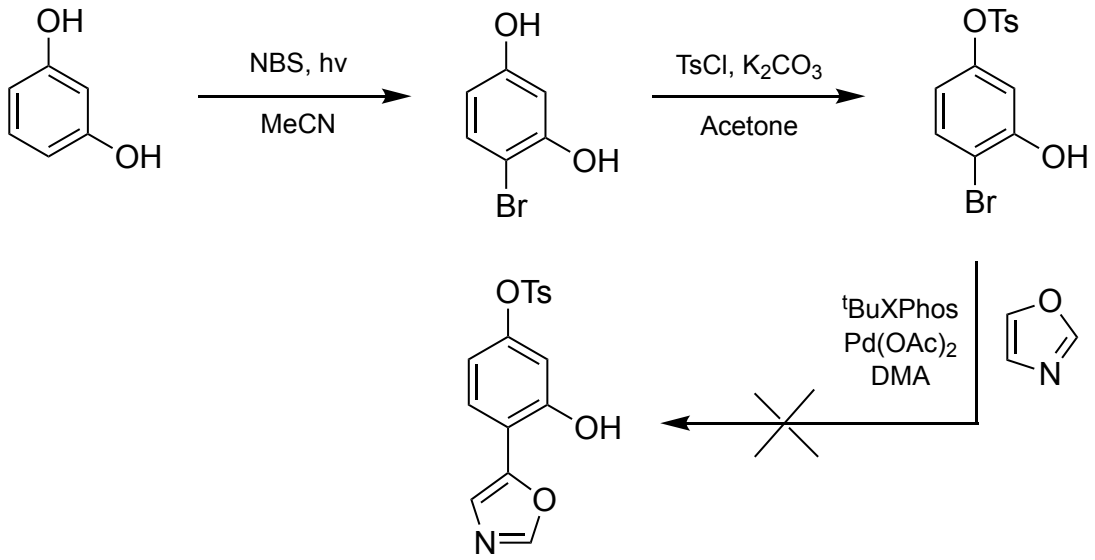

Scheme 4-6. ***Originally proposed synthesis of azole monomer using direct arylation.***

5-(2,4-dimethoxyphenyl)-oxazole

To a Schlenk flask under nitrogen atmosphere was added 2,4-dimethoxybenzaldehyde (1 eq.) and TosMIC (1.1 eq.). MeOH (0.2M) was added followed by K_2CO_3 (2 eq.). The reaction was allowed to reflux for 4 hours. After the reaction, MeOH was removed under reduced pressure. Cold water was added to the crude mixture and the following precipitate was filtered. The dried precipitate was then recrystallized in hexanes to give white needle-like crystals.

5-(2,4-dihydroxyphenyl)-oxazole

To a Schlenk flask under nitrogen atmosphere added 5-(2,4-dimethoxyphenyl)-oxazole (1 eq.) in dichloromethane (0.2 M). The flask was cooled to 0 ^{o}C and BBr_3 (2.2 eq.) was added drop wise. The reaction was allowed to warm to room temperature and was stirred for 24 hours. Aqueous extraction was performed in dichloromethane and saturated sodium bicarbonate solution. The organic layer was dried under reduced pressure resulting in light brown crystals.

Chapter 5. C-H/C-H DARP FOR DFBTA-BASED POLYMERS

5.1 INTRODUCTION TO C-H/C-H DARP

The ultimate challenge for direct arylation reactions would be the activation of two C-H bonds for C-C coupling. In terms of monomer pre-functionalization, this would be the most atom-economical pathway. However, this would also require the use of an external oxidant for regeneration of the catalyst, often used in excess. This type of direct arylation is subsequently known as oxidative direct arylation. In the most ideal case, O_2 would be used as the oxidant to give off water as a byproduct.

Although some oxidative DArP conditions have been reported for homopolymers,[89,90] including ester-functionalized thiophene,[91] exploration donor-acceptor type polymer via oxidative DArP is still lacking. The main challenge of such reaction conditions would be the selectivity of the catalyst towards a certain monomer type, and the potential variable reactivity of the subsequent dimer or trimer after the first coupling products have formed. Additionally, homocoupling can be an issue and high loadings of one monomer with respect to another are often employed, which is effectively wasteful and counterproductive towards sustainability. Larossa reported that tuning the oxidation state of gold can be used to selectively activate arenes with differing electronic character. Gold(I) was found to activate electron rich species, while gold(III) preferentially activated electron deficient arenes.[92] By using excess oxidant, they were able to continually switch the redox state of the gold to continue the cross-coupling. Later, it was also found that silver pivalate was an important additive, not acting exclusively as an oxidant, which allowed for gold-catalyzed oxidative direct arylation.[53] In this case, the oxidant was a hypervalent iodine compound.

5.2 Motivation For Applying DArP to DFBTA

Li and coworkers published the synthesis of a donor-acceptor polymer consisting of a difluorobenzotriazole moiety (DFBTA) (**Scheme 5-1, 3**) and a benzodithiophene-moiety (BDT) with a conjugated thiophenyl side chain.[93] Their aim was to study 2-D conjugated polymers that have exhibited red shifted absorption and higher hole mobilities. Between the donor (BDT) and acceptor (DFBTA) unit, was added a thiophene pi-bridge. Because the conjugated thiophene side chain on the BDT was also alkylated, the pi-bridges were needed as spacers to reduce hindrance of adjacent alkyl chains. They found this contributed to the planarity of the polymer while being able to maintain conjugation along the main chain. Another effect found was the lowering of HOMO levels, which added to the polymer's chemical and thermal stability. Since then, difluorobenzotriazoles have been incorporated into donor acceptor molecules via direct arylation.[94,95]

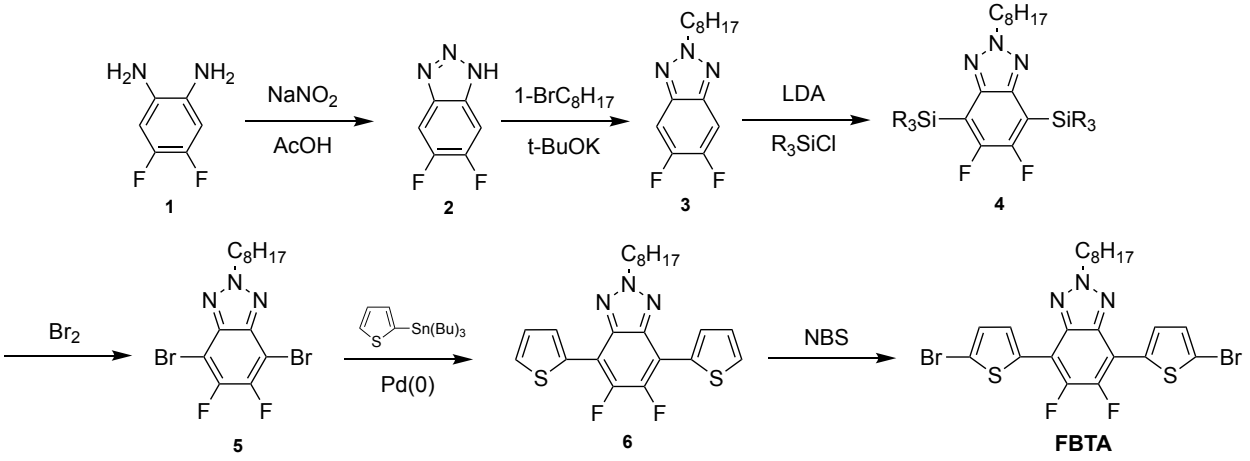

Scheme 5-1. ***Reported difluorobenzotriazole-derivative (FBTA) synthesis.***[93]

However, implementation of oxidative DArP has yet to be explored. It was our aim to use this DFBTA monomer and co-polymerize with 3-hexylhiophene in the hopes of making a donor-acceptor polymer. The reaction scheme for the reported synthesis of the DFBTA monomer is

shown in **Scheme 5-1**. It is apparent that through oxidative DArP methodology, at least six synthetic steps or subsequent purifications would be bypassed, with two of those steps including the bromination and subsequent stannylation of the thiophene precursor to make compound **6**. This step-savings would be non-trivial when considering the synthetic complexity for scalability. The toxicity, reactivity, and sensitivity of some of the reagents employed in the original synthesis are also of potential concern such as the lithiation agent and organotin compound. Therefore, our goal was to start from **3** and apply direct arylation.

5.3 DFBTA Synthesis and General Reaction Screening

Being a fused ring structure, an octyldodecyl alkyl side chain was chosen to enhance the solubility. Based on previous reports of silver as an oxidant in oxidative direct arylation reactions,[94,95] Ag_2CO_3 was used as the stoichiometric oxidant along with $Pd(OAc)_2$ catalyst in the presence of base. From past P3HT DArP conditions,[96] we expect that thiophenes will readily undergo homocoupling in basic conditions with Pd catalysts, so competitive coupling between the co-monomers would likely occur. To mitigate the occurrence of thiophene homocoupling, an excess equivalent up to 4:1 of the 3-hexylthiophene to DFBTA was used.

Initially, small molecule studies were performed to screen for the most reactive conditions (SI, **Scheme 5-5**). This involved using 2-bromo-3-hexylthiophene as the coupling partner in order to limit the products to trimeric species at most. Various thiophene loadings, catalysts, and temperatures were attempted **(SI, Table 5-1).** The goal was to quickly screen reactivity by qualitatively finding conditions that did not yield thiophene homocoupling. In all cases, homocoupling was observed via NMR by looking formation of dimer peaks. The yield and extent of co-monomer coupling was not analyzed in detail.

5.4 POLYMERIZATION TRIALS

Two polymerization trials were performed using varying equivalents of the 3-hexylthiphene (HexThp) (and DFBTA monomers (**Scheme 5-2**). The independent variable chosen was the loading of either monomer. One condition contained 4 equivalents of HexThp with respect to DFBTA, while the other condition used 4 equivalents of DFBTA with respect to HexThp. For the case with 4 equivalents of the thiophene, only P3HT was observed (**SI, Figure 5-2**). When the equivalence ratio was switched and DFBTA was used in an

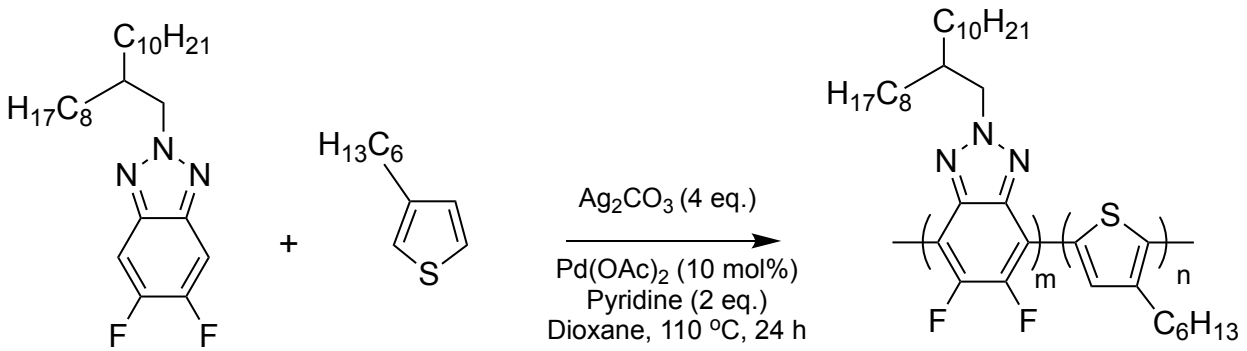

Scheme 5-2. ***DFBTA polymerization trials.***

excess of 4 equivalents, there appeared to be both P3HT and the presence of chains with DFBTA incorporation up to 3 kg/mol. By looking at MALDI-TOF mass spectrometry, the number of DFBTA incorporation was estimated (**SI, Figure 5-3**). Only 1 DFBTA monomer appeared to be incorporated in the series of lower intensity MS signals. Although not ideal, the result is unsurprising based off of the prevalence of thiophene homocoupling in the small molecule studies. As predicted, unbalanced competitive reactivity between the two co-monomers likely hampered the incorporation of the DFBTA unit. Another potential problem could arise from the steric hindrance of the hexyl chain of the thiophene. If the octyl-dodecyl interfere with the hexyl

chain, it might be difficult to obtain a perfectly alternating sequence. It would seem like the most sterically permissive configuration between the DFBTA and hexylthiophene would be that shown in **Figure 5-1**, where the linked hexylthiophenes would be in a head-to-head conformation. Control of the regioselectivity of the thiophenes would be difficult over the course of the polymerization.

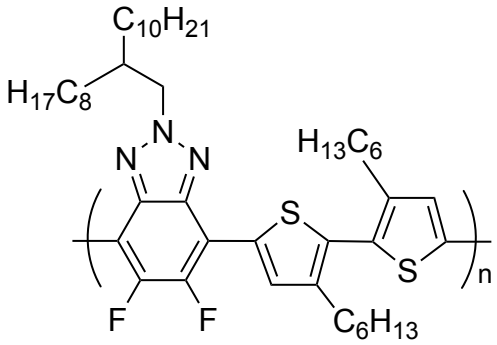

Figure 5-1. ***Proposed connectivity for least steric hindrance between co-monomers.***

5.5 Conclusions and Future Considerations

At least for the system using Ag_2CO_3, it appears that this system favors the more electron-rich monomer, 3-hexylthiophene. This would preclude the possibility of synthesizing polymers with any meaningful distribution of both monomers and certainly not perfectly alternating. In retrospect, it appears that trying to find a single set of conditions, namely a single catalyst, in order to react indiscriminately with two electronically different monomers is quite a difficult task. The Blakey group at Emory shared conditions with us they had used for small molecule coupilngs, which replaced the Ag oxidant with a TEMPO and $CuOAc_2$ system (**SI, Table 5-2**). No homocoupling of thiophene was observed, which was the first set of conditions we observed to show such results (**SI, Figure 5-4**). Polymerization studies have yet to be tested

or examined using these conditions, but perhaps this motif could be used as a basis for probing future DArP work.

A mechanism by which monomer selectivity could be tuned in-situ would allow for orthogonal reactivity and potentially better incorporation of each monomer. The oxidative direct arylation reports featuring a gold (I) and gold (III) system, whereby the oxidation state of the gold controls the selectivity for electron deficient or electron rich species, respectively, might be useful in this case. Despite the atom-economical attractiveness of oxidative DArP, low yields, high monomer loadings, lack of selectivity, and type of stoichiometric oxidant are all issues that still have yet to be fully elucidated.

5.6 SUPPORTING INFORMATION

Experimental Methods

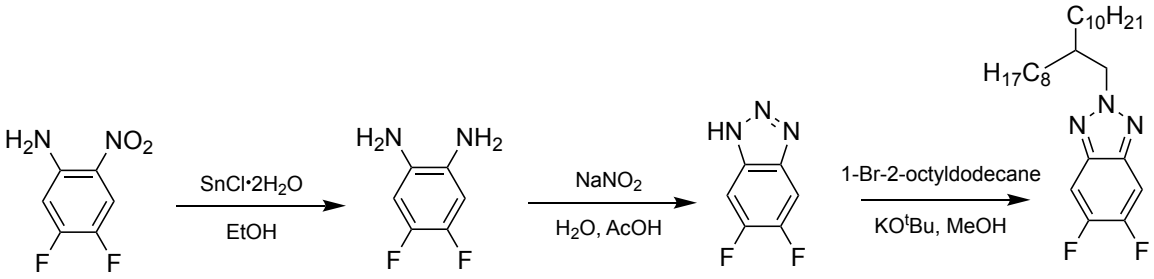

Scheme 5-3. ***Synthetic scheme of DFBTA monomer.***

DFBTA

The procedures found in reference 92 were used to synthesize the DFBTA monomer. Bromooctane (from the original procedure) was replaced with 1-bromo-2-octyldodecane.

1-bromo-2-octyldodecane

To a round bottom flask was added 2-octyl-1-dodecanol (1 eq.) in dichloromethane (2M) at 0 ^{o}C. After stirring for 5 minutes, PPh_3 (1.5 eq.) and NBS (1.5 eq.) were added. The reaction was stirred for 1 hour. Product was purified via silica plug to give a faintly yellow oil.

General small molecule procedure:

To a Schlenk flask under nitrogen atmosphere was added DFBTA (1 eq.). The flask was purged via nitrogen over the course of 10 minutes. 2-bromo-3-hexylthiophene (BrHexThp) was used as the coupling partner to prevent polymerization. All remaining reagents were added followed by the corresponding solvent. See **Table 5-1** and **5-2** for exact reaction conditions. Reaction mixture was worked up via aqueous extraction in dichloromethane. Results were qualitatively analyzed via NMR to observe the presence of thiophene dimerization.

General polymerization reaction conditions:

To a Schlenk flask under nitrogen atmosphere was added DFBTA. The flask was purged via nitrogen over the course of 10 minutes. 3-hexylthiophene and all other reagents were added under positive nitrogen pressure and anhydrous solvent was added via syringe. See **Scheme 5-2** for exact conditions. One trial was carried out with 4 equivalents of DFBTA with respect to 3-hexylthiophene, and another trial was carried out with 4 equivalents of 3-hexylthiophene with respect to DFBTA. This was to done to observe the optimal incorporation of DFBTA units. Polymer was quenched with 5M HCl and suspended in methanol, followed by gravity filtration. The reaction was then washed via acetone before analysis via MALDI-TOF MS.

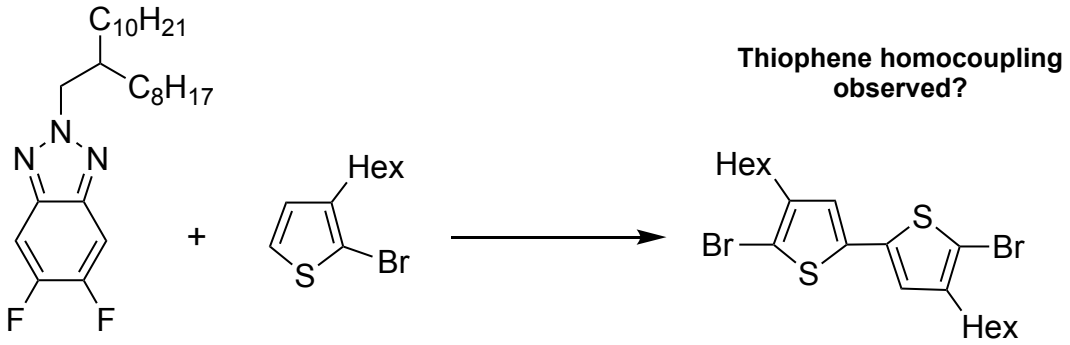

Scheme 5-4. ***Small molecule coupling conditions to observe thiophene homocoupling.***

Entry	BrHexThp (eq.)	Conditions (1 eq. DFBTA, 80 °C, 24 h)
1	4	$Pd(OAc)_2$ (5%) , Ag_2O (4 eq.), DMSO
2	4	$Pd(TFA)_2$ (5%), Ag_2O (4 eq.), DMSO
3	2	$Pd(TFA)_2$ (5%), Ag_2O (2 eq.), DMSO
4	4	$Pd(TFA)_2$ (5%), $AgNO_3$ (4 eq.), DMSO
5	4	$Pd(TFA)_2$ (5%), Ag_2CO_3 (4 eq.), DMSO
6	4	Repeat 2 at 100 °C
7	4	$Pd(TFA)_2$ (5%), Ag_2CO_3 (4 eq.), $(C_6H_{11})_3P \cdot HBF_4$ (10%), DMSO
8	4	$Pd(PPh_3)Cl_2$ (5%), $AgNO_3$ (4 eq.), DMSO
9	4	$Pd(TFA)_2$ (5%), AgF_2 (4 eq.), $P(Cy)_3$ (10%), DMSO
10	1	$Pd(TFA)_2$ (5%), AgF_2 (4 eq.), $P(Cy)_3$ (10%), DMSO

Table 5-1. ***Qualitative thiophene homocoupling trials.*** *All trials showed thiophene homocoupling via NMR.*

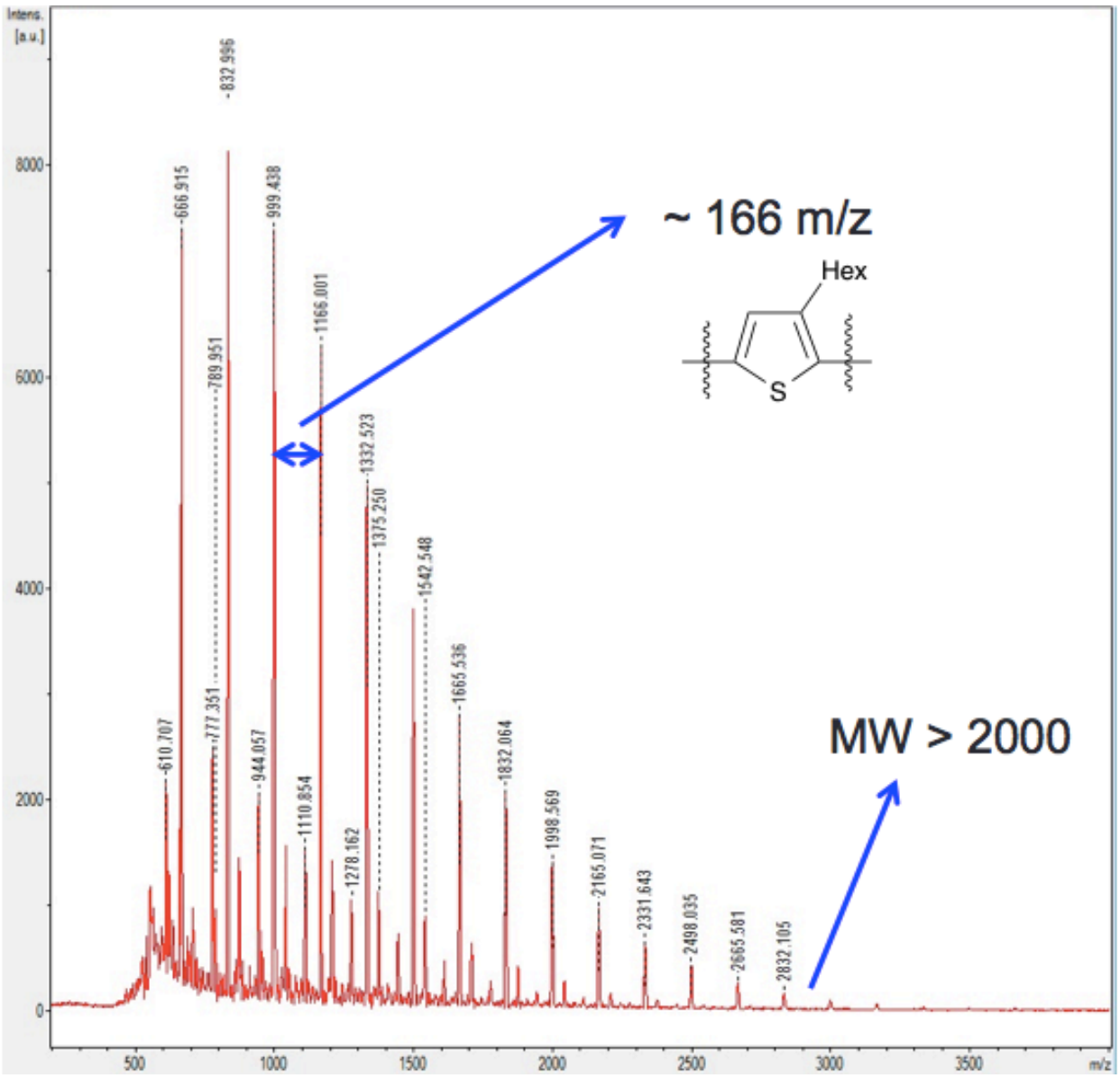

Figure 5-2. MA*LDI-TOF MS for DFBTA (1 eq.) and HexThp (4 eq.) polymerization trials.*

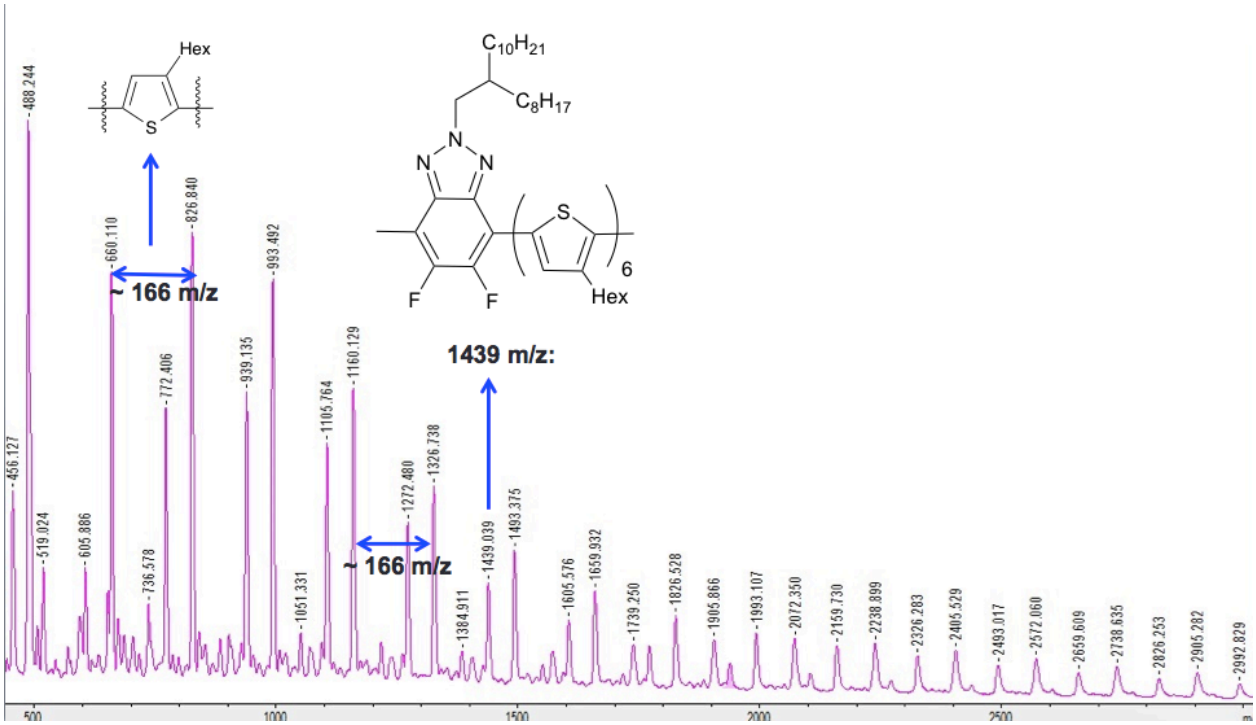

Figure 5-3. ***MALDI-TOF MS for DFBTA (4 eq.) and HexThp (1 eq.) polymerization trials.***

Estimation of DFBTA Incorporation:

Taking the peak at 1439 m/z as an example, we subtract the molar mass of one DFBTA unit, then divide by the molar mass of a 3-hexylthiophene unit. Accounting for the 2 terminal protons, about 6 hexylthiophenes are estimated to be incorporated with one DFBTA unit.

$$\frac{(1439_{Total} - 435_{DFBTA} - 2_{Terminal\ H})}{166_{HexThp}} \sim 6\ hexylthiophenes$$

Entry	Conditions (1 eq. DFBTA, 4 eq. BrHexThp, 110 °C, 24 h)	Thiophene Homocoupling Observed
1	$Pd(TFA)_2$ (5%), TEMPO (1.5 eq.), $Cu(OAc)_2$ (0.1 eq.), DMSO	No
2	$Pd(OAc)_2$ (2.5%), PPh_3 (0.25 eq.), TEMPO (1.5 eq.), $Cu(OAc)_2$ (0.1 eq.), Pyridine (1 eq.), DMSO	Yes

Table 5-2. ***TEMPO oxidant conditions.***

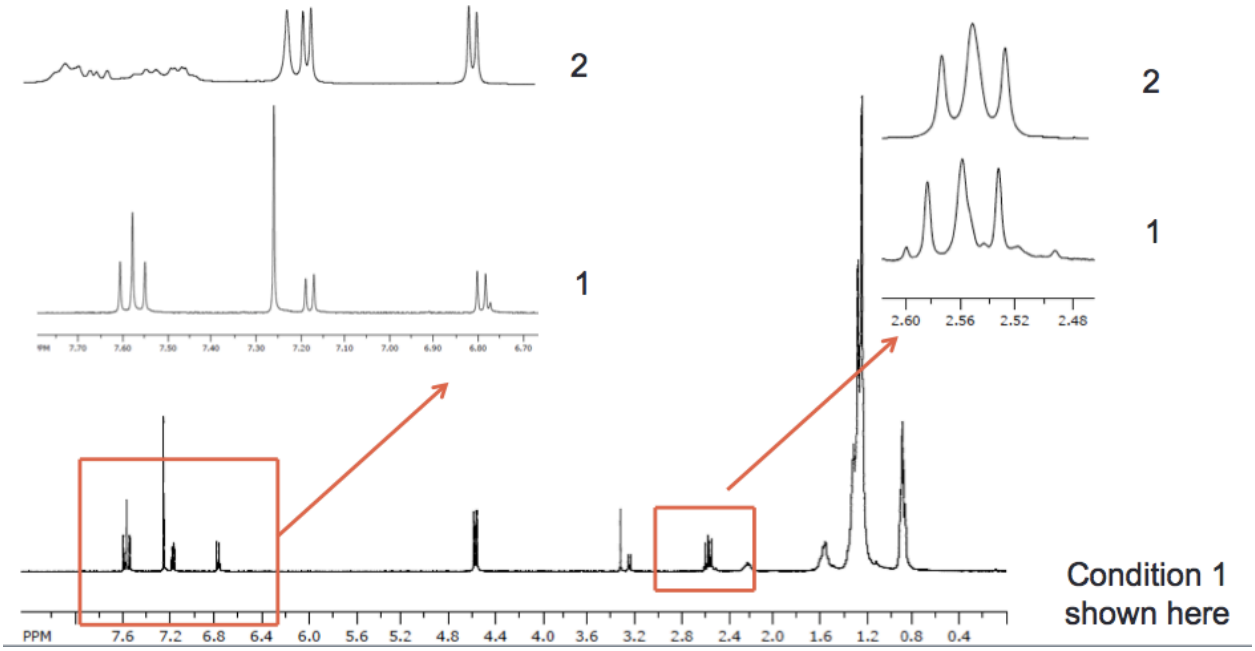

Figure 5-4. ***TEMPO conditions showing 2-bromo-3-hexylthiophene homocoupling (condition 1) and without homocoupling (condition 2).***

Chapter 6. DUAL-METAL GOLD-PALLADIUM DARP OF P3HT

6.1 INTRODUCTION

As stated previously, DArP presents a promising long-term solution towards more environmentally responsible synthetic methods. If we are to look towards novel materials to advance technology and potentially green energy, it does not seem amenable to involve complex polymerization schemes with little consideration for atom economy. Such traditional methodologies, in effect, augment existing problems related to the burden of industrial waste. However, direct arylation reactions have yet to overtake classical coupling reactions as widespread practice in the research community, especially with regards to materials chemistry. For the purpose of polymers, traditional DArP based on small molecule reactions has limitations affecting growth kinetics and characteristics that are unfavorable for reproducibility and control.

Specifically looking at P3HT, the KCTP mechanism that was previously described is a robust and established living polymerization method, albeit reagent-sensitive due to the water-reactive Grignard active species. Traditional DArP cannot yet achieve such characteristics because unlike KCTP, DArP proceeds via step-growth polymerization kinetics. This is inherent in the understood CMD mechanistic pathway of direct arylation reactions. Step-growth leads to higher batch-to-batch variation, lack of control over the molecular weight, and increased dispersities. When considering the reproducibility of device performance, these issues must be resolved. It would be beneficial to address some of these problems in the hopes of eventually developing DArP methodology that could be not only novel but also competitive with existing and tested techniques.

To do this, analogous characteristics of KCTP should be used as a model towards advancing DArP. Our goal is to use a mono-halogenated alkylthiophenes, namely, 2-bromo-3-hexylthiophene, as opposed to the widely used 2,5-dibromo-3-hexylthiophene or the more selectively reactive, but synthetically more complex, 2-bromo-5-iodo-3-hexylthiophene. This will limit the amount of halogenation reagents required. The 5-position will undergo C-H activation and one Br will contribute to retaining regioselectivity of the monomers as well as provide a site for the catalyst species to oxidatively add during the growth of the polymer chain.

6.2 Design of Novel DArP Methodology

To design a new DArP system, analysis of the important steps in the polymerization should be considered. The most important aspect is the activation of the C-H bond in the 5-position of 2-bromo-3-hexylthiophene, which will replace the previously required halogenation step. Additionally, this will also replace the necessity for the Grignardization since the halogenation is essentially pre-activation for the Mg reagent, which gives the active Grignard monomer that participates in the polymerization. It would be necessary to find one metal to both C-H activate and form a metastable metalation of thiophene.

Next, we should consider finding a metal that facilitates C-C coupling. In the case of KCTP, a Ni(II) catalyst or Ni(II)-based external initiator[97–99] are commonly used for a controlled polymerization. From this, we can see that two different metals will be necessary for an analogous KCTP system, whereby one metal (Mg) is necessary for activating the thiophene monomer and one metal is required to carryout carbon-carbon bond formation. Ideally, both metals would have orthogonal reactivity towards the monomer to give predictability and reproducibility for the conditions.

With these considerations in mind, we sought to develop a dual-metal DArP system that would mimic the growth of KCTP. To this point, no such DArP conditions have been reported. The most significant challenge in such a system is identifying the compatibility between metals, orthogonal reactivity towards the monomer, and reasonable stability and reaction kinetics.

6.3 Au as a C-H Activating Agent

We were encouraged by the previously described C-H auration of arenes and heteroarenes from gold chloride complexes showing that 2- and 3-bromo thiophene undergo auration with chloro(tri-*tert*-butylphosphine)gold(I), **3**, in the presence of NaOH in dioxane.[51] We discovered that a similar procedure is applicable for 2-bromo-3-hexylthiophenes as well (**Scheme 6-1**). Therefore, **1** was reacted with **3** in the presence of NaOH in dioxane at 50 °C affording **2** in 82% yield after 48 h. Moreover, in order to match the reaction conditions of the C-H activation with those in P3HT chain growth polymerizations more closely, we also explored THF as solvent, which gives good solubility of P3HT up to high M_n. Using NaO*t*-Bu as a base yielded a conversion of 75%.

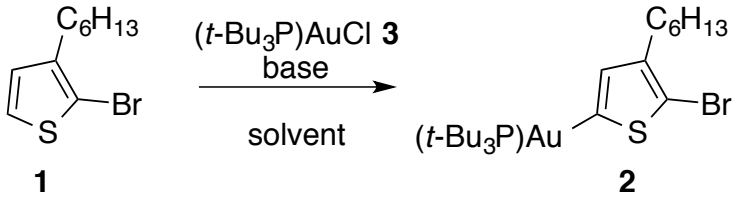

1 **2**

A: 1 / **3** / NaOH (2 : 1 : 2) in dioxane; 50 °C, 48h
B: 1 / **3** / NaO*t*-Bu (2 : 1 : 4) in THF; 60 °C, 17h

Scheme 6-1. ***Synthesis of monomer 2-bromo-3-hexyl-thienyl-5-gold(I) via C-H activation.***

Although the 5-position would be expected to react preferentially, it was possible to have some reactivity at the 4-position. To confirm the identity of **2**, we attempted a more traditional approach to synthesize it using organometallic reagents.[48,49] 2-bromo-3-hexyl-5-iodothiophene was reacted with isopropylmagnesium chloride in the presence of lithium chloride in THF. Transmetalation of magnesium by gold was achieved with the addition of chloro(tri-*tert*-butylphosphine)gold(I) to the Grignard solution. **2** was obtained in 93% yield and was purified by vacuum distillation prior to the following polymerization experiments to remove any remaining thiophene precursor. This monomer maintains stability through both aqueous work-up as well as storage in air for at least several days. High stability of the activated monomer is an advantage over Grignard species that must be kept in strictly anhydrous solvents and reagents while commonly running under inert gas atmosphere. The ability to generate and handle an activated monomer with less stringent conditions could limit unpredictably due to varying levels of dryness during batch conditions. However, when examining the compound by NMR, protodeauration was observed by using as-purchased $CDCl_3$, which was indicative of minor acidic species in the deuterated solvent. Subsequently, all $CDCl_3$ was passed through basic alumina and no Au cleavage was observed. Although the reaction temperature is above room temperature used in KCTP, it is still considerably lower than previously reported DArP conditions running at reflux above 100 ºC.

6.4 Pd-Catalyzed DArP of P3HT

Polymerization of the organogold monomer **2** was performed at 60 °C in THF in order to provide good polymer solubility and prevent precipitation of P3HT from the solution during the

reaction. The use of Pd as the catalyst was based on literature precedent of Pd-Au transmetalation.[100–103] Prescreening of different commonly used Pd catalysts showed that neither $Pd(PPh_3)_2Cl_2$ nor combinations of $Pd_2(dba)_3$ with P^tBu_3 or dppp ligands gave good reactivity since only short oligomers were obtained. In contrast, PEPPSI-iPr showed very good performance in polymerization of monomer **2** and was used for all further experiments (**Scheme 6-2**).

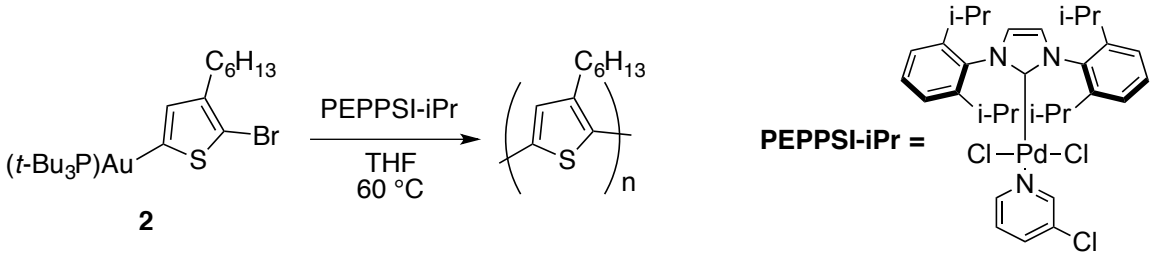

Scheme 6-2. Polymerization of Au-Thiophene monomer. *Reaction was stirred for 4-6 h and quenched with an excess of 2 M HCl solution.*

6.5 Molecular Weight Control

A series of polymerizations were conducted in order to gain insight into the reaction behavior. First, the monomer-to-catalyst ratio was altered to look at the relationship of loading to molecular weight. Four different reactions with 1, 2, 3, and 5 mol% PEPPSI were performed (**Table 6-1**). The number-average molecular weight M_n of the resulting P3HT was determined by GPC and ^1H NMR. Based on previously reported characterization and M_n determination via NMR[13] through end-group analysis, the degree of polymerization was found by comparing the integration of the thiophenyl end group peaks found at 6.825 ppm and 6.9 ppm to the main chain

thiophenyl peak at around 7.0 ppm.[13] Two end group proton signals were used in the estimation of the degree of polymerization to account for the presence of both H/H and H/Br terminated P3HT, as discussed below (See **SI**). The obtained values are in remarkable agreement with the theoretical molecular weight, M_n^{th}, expected for a controlled chain growth polymerization, where the Pd catalyst stays associated with the growing polymer chain.

Entry	PEPPSI-iPr (mol%)	M_n^{th} (g/mol)	M_n^{GPC} (g/mol)	M_n^{NMR} (g/mol)	$M_{n\_2ndAdd}^{NMR}$ (g/mol)[a]	Đ
1	5	3300	3500	3000	-	1.01
2	3	5500	4100	4200	10400	1.20[b]
3	2	8300	10150	10800	-	1.32
4	1	16600	14500	17400	-	1.31

Table 6-1. ***Theoretical and observed M_n at various PEPPSI-iPr catalyst loadings.*** *(a) A second equivalent of monomer was added before quenching to observe continuation of chain growth mechanism. (b) Dispersity in table corresponds to the final polymer after second monomer addition. Before second monomer addition, Đ = 1.04.*

6.6 Determination of Chain Growth

To further investigate the kinetics of the polymerization, we took a closer look at the relationship between M_n versus monomer conversion over the course of the reaction. Aliquots were taken during the course of the polymerization and the M_n was determined by size-exclusion chromatography (SEC). Monomer conversion was monitored via gas chromatography mass

spectrometry (GCMS) using tetradecane as an internal reference. The expected curve for a step growth mechanism would show low M_n at lower to moderate monomer conversion followed by a

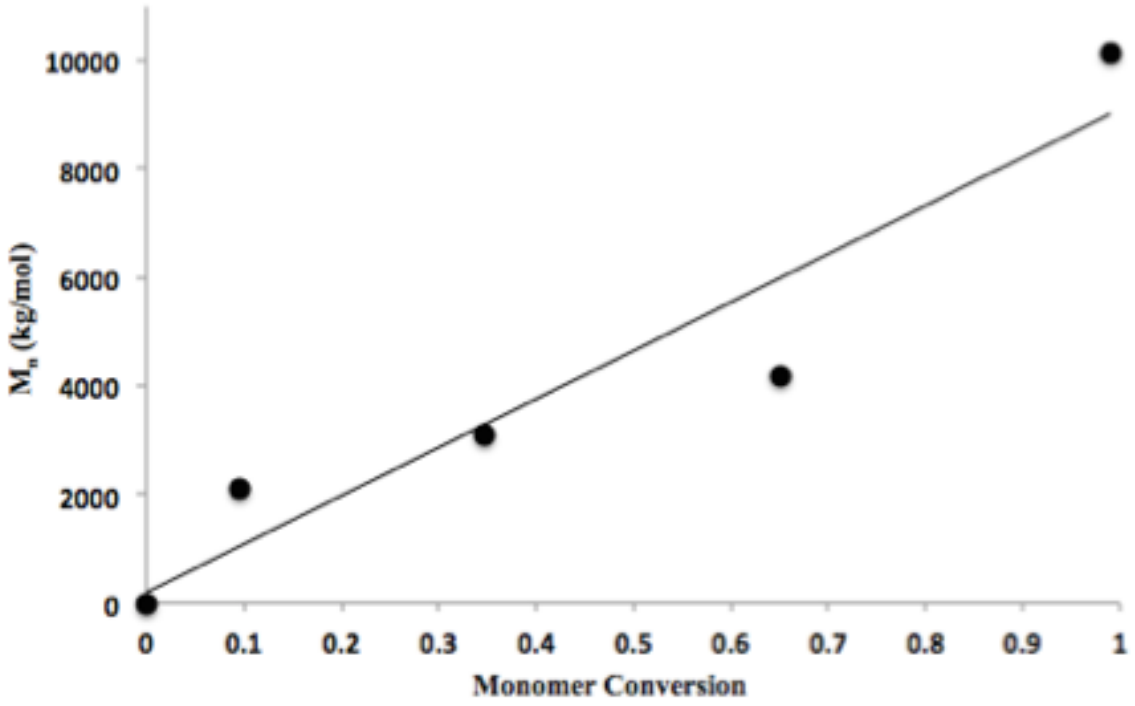

Figure 6-1. ***M_n^{GPC} values for P3HT as a function of monomer conversion.*** *Conversion was determined by GCMS with tetradecane as a reference. PEPPSI-iPr catalyst loading at 2 mol%.*

steep increase in M_n towards complete conversion, signifying the combination of various oligomers. For a polymer exhibiting a controlled chain growth mechanism, a linear relationship is expected between M_n and monomer conversion from onset to completion, suggesting single catalyst association to a single polymer chain. **Figure 6-1** depicts the correlation of monomer conversion and M_n for the polymerization of **2** with 2 mol% PEPPSI-iPr showing a linear relationship and strongly suggesting a controlled chain growth polymerization mechanism.

Additionally, dispersities of aliquots at various monomer conversions showed relatively low values throughout the duration of the polymerization (**Figure 6-2**).

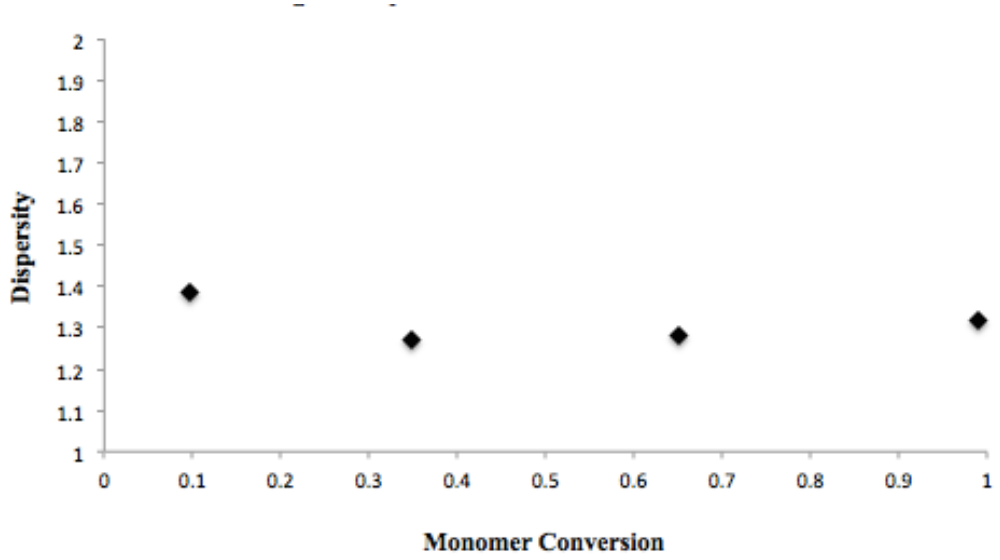

Figure 6-2. ***Dispersity versus monomer conversion at 2 mol% PEPPSI-iPr loading as determined via GPC.***

6.7 Chain Extension Experiments

To further investigate the possibility of a living polymerization occurring, further monomer addition was performed to check if the polymerization could be re-initiated after monomer conversion approached full consumption. Such behavior would suggest true chain association of the catalyst. After completion of the polymerization of **2** in the presence with 3 mol% PEPPSI-iPr was observed by GCMS, a second equal equivalent of monomer **2** was quickly added to the reaction mixture and polymerized further (**Table 6-1, entry 2**). By checking

the M_n, it was seen that indeed addition of another equivalent of monomer proceeded to further polymerize and increase the molecular weight of the previous polymer. Ideally, addition of the

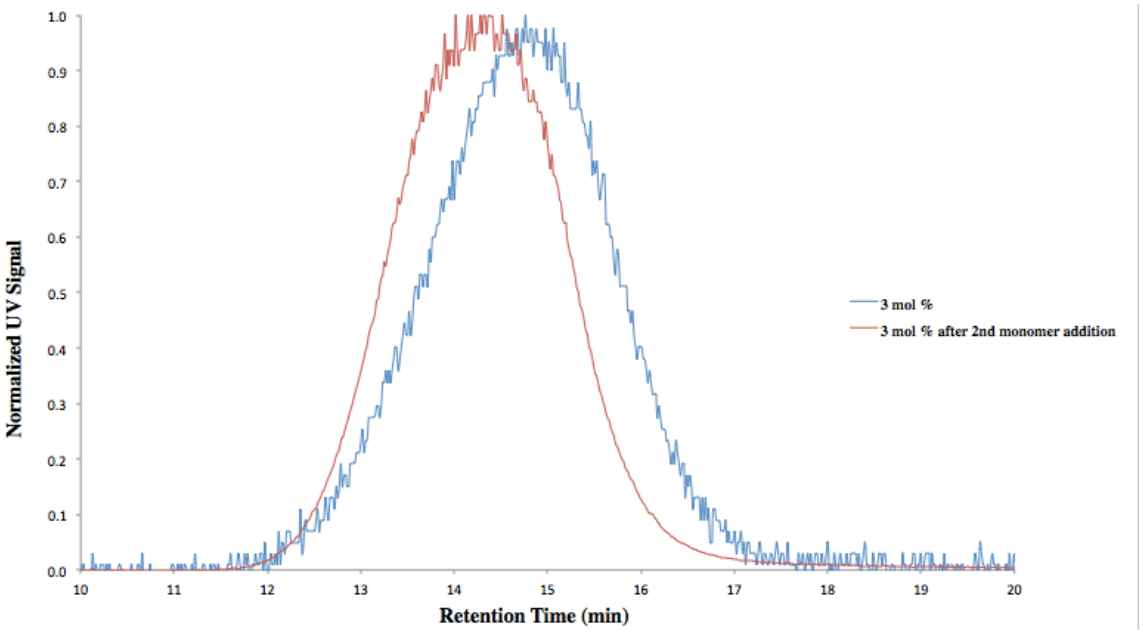

Figure 6-3. ***SEC analysis of 3 mol% PEPPSI-iPr chain extension trials.***

second monomer equivalent should approximately double the theoretical M_n relating to the starting catalyst loading amount. Starting with 3 mol% of catalyst loading, a second equivalent of monomer effectively reduced the catalyst loading to 1.5 mol%, and the result closely matches this value. SEC analysis of an aliquot before addition of the second equivalent of monomer showed a trace with a peak retention time of 14.9 minutes. After the second equivalent was added, the peak retention time shift to 14.3 minutes (**Figure 6-3**). Shorter retention time is expected for linear polymers of longer molecular weight via SEC.

6.8 End-group Analysis

End-group analysis was performed using MALDI-TOF mass spectrometry. It was observed that the major termination pattern for these polymerization reactions was H/H with a smaller distribution of H/Br patterns closer to the lower molecular weight region (**Figure 6-4**).

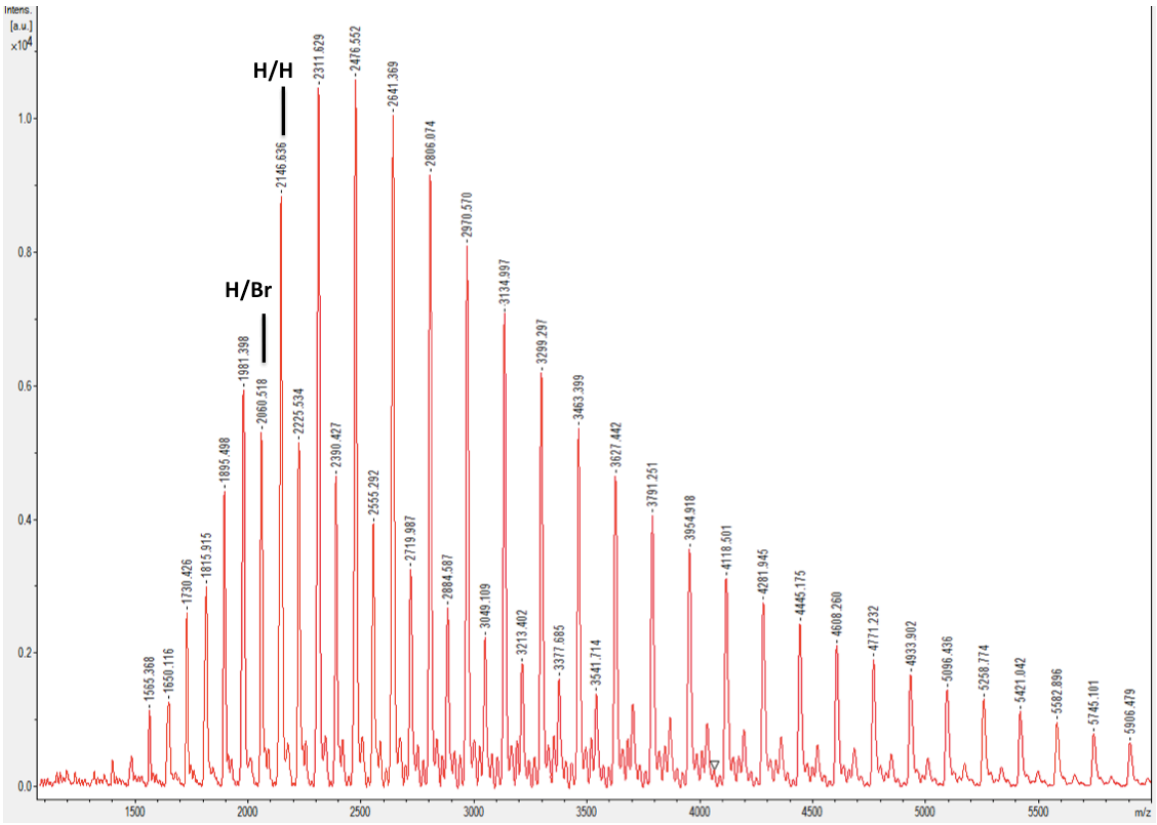

Figure 6-4. ***MALDI-TOF MS end-group analysis of P3HT via Au/Pd DArP.***

This observation is in contrast to traditional KCTP-type polymerizations, which exhibit major H/Br termination, arising from the known mechanism of initiation by the transmetalation of two thiophenes and subsequent acid quenching (**Scheme 6-3**). Although H/Br termination is one

possible indication of catalyst ring-walking and association of the catalyst on the polymer terminus, H/H end groups on their own do not necessarily preclude such a mechanism. Aliquots

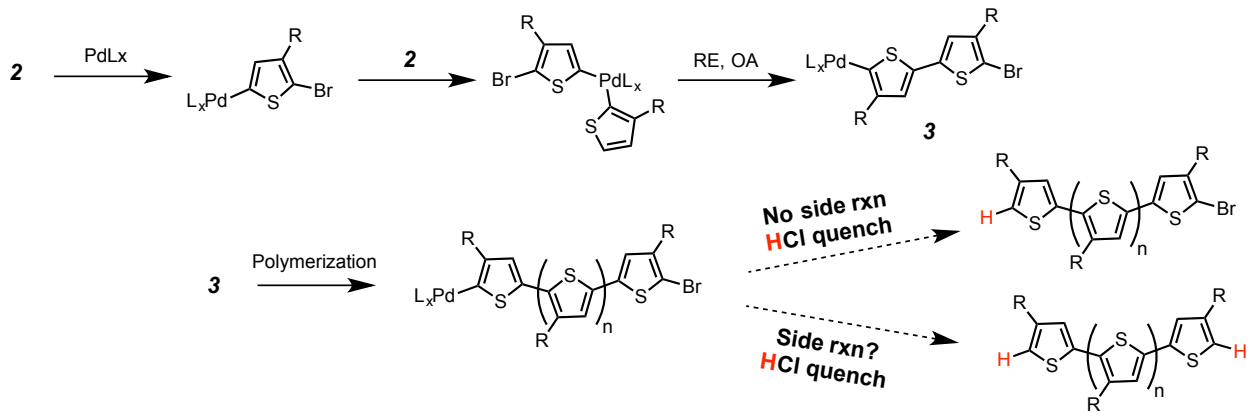

Scheme 6-3. ***Initiation of P3HT synthesis and potential end groups***

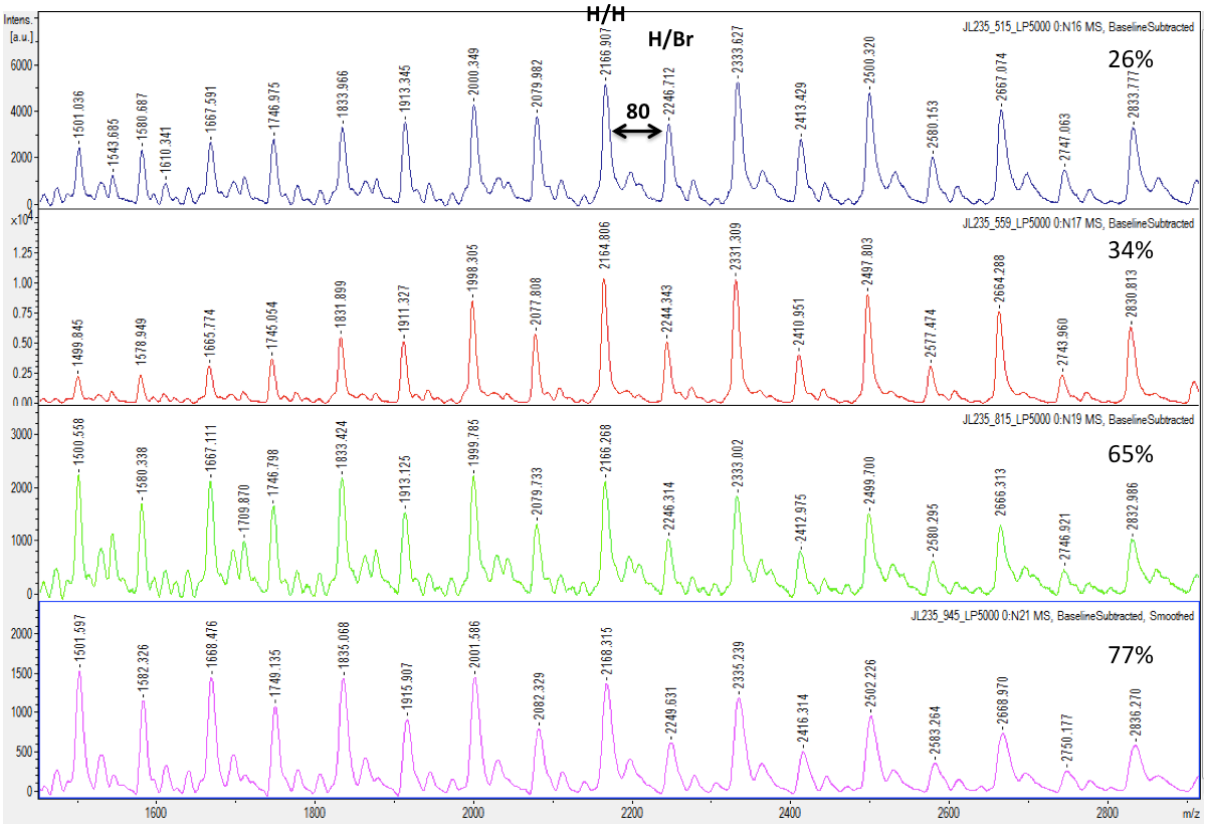

Figure 6-5. ***End-group analysis of aliquots at various monomer conversion.***

were taken at different monomer conversions during the polymerization showing similar relative amounts of H/Br and H/H terminated chains at lower molecular weights (**Figure 6-5**). Since the use of Pd with t-Bu_3P ligand has been shown to give rise to mixed end groups during conjugated polymer synthesis,[11] we hypothesized that a ligand exchange between Au and Pd may be taking place during the polymerization. Indeed, ligand metathesis for Au/Pd systems has been observed by others.[44] However, NMR studies carried out when (t-Bu_3P)Au(I)Cl is mixed with Pd-PEPPSI-iPr showed no signs of a ligand exchange. Mixed end groups have been previously observed in P3HT synthesis with PEPPSI catalysts[51] and side reactions involving dehalogenation in conjugated polymer systems[52] have also given unexpected H/H end groups.

6.9 Catalytic Au Trials

To this point, the polymerization was segregated into two steps. First, the thiophene monomer was activated via stoichiometric aurylation with gold. After purification, this stabilized activated monomer was subjected to Pd catalyst. Although this was a proof-of-concept for a monomer activated via C-H arylation and a polymerization of that monomer exhibiting living chain growth behavior, in practice, it would be ideal to combine the steps into one pot. However, attempts at using catalytic amounts of $AuP(t\text{-}Bu)_3$ and PEPPSI-iPr, did not yield any reaction. We hypothesize that the presence of NaOtBu was detrimental to the catalytic turnover of the Pd. Attempts at using weaker bases such as carbonates or alkyl amines were unsuccessful. If we

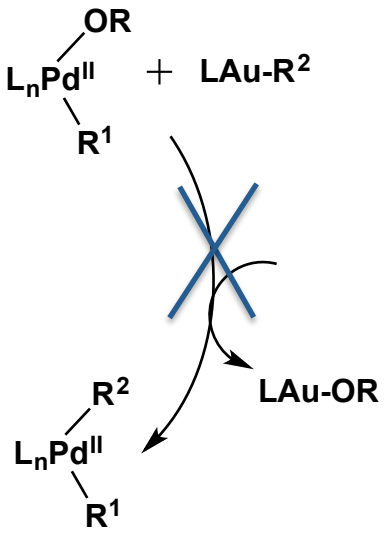

Scheme 6-4. ***Hypothesized lack of Au-O bond formation preventing Pd turnover.***

consider Suzuki coupling as an analogy, whereby alkoxide bases are regularly used, we see that the formation of boron-oxygen bond from Pd-O, is the driving force for the reaction (**Scheme 6-4**). From literature, there is computational study about Au and Pd cross coupling, where it was observed that the Pd-O bond is much stronger than the Au-O bond,[104] which would be unfavorable for successful transmetalation of the aurylated thiophene with the Pd species. This could be expected due to the stability of gold in general and it's low tendency to be oxidized.

6.10 Conclusions and Future Considerations

In summary, we have shown that 2-bromo-3-hexyl-thienyl-5-gold(I) can be used as a monomer for P3HT synthesis. Particularly, reactions with PEPPSI-iPr provided regioregular P3HT with low dispersities. Mechanistic studies were performed to investigate whether or not living character was present in this polymerization. The good accessibility of **2** via CH activation and its ability to undergo controlled palladium catalyzed polymerization open new avenues to

explore overall-catalytic dual metal catalysis with two metals of orthogonal reactivity, one providing CH-activation of the monomer and the other one cross coupling of the activated monomer through a chain growth polymerization mechanism without the use of often sensitive organometallic chemicals based on base metals like Grignard reagents. Additionally, Au (I) has shown high compatibility with electron deficient arenes, which could broaden the scope of monomer reactivities and polymer types.[37,38] Further investigations into such systems are ongoing where the ultimate goal would be to achieve the use of a catalytic amount of Au in the polymerization.

6.11 SUPPORTING INFORMATION

Materials and Methods

2-Bromo-3-hexylthiophene was purchased from TCI America. All other chemicals were purchased from Sigma-Aldrich. All purchased chemicals were used as received. THF was dried on a solvent still before use. Anhydrous dioxane was used as received. Reactions were carried out under inert nitrogen atmosphere, unless otherwise specified. ^{1}H NMR spectra were collected on a Bruker AV 300 spectrometer operating at 300 MHz in deuterated chloroform solution with TMS as reference. Polymer molecular weights were measured by a gel permeation chromatograph (GPC) on a Viscotek Triple Detector Array 305 at 30 °C and THF as the eluent and using a triple detection calibration of a narrow dispersity polystyrene standard. All molecular weights reported are absolute molecular weights. MALDI-TOF measurements were run on a Bruker Autoflex II instrument using *2,2':5',2"*- terthiophene as a matrix. GC-MS measurements were carried out on an Agilent 5973 machine.

Experimental Methods

(5-Bromo-4-hexylthiophen-2-yl)(tri-*tert*-butylphosphine)gold(I)

Condition 1: NaOH/dioxane

2-Bromo-3-hexylthiophene **1** (87.4 mg, 0.354 mmol), chloro(tri-*tert*-butylphosphine)gold(I) (76.4 mg, 0.176 mmol) and freshly grinded sodium hydroxide (15 mg, 0.37 mmol) were placed into a screw cap vial and suspended in dioxane (1.5 mL). The mixture was stirred at 50 °C for 48 h. After cooling down to room temperature hexanes was added, the white solid were filtered

of and the solvent was removed. The resulting oil was dried. NMR analysis indicated a ratio of **2** and 2-bromo-3-hexylthiophene of 0.7:1 and thus a conversion of 82%.

Condition 2: NaO^tBu/THF:

2-Bromo-3-hexylthiophene **1** (20.0 mg, 80.9 µmol), Chloro(tri-*tert*-butylphosphine)gold(I) (17.6 mg, 40.5 µmol) and sodium *tert*-butoxide (16 mg, 0.166 mmol) were placed into a screw cap vial and suspended in THF (2.5 mL). The mixture was stirred at 60 °C for 17 h. NMR indicated 75% conversion. Further stirring for 24 h did not lead to any further reaction. After cooling down to room temperature hexanes was added, the white solid were filtered of and the solvent was removed.

Grignard Method:

2-Bromo-3-hexyl-5-iodothiophene (249 mg, 0.667 mmol), dry lithium chloride (55 mg, 1.3 mmol) were dissolved in dry THF (5 mL) and cooled in an ice bath. Isopropylmagnesium chloride (0. 67 mmol) was added dropwise and the mixture was stirred for 10 min at 0 °C and 50 min without cooling. Chloro(tri-*tert*-butylphosphine)gold(I) (290 mg, 0.667 mmol) in THF (2 mL) was added via cannula to the Grignard-solution at -78 °C and after addition the cold bath was removed. The mixture was allowed to thaw and stirred overnight. Diethylether was added and the mixture was washed with water. The organic phase was collected, dried over K_2CO_3 and the solvent was removed under reduced pressure. NMR indicated 93% conversion.

To obtain pure **2** the mixture was subjected to distillation to remove residual **1**. Monomer is sufficiently stable for storage in air. Before dissolution in NMR solvent, $CDCl_3$ was passed

through basic alumina as a precaution to remove any trace HCl that could cleave the gold functionality.

^{1}H NMR ($CDCl_3$, 300 MHz): 6.75 (d, $^{4}J_{HP}$ = 3.0 Hz, 1H), 2.54 (t, ^{3}J = 7.8 Hz, 2H), 1.53 (d, $^{3}J_{HP}$ = 9.9 Hz, 27H), 1.30 – 1.25 (m, 8H), 0.94 – 0.82 (m, 3H).

General Polymerization Method:

Monomer **2** (0.2 mmol) was placed in a Schlenk flask under nitrogen and dissolved in dry THF (0.05 M). Tetradecane (0.2 mmol) was added as an internal standard for tracking conversion and PEPPSI-iPr (at varying mol %) were added subsequently. A first aliquot was taken (~0.2 mL) prior to heating as a GCMS reference and the reaction mixture was heated to 60 °C. After 4-5 hours GCMS showed conversions of >90%. The reaction was quenched by adding excess 2M HCl. The subsequent suspension was dried under reduced pressure, washed with MeOH, acetone, and cold hexanes before being collected by a chloroform wash. Solvent was once again removed under reduced pressure and polymer samples were analyzed via NMR and GPC.

Block-Polymerization:

Monomer **2** (0.185 mmol) was reacted with 3 mol% PEPPSI-iPr in THF (0.5 M). After 4 hours conversion reached 83% as monitored by GCMS. Thirty minutes later an equal amount of **2** was added as a solution to the reaction mixture (0.185 mmol in 1.37 mL THF) and stirred for 12 hrs. Reaction was quenched and worked up as stated in the general polymerization procedure. M_n correlated with nearly double the value that we would expect for a 3 mol% loading of PEPPSI-iPr (or nearly equivalent to a 1.5 mol% PEPPSI-iPr). Disperties remained low as compared before and after second monomer addition.

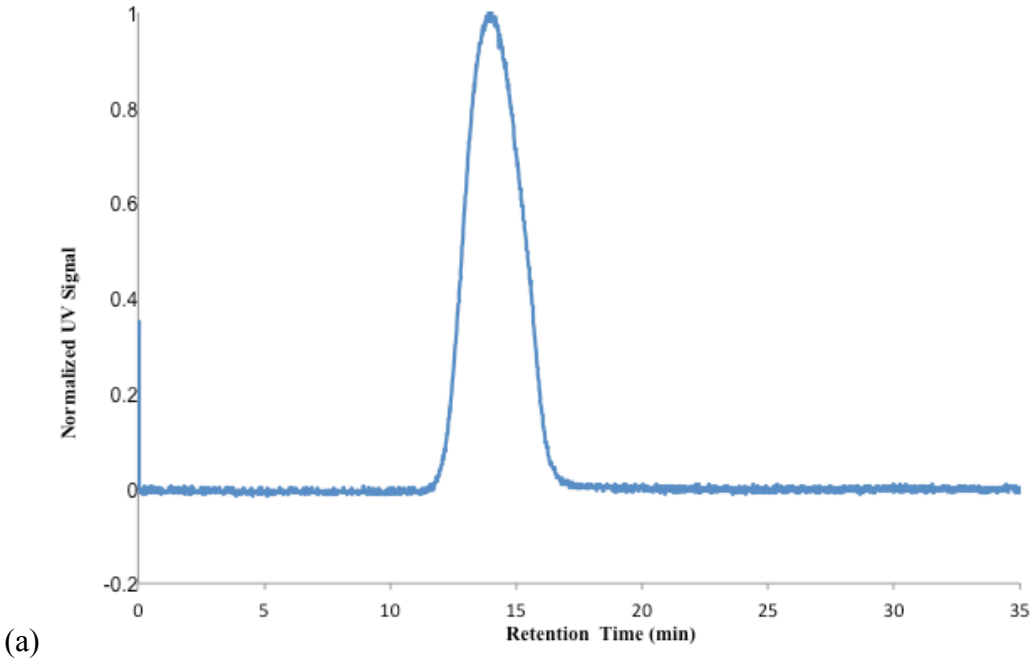

(a)

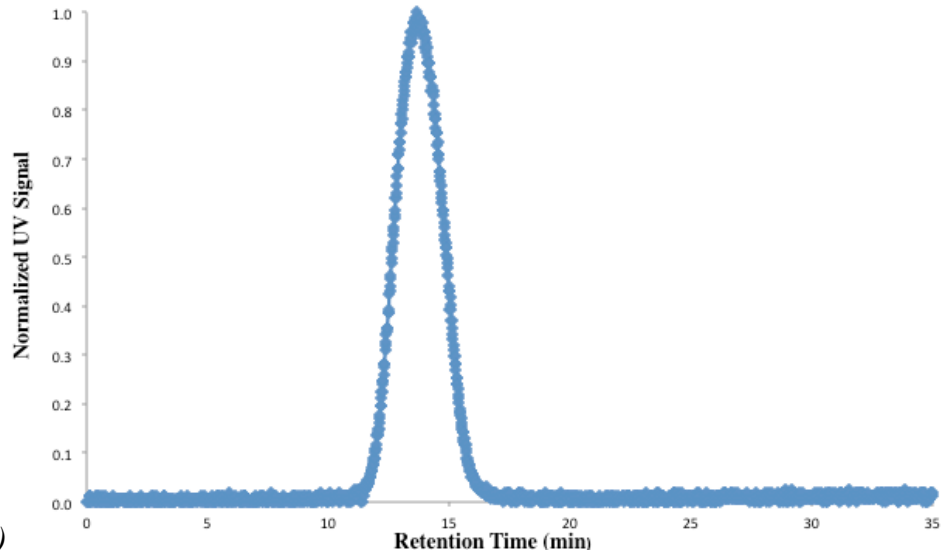

(b)

Figure 6-6. ***Normalized SEC traces of select Au/Pd DArP conditions.*** *(a) Example normalized UV signal with respect to retention time obtained via GPC for 2 mol% PEPPSI-iPr catalyst loading. Peak retention time at 14.1 minutes. (b) Normalized UV signal with respect to retention time for 1 mol% PEPPSI-iPr. Peak retention time at 13.9 minutes.*

Estimation of DP by NMR:

To calculate the degree of polymerization, we considered the presence of both H/H and H/Br terminated polymers. In an H/Br terminated chain, the H-end alpha proton has been shown to be near 6.90 ppm while the beta proton on the Br-end has been shown around 6.825 ppm. To account for all end groups in our mixture, we took the integration of both signals. We then divided this value by 2 to account for every polymer chain containing two end groups in order to estimate the number of chains. The ratio between the main chain thiophenyl protons and the previously calculated value was found to be the estimated degree of polymerization of each polymer chain. This result maintained good agreement with expected molecular weights with respect to catalyst loading.

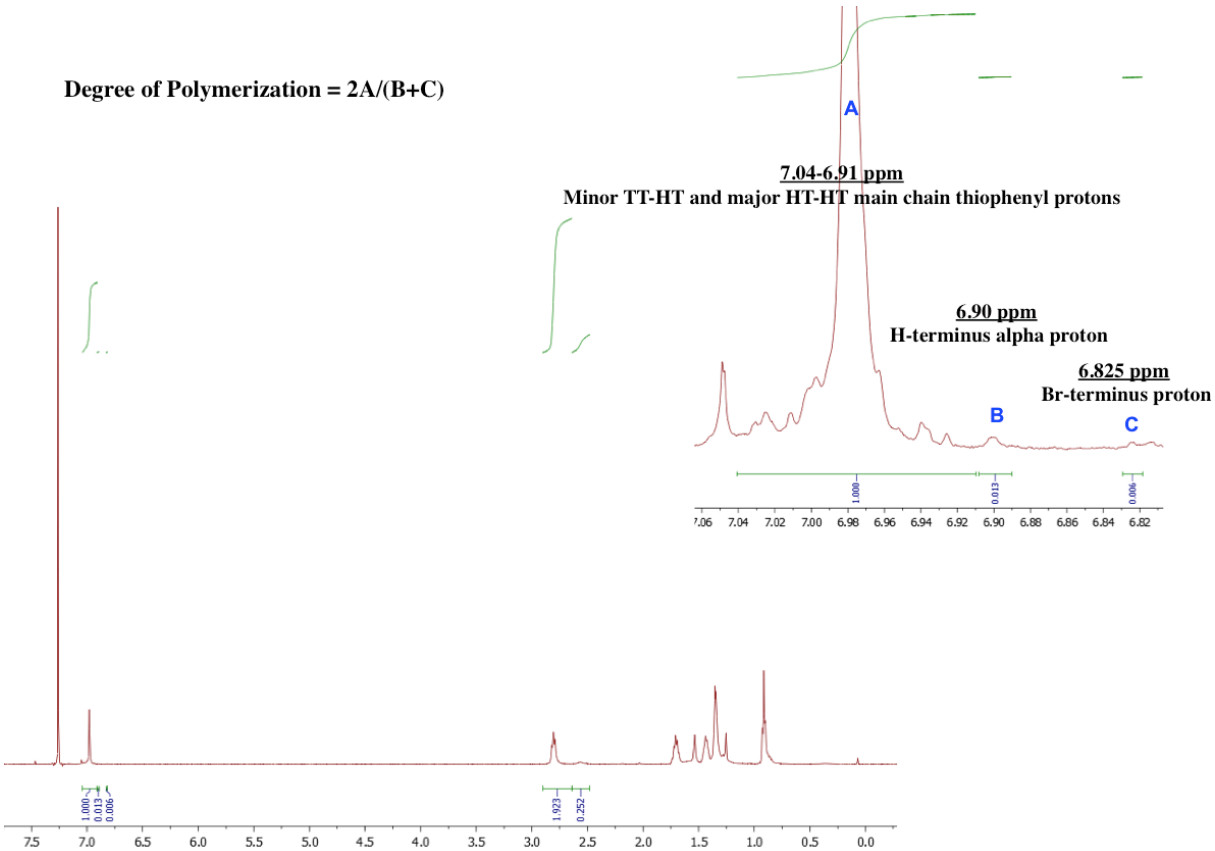

Figure 6-7. ***NMR end-group analysis to estimate M_n for 1mol% PEPPSI-iPr loading.***

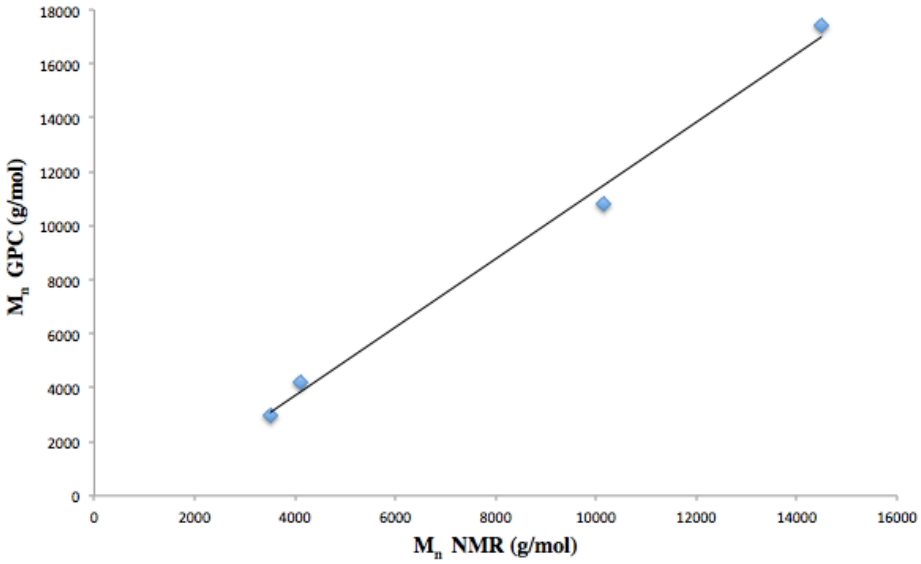

Figure 6-8. ***Comparison of M_n values obtained by GPC versus NMR.*** *Data points correspond to PEPPSI-iPr catalyst loadings of 5, 3, 2, and 1 mol%, respectively.*

Chapter 7. DUAL-CATALYTIC SILVER-PALLADIUM DARP

7.1 INTRODUCTION

DArP has been demonstrated on a variety of heterocyclic monomers and co-monomers, but there still remain areas to improve the methodology. DArP was built upon seminal direct arylation (DA) studies[48,49] intended for small molecule cross-coupling. As such, important polymerization characteristics such as chain-growth kinetics, low dispersity, and molecular weight control remain challenges with few DArP reports attempting to achieve them.[62] This arises from the CMD pathway, which yields less desirable step-growth kinetics.[105] Although discovery of a living DArP conditions would be ideal, pursuing one-pot reaction conditions whereby chain-growth and low dispersities could be achieved would help to advance the utility of DArP, which is the aim in this work (**Scheme 7-1**).

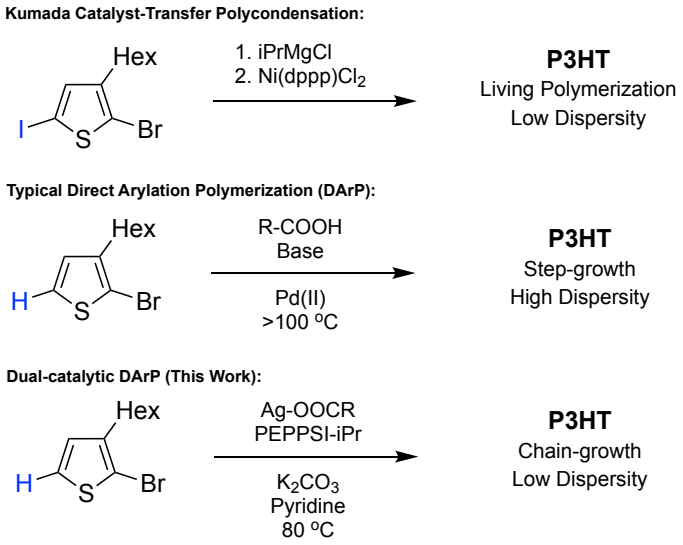

Scheme 7-1. ***Traditional, DArP, and dual-catalytic DArP syntheses of P3HT.***

To overcome the limitations of CMD, namely step-growth leading to high dispersities, a proposed dual-catalytic system could be implemented (**Scheme 7-2**). We had already shown a proof-of-concept using a C-H activated aurylated thiophene monomer with Pd to give a living chain growth polymerization. However, stoichiometric amounts of gold were used, which would be prohibitively expensive in scale-up. Also, this synthesis required the purification of the aurylated monomer, thus adding two more unit steps in the synthetic complexity. Due to incompatibility with the alkoxide base and the Pd species during turnover, a different dual metal system would have to be found. Larossa had published an oxidative DA scheme using gold and silver, without any Pd source.[53] An Au-Ag system would be unfeasible for our model system, especially given the poor ability for either metal to oxidatively add into aryl halogens.[106] However, based on recent reports on the nature of Ag as a C-H activating agent have made it an attractive option.

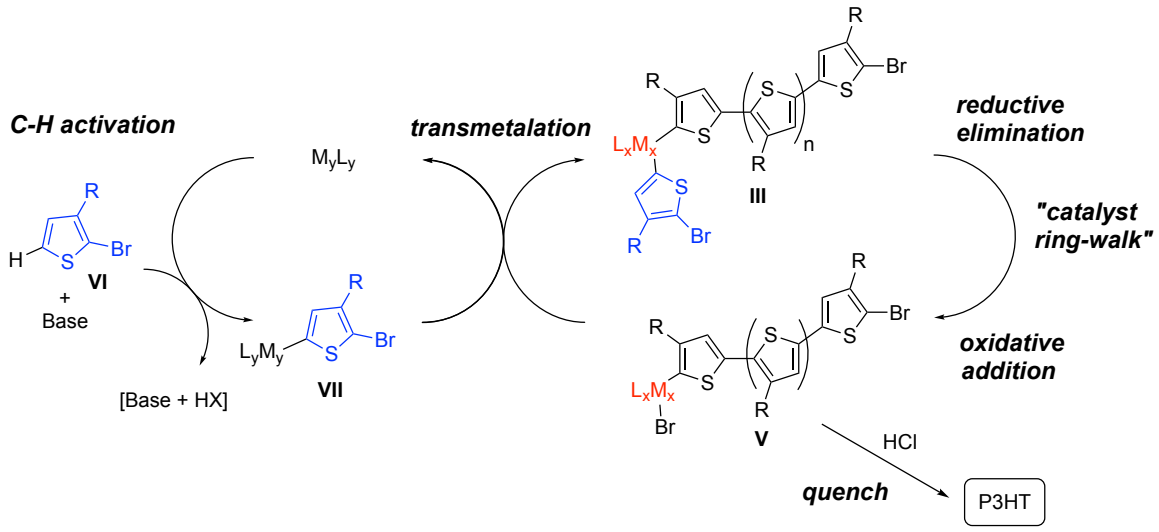

Scheme 7-2. ***Proposed dual-catalytic DArP cycles for P3HT synthesis.*** *In this work, M_y is Ag and M_x is Pd.*

7.2 Selection of Dual-Catalytic System

In general, electron-deficient thiophenes, among other heterocyclic aromatic monomers, have been shown to undergo C-H activation via coinage metals.[101,107] Previously, Ag has been used as an additive to promote C-H activation in many DA and DArP systems.[53,108–110] In 2016, nearly concurrent studies by Larossa and Sanders have suggested that Ag is indeed involved in the rate-limiting C-H activation of electron deficient substrates, which can then undergo transmetalation by Pd.[111,112] We chose to continue developing conditions for the synthesis of P3HT due to its synthetic accessibility and relevance to the field. By incorporating both Ag for C-H activation and Pd for transmetalation and subsequent C-C coupling, we are able to show chain-growth kinetics with low dispersities (<1.5), which are not typically observed characteristics of traditional DArP P3HT syntheses.[61,66],[64] To the best of our knowledge, this is the first report of DArP conditions implementing a dual-catalytic system.

Looking towards specific catalyst species, Ag has exhibited promotion of C-H activation[109] and readily transmetalates with metals such as Pd. Specifically, Ag-carboxylates or Ag(I) salts with carboxylic acid additives have been used in DA small molecule studies.[64] We focused on Ag(I) adamantanoate (AgAd) and Ag(I) neodecanoate (AgNDA) owing to reports[64] of their efficacy in DA conditions and for minimizing C-H activation of open β-positions on thiophene, which leads to undesired branching.[65] PEPPSI-iPr was employed as the Pd(II) source, due to its chemical stability, observed participation in controlled polymerizations of P3HT, and hypothesized chain-association behavior.[41,113]

7.3 Initial Polymerization Conditions

Initial reaction conditions were inspired by reported DArP P3HT literature,[66] with the addition of Ag-carboxylates being novel to our trials (**Scheme 7-3**). At various loadings of PEPPSI-iPr, molecular weights (M_n) up to 25 kg/mol were observed with dispersities in the

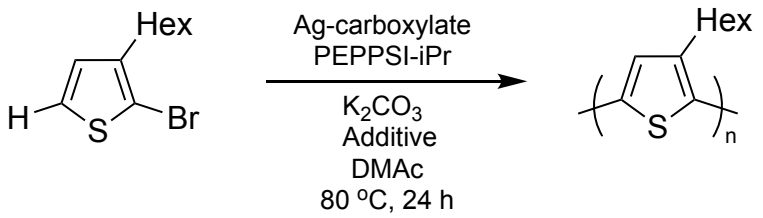

Scheme 7-3. ***General reaction conditions for dual-catalytic DArP for P3HT synthesis.***

range of 1.4-1.5 (**Table 7-1**). In the absence of Ag (**entry 4**), decreased M_n and increased dispersity was observed. Relatively lower dispersities for reactions with AgAd (**entries 1-3**). However, high M_n relative to PEPPSI-iPr loading excluded a controlled polymerization. Lower M_n observed without Ag could indicate lower reactivity, implying a beneficial role of role of Ag in C-H activation in addition to the necessary role of the carboxylate as a proton shuttle during C-H bond activation by Pd. **Entry 4** does show that polymerization occurs with Pd only, which has been reported with PEPPSI-type catalysts,[66] albeit yielding polymers with dispersities approaching 2. We believe two competing C-H activation processes by Ag and Pd need to be considered. For an ideal and predictable dual-catalytic cycle, we would have to reduce or eliminate the C-H activation behavior of Pd for orthogonal catalytic reactivity. Deuterium exchange studies were performed to explore Ag-mediated C-H activation of 2-bromo-3-hexylthiophene (**Table 7-S1**). Conditions with only Ag-carboxylate showed over 64% deuterium conversion, while conditions with only PEPPSI-iPr and carboxylate additive yielded

oligomers. These findings further demonstrated the need to have better control over each catalyst's activity, specifically in limiting Pd-mediated C-H activation.

Entry	Ag Species (eq.)[b]	Additive (eq.)	PEPPSI (mol %)	M_n[c] (kg/mol)	Đ
1[a]	AgAd (0.1)	None	5	16	1.46
2[a]	AgAd (0.1)	None	2.5	21	1.35
3[a]	AgAd (0.1)	None	1.25	25	1.49
4[a]	0	None	5	11	1.80
5[a]	AgNDA (0.1)	None	2.5	30	B[d]
6[a]	AgNDA (0.1)	None	2.5	28	B[d]
7	AgNDA (0.1)	Pyridine (1)	2.5	3.7	1.31
8	AgNDA (0.3)	Pyridine (1)	2.5	1.9	2.05
9	AgAd (0.1)	Pyridine (1)	2.5	5.7	1.28
10	0	Pyridine (1)	2.5	2.6	1.26

Table 7-1. ***Ag-Pd DArP conditions for P3HT synthesis.*** *[a] Reactions run at 100 ^{O}C. [b] All equivalents and mol % are with respect to the monomer. [c] M_n values obtained via size exclusion chromatography. [d] Bimodal distribution.*

When replacing AgAd with AgNDA (**entries 5-6**), bimodality was observed in the molecular weight distribution, however regioregularity generally increased up to 96% versus 86% for AgAd. Because AgNDA was synthesized with a mixture of neodecanoate isomers, there may be different reactivities associated with the competing Pd and carboxylate isomers involved. To narrow the dispersity, lower reaction temperature was attempted to possibly slow activation by Pd (**entry 6**). However, no significant decrease in M_n or bimodality was seen. Despite minimal effect, we decided to continue developing reaction conditions at 80 °C in the interests of a less energy-intensive synthesis compared to commonly reported DArP conditions.

7.4 Effect of Pyridine on Dispersity

Analyzing the structure of PEPPSI-iPr, 3-chloropyridine is considered a stabilizing ligand that dissociates before the Pd catalyst can be active.[114] It was reported that this pyridine moiety can play an inhibitory role in catalytic processes if allowed to re-ligate to the Pd species.[115] With this in mind, several pyridine ligands (2-chloro-pyridine, 3-chloro-pyridine, and pyridine) were screened for effects on dispersity of the resulting polymer. It was only with pyridine at 1 equivalent with respect to the monomer that narrowing of the dispersity (Đ~1.3-1.4) and unimodality (in the AgNDA system) was observed (**Figure 7-1**). We hypothesized that lowering the number of active species of PEPPSI-iPr allowed for C-H activation to be primarily Ag-mediated, promoting orthogonal reactivity of the two metals, thus yielding chain-growth kinetics. The loading of pyridine was quite high with respect to PEPPSI-iPr, however, it is believed to be

necessary to sufficiently slow the C-H activating behavior of the Pd catalyst as even 0.5 equivalents of pyridine continued to exhibit bimodality (**SI, Figure 7-4**).

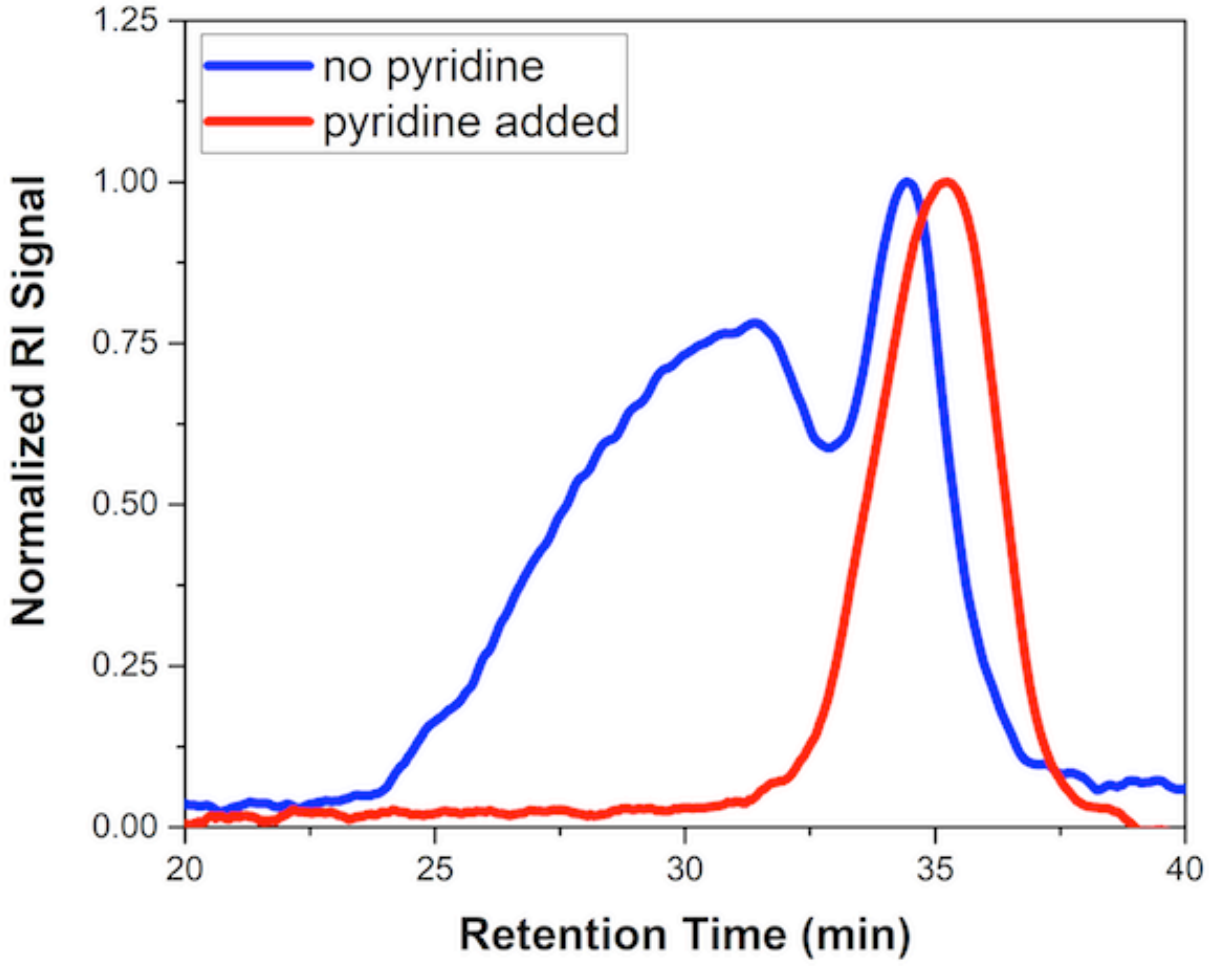

Figure 7-1. ***Normalized RI signals for P3HT synthesized with pyridine (red) and without pyridine (blue).*** *Conditions are using AgNDA.*

Addition of 1 equivalent of 3-chloropyridine did not narrow the dispersity in contrast to pyridine (**SI, Figure 7-5**). This could be explained by the less electron-rich nitrogen in the presence of the chlorine group, which makes it more labile ligand than pyridine. The ability of pyridine to ligate to the active Pd species was examined by observing a mixture of pyridine and

PEPPSI-iPr in CDCl3 via NMR. Disappearance of ligated 3-chloropyridine and the appearance of ligated pyridine peaks showed the efficacy of the ligand exchange. To further show that pyridine is specifically affecting PEPPSI-iPr as an inhibitor rather than due to possible ligand exchange with the NHC, $Pd(OAc)_2$ was used with 1 equivalent of pyridine, which continued to exhibit broad bimodal dispersity (**SI, Figure 7-6**).

7.5 Determination of Chain Growth

Polymer growth behavior was analyzed by looking at a plot of M_n versus monomer conversion (**Figure 7-2**), which showed a linear relationship, indicative of chain-growth. This is a rare example of DArP conditions demonstrating chain-growth kinetics of P3HT combined with comparatively low dispersities.

Next, dependence of M_n on catalyst loading was screened, however polymerization was not controlled based on Pd loading. Allowing the reaction to run past 24 hours yielded high dispersities and the presence of high molecular weight shoulder peaks. This may indicate Ag-species decomposition, as black precipitate formed. If Ag turnover was hindered by decomposition, the addition of higher equivalents might be beneficial. However, it was found that increased Ag was actually detrimental (**Table 7-1, entry 8**). A dark suspension with black particulates and negligible polymer formation was observed. The reason for this effect is unclear since small molecule DA reactions have proceeded with up to 0.7 equivalents of Ag[111]

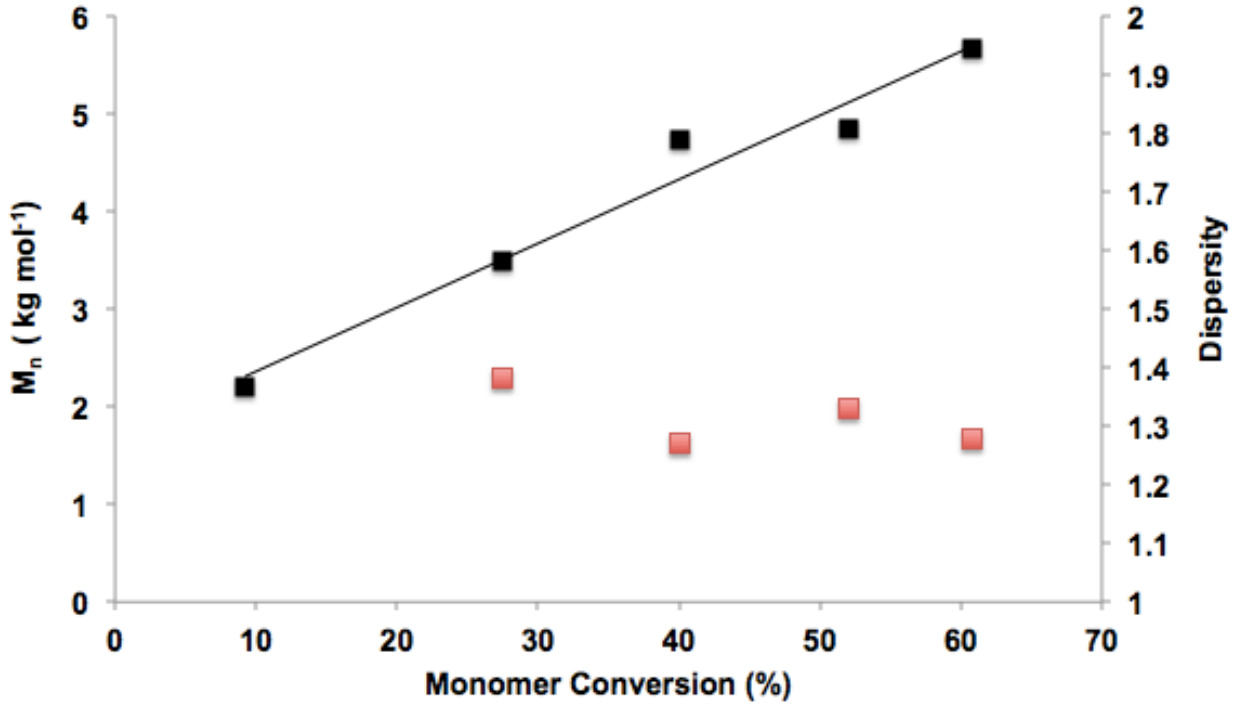

Figure 7-2. ***M_n versus monomer conversion for condition with AgAd and pyridine.***

7.6 Chain Association Behavior of PEPPSI-iPr

Chain association of Pd is another important factor for the eventual development of a controlled polymerization. This was studied by adding bromobenzene (Br-Ph) as a chain transfer agent. If the Pd species dissociates from the chain after reductive elimination, presence of Br-Ph would compete with terminal Br of the thiophene monomer for subsequent oxidative addition of the catalyst, leading to lower M_n P3HT chains and higher dispersities. However, even for up to 5 equivalents of Br-Ph with respect to the monomer, the observed M_n and dispersities remained nearly constant (**SI, Table 7-3**). In similar experiments without Ag present, but in the presence of pyridine, lower M_n with much higher dispersities were observed after more than 2 equivalents of Br-Ph was added. For Kumada catalyst transfer polycondensation (KCTP) reactions, it was

found that excess ligand helps narrow dispersity by possibly limiting chain transfer. However, due to the noticeable evidence of chain transfer in the presence of pyridine without Ag, it is unlikely that the pyridine plays this role for Pd in our system. These findings also suggest different mechanisms for the fate of Pd after reductive elimination in the presence of Ag. The unchanging M_n and dispersities in the Ag condition are supportive of Pd chain association.

7.7 Conclusions and Future Considerations

Observance of chain-growth kinetics and low dispersity is novel and promising for this dual-catalytic Ag-Pd DArP system. It is unclear why the polymerizations reach an upper limit of nearly 6 kg/mol despite lower catalyst loading attempts. Based on the necessity of pyridine additive to induce chain-growth polymerization, we believe the kinetics of both cycles needs further optimization. From the appearance of black particulates in the reaction suspension, the Ag species may be decomposing or forming byproduct complexes yielding lower turnover and lower M_n. In the absence of Ag but in the presence of pyridine, smaller M_n for P3HT are observed, suggesting that the Ag plays an important role in the rate of C-H activation and that pyridine indeed has an inhibitory role on PEPPSI-iPr. Current studies on various Ag-ligand species are being explored, as well as alternative Pd ligands. It would be beneficial to limit the role of Pd in C-H activation based on ligand type, for example, imine-based ligands have shown such characteristics.[116] Further mechanistic insight for additives such as pyridine or other ligands could benefit reaction optimization.

We have demonstrated the first reported dual-catalytic Ag-Pd system for P3HT synthesis via DArP. The observation of chain-growth, low dispersities, Pd chain association, and

regioregularity values up to 96% are encouraging steps towards the potential development of a controlled polymerization via DArP. The high chemical stability of PEPPSI-iPr and Ag-carboxylates as opposed to alternative organometallics facilitates less stringent reaction conditions, which is beneficial for synthetic scalability. Continuing to pursue C-H functionalization methodology that can compete with popular and robust polymerizations such as Kumada-catalyst transfer polycondensation (KCTP), would eventually allow DArP to find widespread adoption in the area of materials research while addressing important considerations for environmental impact.

7.8 SUPPORTING INFORMATION

Materials and Methods

2-Bromo-3-hexylthiophene was purchased from TCI America. All other chemicals were purchased from Sigma-Aldrich. All purchased chemicals were used as received. Anhydrous *N,N*-dimethylacetamide was used without further drying. Reactions were carried out under inert nitrogen atmosphere, unless otherwise specified. All stir-bars were washed in aqua regia and subsequently dried overnight in a 120 °C drying oven. ^{1}H NMR spectra were collected on a Bruker AV 500 spectrometer operating at 500 MHz in deuterated chloroform solution with TMS as reference. Polymer molecular weights were measured by a gel permeation chromatograph (GPC) on a Viscotek Triple Detector Array 305 at 30 °C with chlorobenzene as the eluent at 0.5 mL/min using conventional calibration of a narrow dispersity polystyrene standard. GC-MS measurements were carried out on an Agilent 5973 instrument.

Experimental Methods

Silver carboxylate:

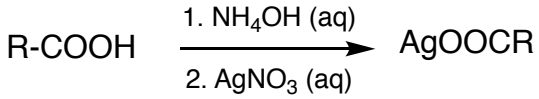

Scheme 7-4. ***General silver carboxylate synthesis.***

Silver neodecanoate and silver adamantanoate were prepared by following literature procedure.[117]

General polymerization procedure:

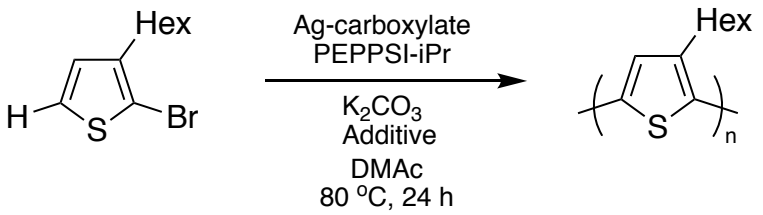

Scheme 7-5. ***Ag/Pd Dual-catalytic DArP of 2-bromo-3-hexylthiophene***

Poly(3-hexylthiophene). To a 4 mL dark vial with a septa cap was added PEPPSI-iPr (2.5 mol%), Ag carboxylate (0.1 eq), K_2CO_3 (0.1 eq). 2-bromo-3-hexylthiophene (0.1 mmol, 1 eq.) was then added. The vial was purged with nitrogen before pyridine (0.1 eq.) was added. *N,N*-dimethylacetamide (1.5 mL) was added to the reaction mixture via syringe, and the reaction was allowed to stir for 24 hours in a reaction block at 80 °C. The reaction was quenched with 0.3 mL of 3M HCl and was subsequently filtered and washed with methanol finally acetone until each filtrate was clear. Finally, the polymer was dissolved in chloroform and dried in a vial *in vacuo*.

Mn vs Conversion Aliquot Procedure:

The aforementioned procedure for P3HT synthesis was followed with the exception that tetradecane (1 eq.) was added as an internal standard. Conversion of 2-bromo-3-hexylthiophene was analyzed via GC-MS.

Deuterium exchange experiments

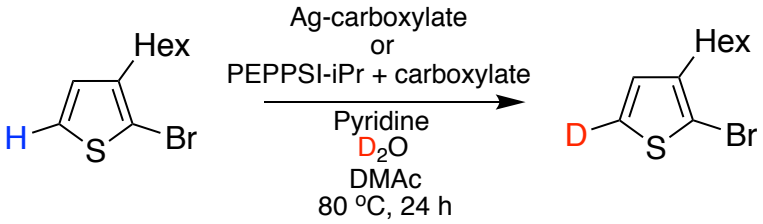

Scheme 7-6. ***General reaction conditions for deuterium exchange studies.***

Entry	AgNDA (eq)	Pyridine (eq)	PEPPSI-iPr (eq)	Average Deuterium Conversion (%)
1	0.1	0.1	0	73 +/- 6
2	0.1	0	0	64 +/- 3
3	0	0	0.025	Trace
4	0	0	0	Trace
5	0	0	0.025 + 0.1 eq NDA	Trace (dimer formation)

Table 7-2. ***Deuterium exchange studies.***

The aforementioned general procedure for P3HT synthesis was followed with the exception that D_2O (10 equivalents) was added as a deuterium source. Work-up procedures followed previously reported literature by Sanford.[112] Acetone-d6 was used as an internal standard to estimate deuterium exchange conversion.

Deuterium incorporation was not observed for the Pd-only trials, possibly due to the stability of aryl-Pd intermediates and quick formation of coupling products.

PEPPSI-iPr and pyridine exchange

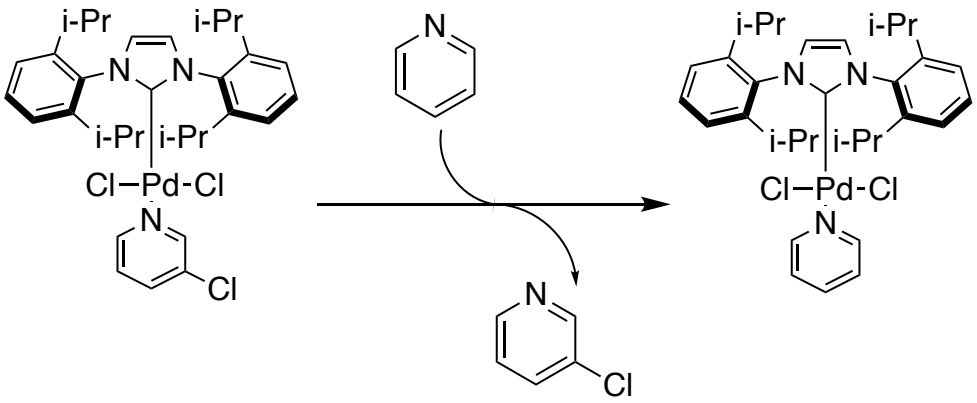

Scheme 7-7. ***Pyridine exchange on PEPPSI-iPr, inhibiting Pd-mediated C-H activation.***

We hypothesize that ligand exchange of 3-chloropyridine with excess pyridine suppresses Pd-mediated C-H activation of the 2-bromo-3-hexylthiophene monomer, allowing for Ag-mediated C-H activation to dominate in order to achieve orthogonal dual-catalytic activity. Attempts at using 2-chloropyridine or 3-chloropyridine in excess (0.1 eq.) did not yield low dispersity (<1.5) or unimodal (for AgNDA) distributions.

Procedure for NMR pyridine exchange study:

To a J. Young NMR tube was added 1.3 mg of PEPPSI-iPr (0.0019 mmol) with 6 uL (0.075 mmol) of pyridine and 1.5 mL of $CDCl_3$. This was heated at 80 °C for 24 hours. NMR spectrum was taken after 24 hours to determine replacement of 3-chloropyridine by pyridine.

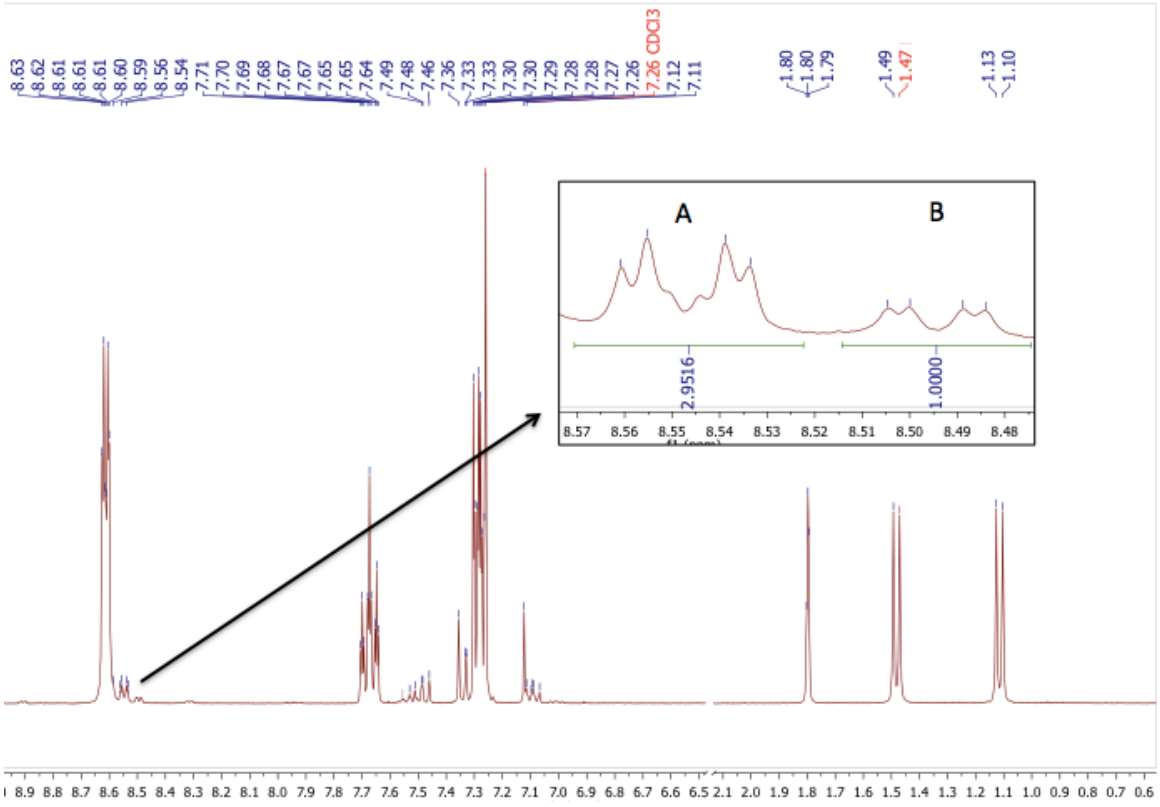

Figure 7-3. ***Pyridine Ligand Exchange NMR.*** *Crude NMR spectra of pyridine exchange reaction. Peaks A correspond to PEPPSI-ligated pyridine while peaks B correspond to PEPPSI-ligated 3-chloropyridine. The ratio of these peaks after heating at 80 °C for 24 hours estimates 74% 3-chloropyridine replacement by pyridine.*

Additional SEC analysis

Note: *These data were collected on a GPC consisting of an: Agilent 1260 Infinity II HPLC pump, three in-line MZ-Gel 10 µm size-exclusion columns (pore sizes = 10^3 , 10^3 , and 10^5 Å), miniDAWN-TREOS 3-angle multi-angle laser light scatter and OptiLab T-rEx refractive index detectors from Wyatt Technologies Corporation, using universal calibration.*

This data is meant to qualitatively compare the effect of various conditions on the dispersity and modality of the synthesized P3HT. These conditions utilize AgNDA as the silver species and the previously described general polymerization procedure above. Any changes in the conditions are listed in the figure descriptions.

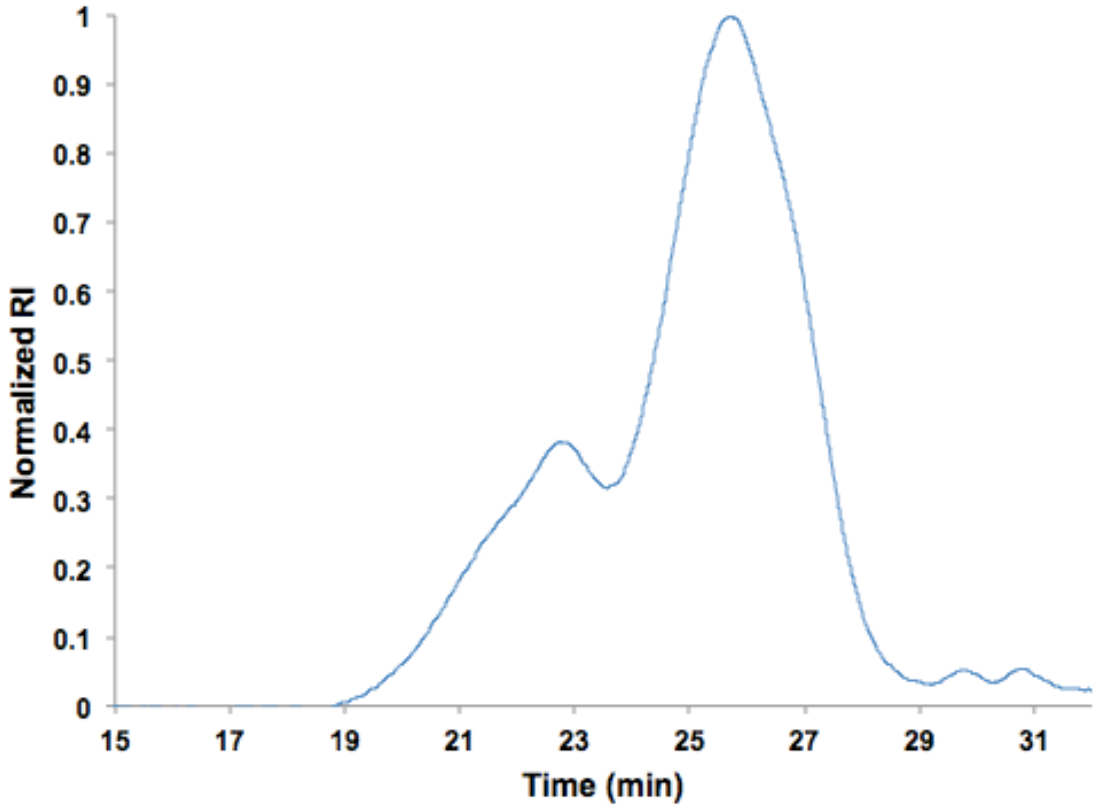

Figure 7-4. ***0.5 Equivalent of pyridine added.*** *Bimodal distribution was still observed. Dispersity = 1.99*

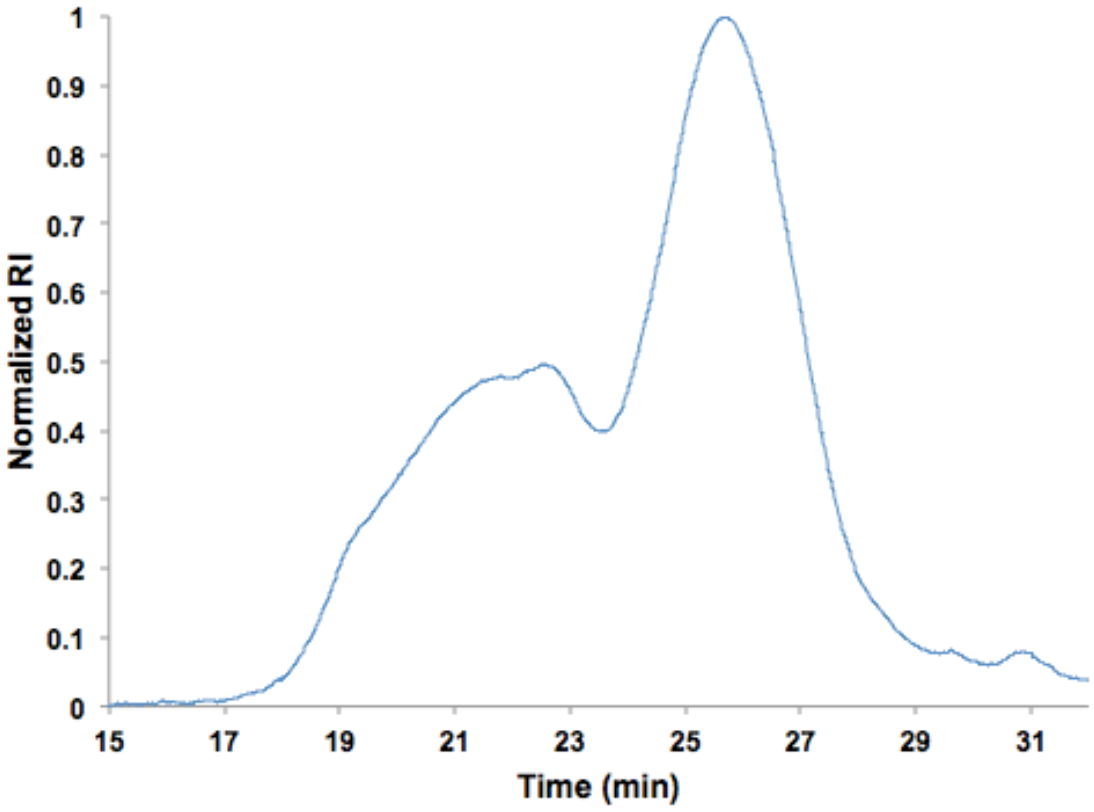

Figure 7-5. ***One equivalent of 3-chloropyridine.*** *Bimodality was not controlled in this case, likely due to the more labile nature of the electron deficient 3-chloropyridine compared to pyridine. Dispersity = 1.53*

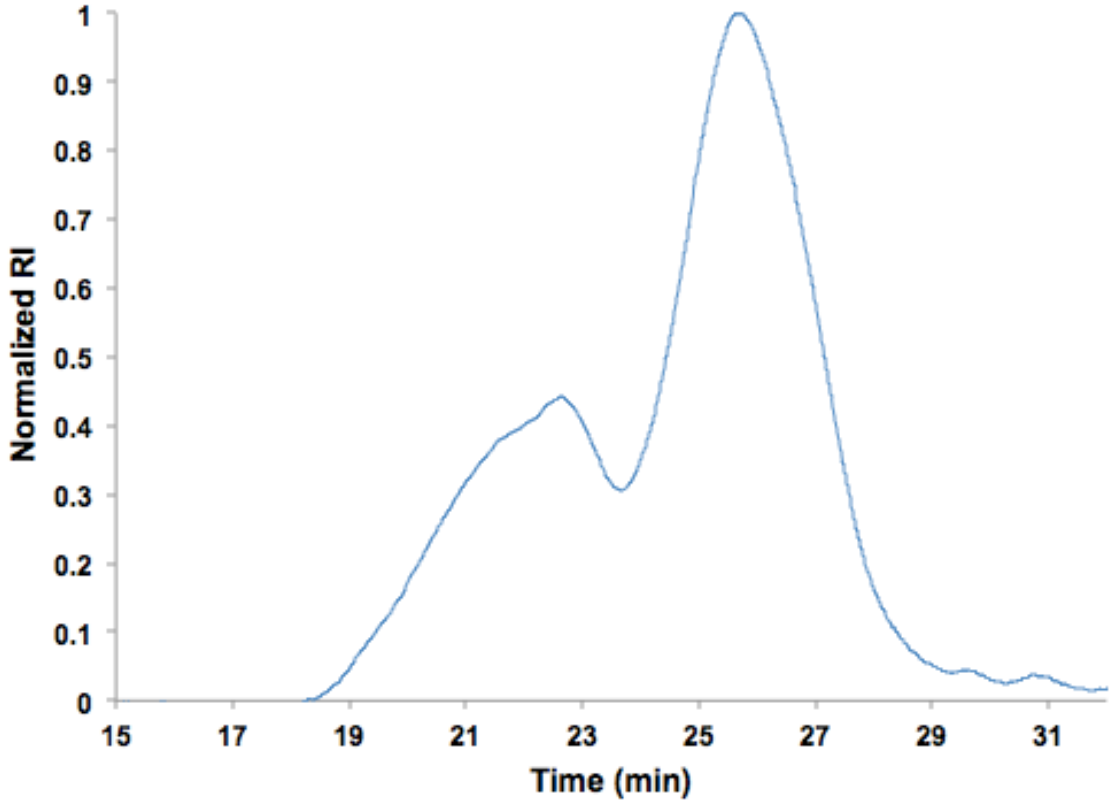

Figure 7-6. *Pd(OAc)$_2$ instead of PEPPSI-iPr.* *Pd(OAc)$_2$, a non-NHC Pd catalyst, was used at 2.5 mol%. This was to probe the uniqueness of the pyridine additive as an inhibitor for PEPPSI-iPr. Narrowing of dispersity was not observed, supporting the mechanism for reducing Pd-mediated C-H activation. Dispersity = 2.62*

d

MALDI-TOF Mass Spectrometry End Group Analysis

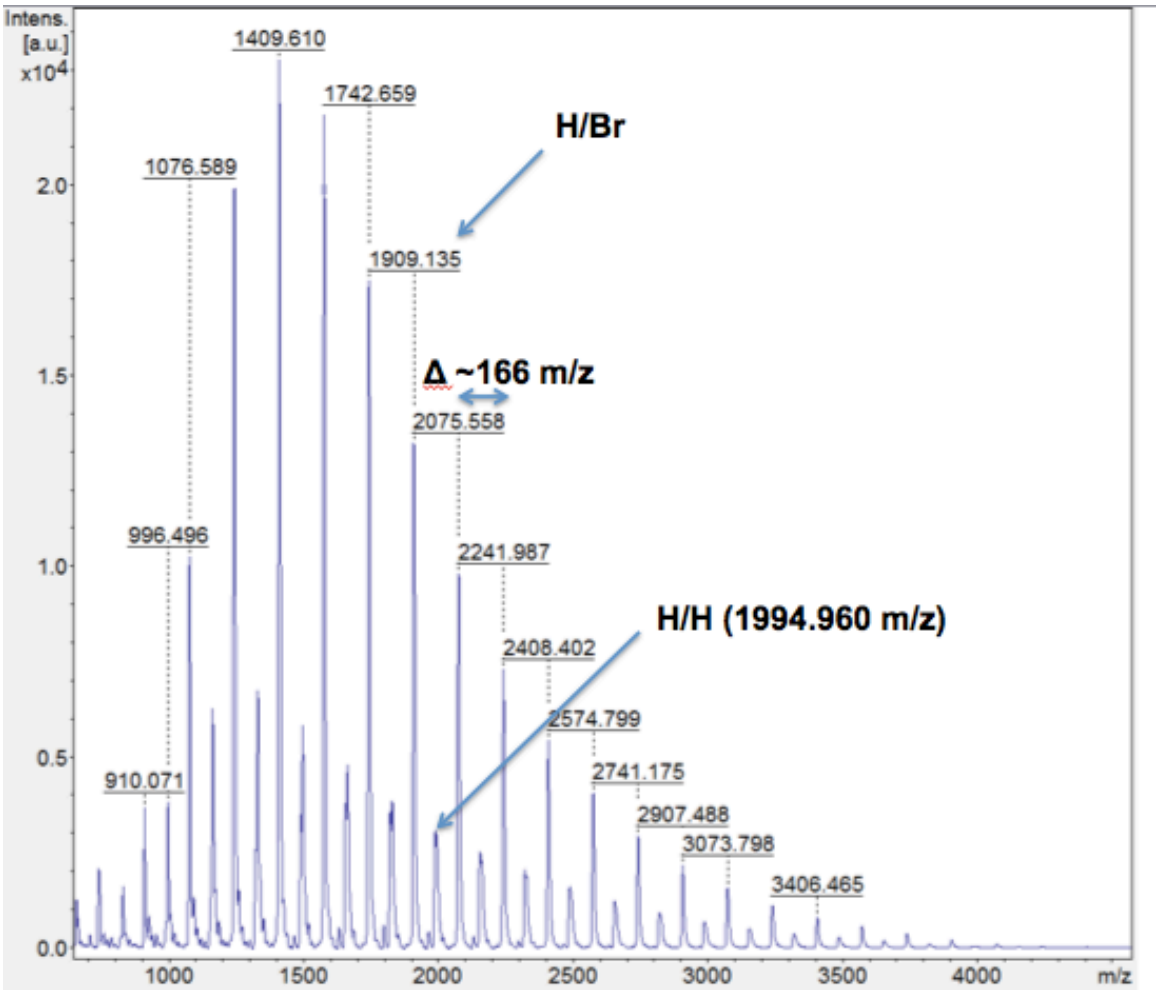

Figure 7-7. ***Ag-Pd system end-group analysis***. *A mixture of H/Br and H/H end groups are observed (condition using AgNDA).*

Chain transfer agent reactions

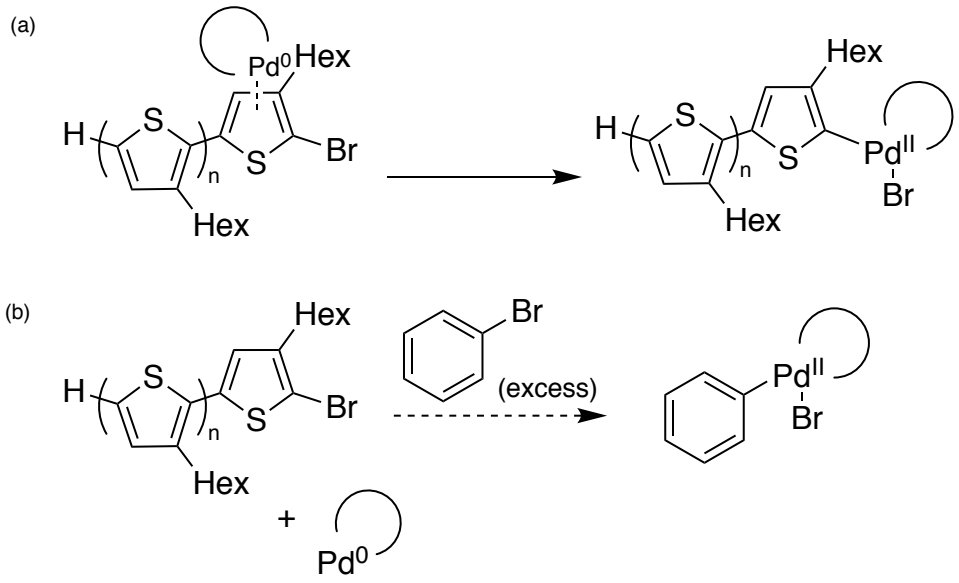

Scheme 7-8. ***Chain transfer agent reaction possible outcomes.*** *(a) Proposed Pd pi-complex that stays associated to thiophene ring after reductive elimination followed by oxidative addition into terminal thiophenyl bromine bond. (b) In the absence of a Pd pi-complex, excess bromobenzene would compete with the growing chain for oxidative addition by Pd.*

Entry	Br-Ph (eq)	Mn (kg/mol)	Dispersity
1	0	3.5	1.37
2	1	3.4	1.39
3	2	3.3	1.44
4	3	3.5	1.38
5	4	3.9	1.40
6	5	3.8	1.33
7[a]	0	9.2	2.80
8[a]	2	8.6	2.37
9[a]	3	6.3	2.90
10[a]	4	5.8	2.19
11[a]	5	5.1	1.76

Table 7-3. ***M_n and dispersity values for chain transfer trials.*** *[a] Entries 7-10 did not have any Ag-carboxylate.*

The aforementioned general procedure for P3HT synthesis was followed (AgNDA used in each trial), with the exception that varying equivalents of 2-bromobenzene were added as a chain transfer agent.

Regioregularity reaction screening

Entry	PEPPSI-iPr (mol %)	Ag-Carboxylate (eq.)	Regioregularity	Yield (%)
1	2.5	AgNDA (0.1)	96	48
2	2.5	AgAd (0.1)	86	20
3[a]	0	AgNDA (0.1)	96	-
4[a]	5	AgNDA (0.1)	94	-
5[a]	5	AgAd (0.1)	92	-
6[a]	2.5	AgAd (0.1)	87	-
7[a]	1.25	AgAd (0.1)	87	-
8[a]	0[b]	AgNDA (0.1)	89	-
9[a]	2.5	AgOAc (0.1)	89	-
10[a]	0[c]	AgAd (0.1)	No Reaction	-

Table 7-4. ***Preliminary reaction screening for Ag species and PEPPSI-iPr equivalents.*** *Yields not calculated for entries 3-10. [a] Reaction run at 100°C without pyridine. [b] 5 mol% Hermann-Beller Pd catalyst used [c] 5 mol % Ni(dppp)*Cl_2.

REFERENCES

[1] H. Shirakawa, J. Louis, A. G. Macdiarmid, *J. C. S. Chem. Comm* **1977**, 578–580.

[2] A. Facchetti, *Chem. Mater.* **2011**, *23*, 733–758.

[3] C. Li, M. Liu, N. G. Pschirer, M. Baumgarten, K. Müllen, *Chem. Rev.* **2010**, *110*, 6817–6855.

[4] P. M. Beaujuge, J. M. J. Fréchet, *J. Am. Chem. Soc.* **2011**, *133*, 20009–20029.

[5] J. Onorato, V. Pakhnyuk, C. K. Luscombe, *Polym. J.* **2017**, *49*, 41–60.

[6] S. E. Root, S. Savagatrup, A. D. Printz, D. Rodriquez, D. J. Lipomi, *Chem. Rev.* **2017**, *117*, 6467–6499.

[7] M. A. Green, Y. Hishikawa, E. D. Dunlop, D. H. Levi, J. Hohl-Ebinger, A. W. Y. Ho-Baillie, *Prog. Photovoltaics Res. Appl.* **2018**, *26*, 3–12.

[8] M. S. Vezie, S. Few, I. Meager, G. Pieridou, B. Dörling, R. S. Ashraf, A. R. Goñi, H. Bronstein, I. McCulloch, S. C. Hayes, et al., *Nat. Mater.* **2016**, *15*, 746–753.

[9] H. Usta, A. Facchetti, T. J. Marks, *Acc. Chem. Res.* **2011**, *44*, 501–10.

[10] Y. Takeda, T. L. Andrew, J. M. Lobez, A. J. Mork, T. M. Swager, *Angew. Chem. Int. Ed.,* **2012**, *51*, 9042–9046.

[11] ASTM, *ASTM* **2013**, *3*, 1–21.

[12] Y. Tamai, H. Ohkita, H. Benten, S. Ito, *J. Phys. Chem. Lett.* **2015**, *6*, 3417–3428.

[13] Y. Kim, S. Cook, S. M. Tuladhar, S. A. Choulis, J. Nelson, J. R. Durrant, D. D. C. Bradley, M. Giles, I. McCulloch, C.-S. Ha, et al., *Nat. Mater.* **2006**, *5*, 197–203.

[14] R. Noriega, J. Rivnay, K. Vandewal, F. P. V Koch, N. Stingelin, P. Smith, M. F. Toney, A. Salleo, *Nat. Mater.* **2013**, *12*, 1038–44.

[15] R. S. Loewe, P. C. Ewbank, J. Liu, L. Zhai, R. D. McCullough, *Macromolecules* **2001**, *34*, 4324–4333.

[16] T. Yokozawa, A. Yokoyama, *Chem. Rev.* **2009**, *109*, 5595-5619.

[17] R. Miyakoshi, A. Yokoyama, T. Yokozawa, *Macromol. Rapid Commun.* **2004**, *25*, 1663–1666.

[18] A. Yokoyama, H. Suzuki, Y. Kubota, K. Ohuchi, H. Higashimura, T. Yokozawa, *J. Am. Chem. Soc.* **2007**, *129*, 7236–7237.

[19] A. Babel, S. a. Jenekhe, *Synth. Met.* **2005**, *148*, 169–173.

[20] B. Friedel, C. R. McNeill, N. C. Greenham, *Chem. Mater.* **2010**, *22*, 3389–3398.

[21] A. Cadisa, W. D. Oosterbaan, K. Vandewal, J. C. Bolsée, S. Bertho, J. D'Haen, L. Lutsen, D. Vanderzande, J. V. Manca, *Adv. Funct. Mater.* **2009**, *19*, 3300–3306.

[22] H. Sirringhaus, P. J. Brown, R. H. Friend, M. M. Nielsen, K. Bechgaard, A. J. H. Spiering, *Nature,* **1999**, *401,* 685–688.

[23] C. H. Woo, B. C. Thompson, B. J. Kim, M. F. Toney, J. M. J. Frechet, *J. American Chem. Soc.* **2008**, *130,* 16324–16329.

[24] S. Holliday, R. S. Ashraf, A. Wadsworth, D. Baran, S. A. Yousaf, C. B. Nielsen, C. H. Tan, S. D. Dimitrov, Z. Shang, N. Gasparini, et al., *Nat. Commun.* **2016**, *7*, 1–11.

[25] X. Guo, C. Cui, M. Zhang, L. Huo, Y. Huang, J. Hou, Y. Li, *Energy Environ. Sci.* **2012**, *5*, 7943-7949.

[26] H. Seyler, J. Subbiah, D. J. Jones, A. B. Holmes, W. W. H. Wong, *Beilstein J. Org. Chem.* **2013**, *9*, 1492–1500.

[27] J. H. Bannock, S. H. Krishnadasan, A. M. Nightingale, C. P. Yau, K. Khaw, D. Burkitt, J. J. M. Halls, M. Heeney, J. C. De Mello, *Adv. Funct. Mater.* **2013**, *23*, 2123–2129.

[28] M. Mizuno, H. Tateno, Y. Matsumura, M. Atobe, *React. Chem. Eng.* **2017**, *2*, 642–645.

[29] X. Wang, Y. Sun, S. Chen, X. Guo, M. Zhang, X. Li, Y. Li, H. Wang, *Macromolecules* **2012**, *45*, 1208–1216.

[30] J.-H. Kim, J. B. Park, F. Xu, D. Kim, J. Kwak, A. C. Grimsdale, D.-H. Hwang, *Energy Environ. Sci.* **2014**, *7*, 4118–4131.

[31] A. Kiriy, V. Senkovskyy, M. Sommer, *Macromol. Rapid Commun.* **2011**, *32*, 1503–1517.

[32] F. Pammer, U. Passlack, *ACS Macro Lett.* **2014**, *3*, 170–174.

[33] E. E. Sheina, J. Liu, M. C. Iovu, D. W. Laird, R. D. Mccullough, *Macromolecules* **2004**, *37,* 3526–3528.

[34] M. C. Iovu, E. E. Sheina, R. R. Gil, R. D. Mccullough, *Macromolecules* **2005**, *38*, 8649–8656.

[35] P. Thieno, P. Willot, G. Koeckelberghs, *Macromolecules* **2014**, 47, 8548-8555.

[36] K. Okamoto, C. K. Luscombe, *Chem. Commun.* **2014**, *50*, 5310–5312.

[37] G. Zhang, Y. Ohta, T. Yokozawa, *Macromol. Rapid Commun.* **2018**, *39*, 1–5.

[38] M. Verswyvel, P. Verstappen, L. De Cremer, T. Verbiest, G. Koeckelberghs, *J. Polym. Sci. Part A Polym. Chem.* **2011**, *49*, 5339–5349.

[39] S. Kang, R. J. Ono, C. W. Bielawski, *J. Am. Chem. Soc.* **2013**, *135*, 4984–4987.

[40] M. Nath, *Appl. Organomet. Chem.* **2008**, *22*, 598–612.

[41] Y. Qiu, J. Mohin, C.-H. Tsai, S. Tristram-Nagle, R. R. Gil, T. Kowalewski, K. J. T. Noonan, *Macromol. Rapid Commun.* **2015**, *36*, 840–4.

[42] T. Yokozawa, R. Suzuki, M. Nojima, Y. Ohta, A. Yokoyama, *Macromol. Rapid Commun.* **2011**, *32*, 801–806.

[43] M. P. Bhatt, H. D. Magurudeniya, P. Sista, E. E. Sheina, M. Jeffries-EL, B. G. Janesko, R. D. McCullough, M. C. Stefan, *J. Mater. Chem. A* **2013**, *1*, 12841-12849.

[44] Q. Shi, S. Zhang, J. Zhang, V. F. Oswald, A. Amassian, S. R. Marder, S. B. Blakey, *J. Am. Chem. Soc.* **2016**, *138*, 3946–3949.

[45] X. Liu, X. Zhao, F. Liang, B. Ren, *Org. Biomol. Chem.* **2018**, 886–890.

[46] H. M. L. Davies, J. R. Manning, *Nature* **2008**, *451*, 417–424.

[47] T. Itahara, *J. Org. Chem.* **1985**, *50*, 5272–5275.

[48] B. Liegault, D. Lapointe, L. Caron, A. Vlassova, K. Fagnou, *J. Org. Chem.,* **2009**, *74,* 1826–1834.

[49] M. Lafrance, K. Fagnou, *J. Am. Chem. Soc.* **2006**, *128*, 16496–16497.

[50] X. Chen, K. Engle, D.-H. Wang, J.-Q. Yu, *Angew. Chemie Int. Ed.* **2009**, *48*, 5094–5115.

[51] N. Ahlsten, G. J. P. Perry, X. C. Cambeiro, T. C. Boorman, I. Larrosa, *Catal. Sci. Technol.* **2013**, *3*, 2892-2897.

[52] T. C. Boorman, I. Larrosa, *Chem. Soc. Rev.* **2011**, *40*, 1910–25.

[53] X. C. Cambeiro, N. Ahlsten, I. Larrosa, *J. Am. Chem. Soc.* **2015**, *137*, 15636–15639.

[54] L.-C. Campeau, M. Parisien, A. Jean, K. Fagnou, *J. Am. Chem. Soc.* **2006**, *128,* 581–597.

[55] D. Lapointe, K. Fagnou, *Chem. Lett.* **2010**, *39*, 1118–1126.

[56] S. I. Gorelsky, D. Lapointe, K. Fagnou, *J. Org. Chem.* **2012**, *77*, 658–668.

[57] S. I. Gorelsky, D. Lapointe, K. Fagnou, *J. Am. Chem. Soc.* **2008**, *130,* 10848–10849.

[58] B. Liégault, I. Petrov, S.I. Gorelsky, K. Fagnou, *J. Org. Chem.* **2010**, *75*, 1047–1060.

[59] K. Okamoto, J. Zhang, J. B. Housekeeper, S. R. Marder, C. K. Luscombe, *Macromolecules,* **2013**, *46*, 8059-8078.

[60] L. G. Mercier, M. Leclerc, *Acc. Chem. Res.* **2013**, *46*, 1597–1605.

[61] Q. Wang, R. Takita, Y. Kikuzaki, F. Ozawa, *J. Am. Chem. Soc.* **2010**, *132*, 11420–11421.

[62] Q. Wang, M. Wakioka, F. Ozawa, **2012**, 1203–1207.

[63] T. Bura, P.-O. Morin, M. Leclerc, *Macromolecules* **2015**, *48*, 5614–5620.

[64] A. E. Rudenko, B. C. Thompson, *Macromolecules* **2015**, *48*, 569–575.

[65] A. E. Rudenko, A. A. Latif, B. C. Thompson, *Nanotechnology* **2014**, *25*, 14005.

[66] Y. Y. Lai, T. C. Tung, W. W. Liang, Y. J. Cheng, *Macromolecules* **2015**, *48*, 2978–2988.

[67] T. P. Osedach, T. L. Andrew, V. Bulović, S. R. Forrest, L. Dou, J. You, J. Yang, C.-C. Chen, Y. He, S. Murase, et al., *Energy Environ. Sci.* **2013**, *6*, 711-718.

[68] R. Po, G. Bianchi, C. Carbonera, A. Pellegrino, *Macromolecules* **2015**, *48*, 453–461.

[69] C. Gao, D. Yan, *Prog. Polym. Sci.* **2004**, *29*, 183–275.

[70] T. V Richter, S. Link, R. Hanselmann, S. Ludwigs, *Macromol. Rapid Commun.* **2009**, *30*, 1323–7.

[71] H. S. Mangold, T. V Richter, S. Link, U. Würfel, S. Ludwigs, *J. Phys. Chem. B* **2012**, *116*, 154–9.

[72] T. V. Richter, C. Bühler, S. Ludwigs, *J. Am. Chem. Soc.* **2012**, *134*, 43–46.

[73] C. Kub, J. Tolosa, A. J. Zucchero, P. L. McGrier, C. Subramani, A. Khorasani, V. M. Rotello, U. H. F. Bunz, *Macromolecules* **2010**, *43*, 2124–2129.

[74] Y. Wang, A. La, Y. Ding, Y. Liu, Y. Lei, *Adv. Funct. Mater.* **2012**, *22*, 3547–3555.

[75] K. Li, B. Liu, *J. Mater. Chem.* **2012**, *22*, 1257–1264.

[76] K. Y. Pu, K. Li, J. Shi, B. Liu, *Chem. Mater.* **2009**, *21*, 3816–3822.

[77] J. L. Novotney, W. R. Dichtel, *ACS Macro Lett.* **2013**, *2*, 423–426.

[78] X. Wu, H. Li, B. Xu, H. Tong, L. Wang, *Polym. Chem.* **2014**, *5*, 4521.

[79] W. Huang, E. Smarsly, J. Han, M. Bender, K. Seehafer, I. Wacker, R. R. Schröder, U. H. F. Bunz, *ACS Appl. Mater. Interfaces* **2017**, *9*, 3068–3074.

[80] Y. Segawa, T. Higashihara, M. Ueda, *Polym. Chem.* **2013**, *4*, 1746–1759.

[81] K. Okamoto, J. B. Housekeeper, F. E. Michael, C. K. Luscombe, *Polym. Chem.* **2013**, *4*, 3499-3506.

[82] K. Funaki, T. Sato, S. Oi, *Org. Lett.* **2012**, *14*, 6186–9.

[83] K. Muto, J. Yamaguchi, K. Itami, *J. Am. Chem. Soc.* **2012**, *134*, 169–172.

[84] H. Xu, K. Muto, J. Yamaguchi, C. Zhao, K. Itami, D. G. Musaev, *J. Am. Chem. Soc.* **2014**, *136*, 14834–14844.

[85] K. Muto, J. Yamaguchi, A. Lei, K. Itami, *J. Am. Chem. Soc.* **2013**, *135*, 16384–16387.

[86] A. Kiriy, V. Senkovskyy, M. Sommer, *Macromol. Rapid Commun.* **2011**, *32*, 1503–1517.

[87] N. A. Strotman, H. R. Chobanian, Y. Guo, J. He, J. E. Wilson, *Org. Lett.* **2010**, *12*, 3578–3581.

[88] A. M. van Leusen, B. E. Hoogenboom, H. Siderius, *Tetrahedron Lett.* **1972**, *13*, 2369–2372.

[89] Q. Guo, D. Wu, J. You, *ChemSusChem* **2016**, *9*, 2765–2768.

[90] A. Faradhiyani, Q. Zhang, K. Maruyama, J. Kuwabara, T. Yasuda, T. Kanbara, *Mater. Chem. Front.* **2018**, 2–5.

[91] N. S. Gobalasingham, S. Noh, B. C. Thompson, *Polym. Chem.* **2016**, *7*, 1623–1631.

[92] X. C. Cambeiro, T. C. Boorman, P. Lu, I. Larrosa, *Angew. Chem. Int. Ed. Engl.* **2013**, *52*, 1781–4.

[93] J. Min, Z. G. Zhang, S. Zhang, Y. Li, *Chem. Mater.* **2012**, *24*, 3247–3254.

[94] C. Y. He, C. Z. Wu, F. L. Qing, X. Zhang, *J. Org. Chem.* **2014**, *79*, 1712–1718.

[95] C.-Y. He, C.-Z. Wu, Y.-L. Zhu, X. Zhang, *Chem. Sci.* **2014**, *5*, 1317–1321.

[96] J. Pouliot, M. Wakioka, F. Ozawa, Y. Li, M. Leclerc, *Macromol. Chem. Phys.* **2016**, *217*, 1493–1500.

[97] H. Bronstein, C. Luscombe, *J. Am. Chem. Soc.,* **2009**, *131*, 12894–12895.

[98] N. Doubina, S. A. Paniagua, A. V. Soldatova, A. K. Y. Jen, S. R. Marder, C. K. Luscombe, *Macromolecules* **2011**, *44*, 512–520.

[99] N. Doubina, M. Stoddard, H. A. Bronstein, A. K. Y. Jen, C. K. Luscombe, *Macromol. Chem. Phys.* **2009**, *210*, 1966–1972.

[100] J. J. Hirner, Y. Shi, S. A. Blum, *Acc. Chem. Res.* **2011**, *44*, 603–13.

[101] A. S. K. Hashmi, C. Lothschütz, R. Döpp, M. Rudolph, T. D. Ramamurthi, F. Rominger, *Angew. Chemie Int. Ed.* **2009**, *48*, 8243–8246.

[102] K. E. Roth, S. A. Blum, *Organometallics* **2011**, *30*, 4811–4813.

[103] M. Al-Amin, K. E. Roth, S. A. Blum, *ACS Catal.* **2014**, *4*, 622–629.

[104] M. M. Hansmann, M. Pernpointner, R. Döpp, A. S. K. Hashmi, *Chem. – A Eur. J.* **2013**, *19*, 15290–15303.

[105] D. Lapointe, K. Fagnou, *Chem. Lett*., **2010**, *39,* 1118–1126.

[106] M. Livendahl, C. Goehry, F. Maseras, A. M. Echavarren, *Chem. Commun.* **2014**, *50*, 1533–1536.

[107] M. Y. and H. V. R. D. Venkata A. K. Adiraju, *Dalt. Trans.* **2015**, *44*, 4449–4454.

[108] H. A. Ioannidou, P. A. Koutentis, *Org. Lett.* **2011**, *13*, 1510–1513.

[109] S. Y. Lee, J. F. Hartwig, *J. Am. Chem. Soc,* **2016**, *138,* 15278-15284.

[110] M. Anand, R. B. Sunoj, H. F. Schaefer, *ACS Catal.* **2016**, *6*, 696–708.

[111] D. Whitaker, J. Burés, I. Larrosa, *J. Am. Chem. Soc.* **2016**, *138*, 8384–8387.

[112] M. D. Lotz, N. M. Camasso, A. J. Canty, M. S. Sanford, *Organometallics* **2017**, *36,* 165-171.

[113] S.-L. Suraru, J. A. Lee, C. K. Luscombe, *ACS Macro Lett.* **2016**, *5*, 533–536.

[114] C. J. O'Brien, E. A. B. Kantchev, C. Valente, N. Hadei, G. A. Chass, A. Lough, A. C. Hopkinson, M. G. Organ, *Chem. – A Eur. J.* **2006**, *12*, 4743–4748.

[115] Y. Zhao, A. J. Nett, A. J. Mcneil, P. M. Zimmerman, *Macromolecules* **2016**, *49,* 7632–7641.

[116] J. Kim, S. H. Hong, *ACS Catal.* **2017**, *7,* 3336–3343.

[117] K. F. Teng, R. W. Vest, *IEEE Trans. components, hybrids, Manuf. Technol.* **1988**, *11*, 291–297.

VITA

Jason A. Lee was born and raised in southern California. His first interest in chemistry developed during his time at Gabrielino High School, where he took honors chemistry and AP chemistry with Mr. Cameron and Mrs. Strom, respectively. His first exposure to research was in 2010 via the Caltech Summer Undergraduate Research Fellowship (SURF) in the lab of Professor Robert H. Grubbs, under the mentorship of Dr. Rosemary Kiser. There, he worked on trying to develop a polymeric bioadhesive. From the fall of 2010 until graduation, he worked in the lab of Professor Paula Diaconescu at UCLA, performing research on synthesizing group 3 transition metal catalysts. He received his BS in chemical engineering with a biomolecular option from UCLA in 2012. In the fall of 2012, Jason joined the lab of Professor Christine K. Luscombe at the University of Washington to study C-H functionalization, specifically direct arylation polymerization for novel and atom-economical methods of conjugated polymer syntheses.